Anna Costa

Basin-scale sediment dynamics of an alpine catchment: understanding the impacts of hydroclimatic forcing and hydropower

ETH zürich

Institute of Environmental Engineering
Diss. ETH No. 25087

Diss. ETH No. 25087

Basin-scale sediment dynamics of an alpine catchment: understanding the impacts of hydroclimatic forcing and hydropower

A thesis submitted to attain the degree of

DOCTOR OF SCIENCES of ETH ZURICH

(Dr. sc. ETH Zurich)

presented by

ANNA COSTA

MSc in Environmental Engineering, University of Trento, Italy
MAS Institute of Environmental Engineering, ETH Zurich

born on 24 August 1980

citizen of Italy

accepted on the recommendation of

Prof. Dr. Peter Molnar, examiner
Prof. Dr. Paolo Burlando, co-examiner
Prof. Dr. Stuart N. Lane, co-examiner
Prof. Dr. Hervé Piégay, co-examiner

2018

Abstract

Erosion and sediment transport processes play an important role in many aspects of landscape dynamics and society, affecting land degradation, agricultural productivity, river stability, flood risk, coastal change, and many others. Consequently, they have increasing economic, environmental, and scientific relevance worldwide. The Alpine region has been recognized to represent a critical sediment source for the European continent. Tectonic and seismic activity, high relief, the presence of glaciers, orographic precipitation combined with a favorable lithology, result in some of the highest denudation rates in Europe. Alpine-derived sediments represent a significant contribution to the sediment yield of continental drainage systems. The Alps also represent a very sensitive environment with regard to climate change and human development. Changes in precipitation intensity and snow cover duration are expected to affect erosion. Temperature driven changes in snow and ice melt processes may significantly impact sediment transport in Alpine streams. In addition, accelerated glacier retreat may disclose large amounts of unconsolidated sediment, substantially increasing sediment supply in headwater regions. Moreover, during the last century, anthropogenic activities such as river channelization, gravel mining for construction purposes, and hydropower production based on water storage and transfer have significantly impacted mountainous catchments. Hydropower systems affect sediment dynamics mainly by reducing sediment supply due to trapping behind dams, and by altering sediment transport due to streamflow regulation associated with hydropower operations.

The main aim of this thesis is to explore how climate and human activities have impacted the fate of sediment in Alpine environments during the Anthropocene. The focus is on the upper Rhône Basin, a 5338 km^2 large Alpine catchment in southwestern Switzerland. The catchment covers a wide elevation range (372-4634 m a.s.l.). Precipitation shows a strong orographic variability, with basin-averaged mean annual values around 1400 mm $year^{-1}$. More than 10% of the catchment is covered by glaciers, among which is Aletsch Glacier, the largest glacier in the European Alps. The basin is characterized by a pluvioâglacioânival hydrological regime typical of Alpine environments. Ongoing climate driven changes in the hydrological regime, observed in the Alpine region, have occurred in this basin as well, and may have impacted the sediment dynamics of the catchment. The Rhône Basin has been heavily affected by humans during the last century. Major projects of river channelization have been implemented on the main river to ensure flood protection and gravel mining activities are ongoing along several tributaries. Most importantly, several large dams have been built in the basin, with a total storage capacity equal to almost 20% of the total annual runoff at the outlet of the catchment into Lake Geneva. A network of intakes,

tunnels and pumping stations extract water from headwater channels and transfer it to hydropower reservoirs. Effects of hydropower vary greatly in space: while downstream of dams and intakes flow is often reduced almost to zero, downstream of hydropower stations flow in the summer is substantially reduced and winter discharge increases in response to hydropower operations. It is hypothesized that hydropower operation will have major impacts on sediment dynamics. Sediment trapping behind dams may reduce sediment supply, regulation may alter the sediment transporting capacity of flow. However, there have been relatively few studies which have analyzed and quantified the impacts of hydropower on sediment transport. Important features are in-stream water intakes which divert water to reservoirs, but also trap sediment and intermittently flush it downstream. In this way they also represent a significant disturbance of the sediment transfer. All these characteristics make the Rhône Basin a suitable site for exploring the joint effect of hydroclimate and hydropower on the sediment dynamics in an Alpine environment.

To explore the control of hydroclimatic factors and hydropower on suspended sediment fluxes, the catchment is conceptualized as a series of sediment sources which are activated/deactivated throughout the hydrological year by three main hydroclimatic forcings: erosive rainfall, defined as liquid precipitation over snow free areas, snow/ice melt. Taking into consideration that the various erosional and sediment transport processes (e.g. soil erosion by raindrop impacts, soil detachment by snowmelt-driven overland flow, glacial erosion) and the sediment sources involved (e.g. hillslopes, channels, glaciers) are related to sediment concentration at the catchment outlet, we examined the relations of hydroclimatology to suspended sediment yield in the following way. First, we simulate the hydroclimatic variables, erosive rainfall, snow cover, snowmelt and ice melt by applying spatially distributed degree-day models for melting and a temperature threshold for the snow/rain division. In addition, we estimate hydropower releases by a conceptual approach with a unique virtual reservoir regulated on the basis of a targetâvolume function. Second, we explore the link between hydroclimatic factors and values of mean daily suspended sediment concentration (SSC) derived from turbidity measurements collected at the outlet of the catchment. The relations are quantified by an objective input variable selection algorithm which identifies the variables with the highest predictive power for SSC, their characteristic time lags, and explained variance. To quantify the individual contributions of hydroclimatic forcing variables, we develop a nonâlinear multivariate rating curve (Hydroclimate Multivariate Rating Curve, HMRC), which relates SSC to the main hydroclimatic factors driving suspended sediment fluxes in the catchment. To investigate the impacts of hydropower on coarser grains, a new model for bedload transport at the river network scale was developed. The river network is conceptualized as a series of links connected through nodes. The model computes 1-D flow depth, bedload

transport, erosion and deposition, channel bed volume and the grain size distribution (GSD) at daily time step, given discharge and the geometric characteristics of the links. Discharge in each link are simulated with the spatially-distributed, physically-based hydrological model Topkapi-ETH, in which a detailed scheme of the hydropower system operating in the catchments has been implemented and successfully calibrated in a previous study. Sediment trapping behind dams is accounted for by removing the sediment supply entering river reaches downstream of dams. Impacts of flow regulation are analyzed by running the model under the hydrological conditions before ("natural" scenario) and after ("hydropower" scenario) dam construction.

Our results show that all three hydroclimatic processes - erosive rainfall, ice melt and snowmelt - are significant predictors of mean daily SSC at the outlet of the upper Rhône Basin. Erosive rainfall explains 75% of the total observed variance in SSC, ice melt and snowmelt explain respectively 12% and 4%, while hydropower releases do not play a significant role. This is likely because released water is poorer in sediment. Coefficients of the HMRC indicate that, although erosive rainfall is responsible for the peaks in SSC during intense rainfall events, ice melt generates the greatest contribution to SSC per unit of water volume and contributes the most to the annual sediment yield from the catchment. In agreement with these results, we found that despite the substantial effect of hydropower, the catchment has experienced a significant rise in mean annual SSC ($\sim$40%) at the outlet in mid 1980s. This rise occurred simultaneously with an increase in basin-wide mean air temperature. Statistical analysis revealed that temperature driven enhanced ice melt and glacier retreat have likely played a dominant role in the observed SSC rise, through increased contribution of sediment-rich glacial meltwater and increased sediment availability due to glacier recession. Reduced snow cover duration and extent might have contributed to increase SSC as well, by enhancing erosion over snow-free hillslopes. Results of the river-network bedload model indicate that bedload rates are substantially lower in the "hydropower" scenario, compared to the "natural" conditions (-48% averaged over the river network). Bedload reduction occurs mainly in summer and for coarser grains. After hydropower, the river network is subject to less erosion and more deposition. However, spatial patterns of erosion and deposition are similar to the pre-dam condition. Likewise, the channel bed GSDs do not show significant changes between pre- and post-dam. Fining of the GSD occurs only locally and after 100 years of simulation. Model results suggest that flow regulation has a substantial impact on bedload, exceeding the effect of sediment trapping behind reservoirs. This could be related to presence of many water diversion schemes in the catchment, which lead to reduced transport capacity almost without limitation on sediment supply. Results show that perturbations in bedload propagate along the entire river network. The comparison between streams of different

orders, shows that the hierarchical structure of the river network controls the effects of the perturbations, which result either dampened or enhanced in the downstream direction. Bedload transport is shown to be sensitive to runoff increases due to temperature rise, as would be expected form climate change in the region. Scenarios with warmer temperatures exhibit shifts in the seasonal pattern of bedload and an overall increase in the annual sediment yield, which is, however, lower than the decrease induced by flow regulation. This study suggests that glaciers are crucial sediment sources in mountainous region, especially of fine sediment transported in suspension. Results further demonstrate that the climate signal in suspended sediment dynamics may be visible even in highly regulated and human-impacted Alpine catchments like the upper Rhône Basin. In addition, we conclude that to explore changes in suspended sediment dynamics in mountainous regions it is necessary to apply a perspective that includes an understanding of the sediment sources involved and their hydroclimatic activation. This presents an advantage over traditional rating curves which relate SSC to discharge only, as it allows analyzing climateâinduced changes in sediment dynamics. We show that flow regulation driven by hydropower operation has dominating impacts on bedload transport in the Rhône Basin. The river network modelling approach we have taken allows us to study the effects of perturbations and their propagation throughout the river network. It provides a perspective which enhances local reach-scale studies of sediment dynamics. The model can be applied to any other mountainous catchment to quantify the impacts of perturbation in sediment transport and sediment supply. In addition, due to the low computational effort, this modelling framework can be used to evaluate long term changes in bedload of Alpine river networks including uncertainty analysis.

Sommario

I processi di erosione e trasporto di sedimenti rivestono un ruolo importante in molti aspetti legati sia alla società che alle dinamiche morfologiche, influenzando la degradazione del suolo, la produttività agricola, la stabilità dei corsi d'acqua, il rischio d'inondazioni, l'erosione costiera e molti altri aspetti. Di conseguenza, l'erosione ed il trasporto di sedimenti stanno assumendo sempre più importanza economica, ambientale e scientifica a livello globale. La regione alpina è riconosciuta come una cruciale risorsa di sedimenti per il continente europeo. L'attività tettonica, l'attività sismica, le elevate pendenze, la presenza di ghiacciai e le intense precipitazioni, associate ad una litologia favorevole, si riflettono in tassi di erosione fra i più alti in Europa. I sedimenti prodotti nella regione alpina rappresentano un notevole contributo all'apporto totale di sedimenti che costituisce i sistemi di drenaggio continentale. Le Alpi rappresentano anche un ambiente molto sensibile ai cambiamenti climatici e a quelli associati allo sviluppo di attività umane. Per esempio, alterazioni dell'intensità di precipitazione e della durata ed estensione della copertura nevosa possono influenzare l'erosione. Allo stesso modo, cambiamenti nei processi di scioglimento di ghiaccio e neve, dovuti all'aumento della temperatura, possono alterare il trasporto di sedimenti nei torrenti alpini. Inoltre, ci si aspetta che l'accelerato ritiro dei ghiacciai rilasci un'elevata quantità di sedimenti non consolidati, aumentando in maniera sostanziale il volume di sedimenti disponibile nelle zone di alta quota. Le attività umane, come la canalizzazione dei fiumi, l'estrazione della ghiaia a scopi edili, e l'installazione degli impianti idroelettrici basati sullo stoccaggio e sul trasferimento di acqua, hanno notevolmente influenzato i bacini montani durante il secolo scorso. Gli impianti idroelettrici influenzano le dinamiche dei sedimenti in due modi principali: attraverso l'accumulo di sedimento nelle dighe e conseguente riduzione del volume di sedimento disponibile per il trasporto, e attraverso la regolazione del flusso dovuto alle operazioni di produzione di energia idroelettrica.

L'obiettivo principale di questa tesi è di analizzare come il clima e le attività umane abbiano influenzato il destino dei sedimenti nella regione alpina durante lo scorso secolo. L'analisi si concentra sul bacino dell'alto Rodano, un bacino alpino di estensione pari a 5338 km^2, collocato nel sudovest della Svizzera. Il bacino copre un ampio dislivello altimetrico (372-4634 m a.s.l.). La precipitazione, il cui valore medio annuale è di circa 1400 mm $year^{-1}$, è caratterizzata da una forte gradiente orografico. Più di 10% del bacino è coperto da ghiacciai, tra cui l'Aletsch Glacier, il più grande ghiaccio d'Europa. Il bacino è caratterizzato da un regime idrologico tipico della regione alpina, in cui precipitazione e le acqua di scioglimento di ghiaccio e neve rappresentano le componenti idrologiche principali. Alterazioni del regime idrologico, osservate nella regione alpina, stanno inter-

essando anche il bacino dell'alto Rodano, e potrebbero aver un impatto sulla dinamiche dei sedimenti. Il bacino dell'alto Rodano è stato pesantemente influenzato dalle attività umane durante il secolo scorso. Grossi interventi di canalizzazione sono stati implementati per ridurre il rischio di inondazioni, e attività di estrazione della ghiaia sono operative lungo il corso di molti affluenti. Soprattutto, molte dighe di notevoli dimensioni sono state costruite nel bacino, per una capacità di ritenzione totale pari a 20% del volume annuale di acqua scaricato dal fiume Rodano nel lago di Ginevra.

Un'intricata rete di captazioni, tubature, e stazioni di pompaggio estrae acqua dai torrenti di alta quota e la trasferisce alle dighe per la produzione di energia elettrica. Gli effetti legati all'idroelettrico variano sostanzialmente nello spazio: mentre a valle di dighe e punti di prelievo, il flusso d'acqua è ridotto circa a zero, a valle di stazioni idroelettriche, il flusso è notevolmente ridotto in estate e aumentato in inverno, a causa delle operazioni di rilascio per la produzione di energia. Ci si aspetta che i sistemi idroelettrici abbiano un impatto considerevole anche sulle dinamiche dei sedimenti. Da un lato, l'accumulo di sedimenti nelle dighe potrebbe ridurre il volume di sedimenti disponibile, dall'altro la regolazione del flusso potrebbe portare alla riduzione della capacità di trasporto. Tuttavia, ad oggi, ci sono relativamente pochi studi che analizzano e quantificano l'impatto dell'idroelettrico sul trasporto dei sedimenti. Nelle strutture di prelievo e trasferimento dell'acqua collocate lungo il corso dei torrenti, i sedimenti sono prima accumulati e poi rilasciati a valle regolarmente durante operazioni si svuotamento. Di conseguenza essi rappresentano un considerevole elemento di disturbo nel trasferimento dei sedimenti. Riassumendo, tutte queste caratteristiche rendono il bacino dell'alto Rodano molto adatto ad analizzare l'effetto congiunto di idrologia, clima ed attività idroelettriche sul trasporto dei sedimenti in ambiente alpino.

Per analizzare il controllo esercitato dai fattori idrologici, climatici e legati all'idroelettrico sui flussi di sedimenti trasportati in sospensione, abbiamo concettualizzato il bacino come una serie di fonti di sedimento che sono attivate/disattivate, durante l'anno, da tre fattori principali: la pioggia erosiva, definita come la precipitazione liquida che cade su superfici non coperte da neve, e le acque di scioglimento di neve e ghiaccio. Tendendo in considerazione che i vari processi di erosione e trasporto di sedimenti (per esempio, erosione del suolo dovuta all'impatto delle gocce di pioggia, erosione dovuta al flusso generato dallo scioglimento della neve, o erosione dovuta ai ghiacciai) e le varie fonti di sedimento coinvolte (per esempio, pendii, torrenti, ghiacciai) sono legate alla concentrazione di sedimento trasportato in sospensione (CSS) allo sbocco del bacino, abbiamo esaminato la relazione che lega idrologia, clima e CSS, come spiegato di seguito. Innanzitutto, abbiamo simulato la pioggia erosiva, la copertura nevosa, e lo scioglimento di neve e ghiaccio, utilizzando modelli spazialmente distribuiti, basati su gradienti di temperature (degree-day models)

per lo scioglimento e su una soglia di temperatura per la divisione pioggia/neve. Abbiamo poi stimato i rilasci dagli impianti idroelettrici con un modello concettuale basato su un'unica diga virtuale, regolata sulla base di funzioni di obiettivo del volume d'acqua. In un secondo passaggio, abbiamo esplorato il legame tra fattori idroclimatici e valori di CSS, derivati da valori di torbidità, misurati allo sbocco del bacino. La relazione è stata quantificata con un algoritmo di selezione delle variabili, che identifica le variabili con il massimo potere di predire CSS, i loro caratteristici lag temporali, e la varianza spiegata. Per quantificare i contributi individuali di ogni fattore idroclimatico, abbiamo sviluppato una curva di taratura multivariabile, non-lineare (Hydroclimate Multivariate Rating Curve, HMRC) che lega CSS ai principali fattori idroclimatici.

Per analizzare gli effetti dell'idroelettrico sui sedimenti di dimensioni maggiori, abbiamo sviluppato un modello per il trasporto solido di fondo a scala di rete fluviale. La rete fluviale è concettualizzata come una serie di segmenti collegati da nodi. Il modello calcola il flusso, il trasporto solido, l'erosione, la deposizione, e la curva granulometrica del letto del fiume, in una dimensione e su scala giornaliera, date la portata e le caratteristiche geometriche dei segmenti fluviali. La portata è simulata, ad ogni nodo, con il modello idrologico spazialmente distribuito e fisicamente basato Topkapi-ETH, dove uno schema dettagliato degli impianti idroelettrici funzionanti nel bacino è stato implementato e calibrato in un precedente analisi. L'accumulo dei sedimenti è riprodotto nel modello rimuovendo l'apporto di sedimento a monte di segmenti fluviali collocati a valle delle dighe. Gli effetti della regolazione del flusso sono analizzati usando il modello in condizioni idrologiche prima (scenario ânaturaleâ) e dopo la costruzione delle dighe (scenario âidroelettricoâ).

I risultati dimostrano che tutti e tre i fattori climatici, pioggia erosiva, e acque di scioglimento di neve e ghiaccio, sono rilevanti per la CSS trasportata allo sbocco del bacino dell'alto Rodano. La pioggia erosiva spiega il 75% della varianza totale osservata in CSS, mentre l'acqua da scioglimento di ghiaccio e neve rappresenta rispettivamente il 12% ed il 4% della varianza totale. Al contrario, i rilasci idroelettrici non hanno un impatto significativo sulla variabilità di CSS, probabilmente perché i flussi d'acqua rilasciati dalle dighe sono molto poveri di sedimento. I coefficienti della HMRC indicano che, sebbene la pioggia erosiva sia responsabile per i picchi di CSS generati durante piogge intense, l'acqua da scioglimento di ghiaccio genera il contributo maggiore di CSS per unità di volume d'acqua e produce quindi la maggior parte del volume totale annuale di sedimento sospeso allo sbocco.

In accordo con questi risultati, abbiamo trovato che, nonostante l'effetto sostanziale indotto dall'idroelettrico, il bacino ha subito un aumento notevole della CSS media annuale ($\sim$40%) a metà degli anni 80. L'aumento di CSS è avvenuto contemporaneamente

ad un aumento della temperatura media del bacino. L'analisi statistica ha rivelato che l'aumento dello scioglimento dei ghiaccio ed il ritiro dei ghiacciai ha avuto un ruolo dominante nell'aumento di CSS osservato nel bacino dell'alto Rodano, grazie all'aumentato contributo di acqua glaciali ricche in sedimenti sottili, ed all'aumentata disponibilità di sedimento nelle aree prossime ai ghiacciai.

I risultati del modello di trasporto solido indicano che le quantità di volume trasportato sul fondo sono considerevolmente più basse nello scenario âidroelettricoâ (mediamente -48%). La riduzione del trasporto avviene soprattutto in estate e per sedimenti di dimensioni maggiori. Dopo l'attivazione degli impianti idroelettrici, la rete fluviale è soggetta a minor erosione ed a maggior deposizione. In ogni caso, la distribuzione spaziale di erosione e deposizione è molto simile a prima dell'idroelettrico. Allo stesso modo, le curve granulometriche del letto dei fiumi non variano in maniera significativa tra prima e dopo la costruzione delle dighe. Una riduzione nei diametri dei sedimenti è visibile solo localmente e dopo 100 anni di simulazione. I risultati indicano che la regolazione del flusso ha un impatto molto forte sul trasporto, maggiore dell'accumulo di sedimenti nelle dighe. Questo potrebbe anche essere legato al fatto che il bacino contiene molti punti di prelievo d'acqua che comportano la riduzione della capacità di trasporto senza ridurre la disponibilità di sedimento. Le simulazioni mostrano che perturbazioni locali del trasporto si propagano lungo la rete fluviale. Il confronto tra segmenti fluviali di diversi ordini indica che la struttura gerarchica della rete fluviale controlla gli effetti delle perturbazioni, che risultano essere aumentati o diminuiti verso valle. Il trasporto di fondo risulta sensibile alla crescita del flusso legato all'aumento di temperatura previsto nella regione. Temperature più elevate comportano un cambiamento nella stagionalità del trasporto solido, e un aumento del volume annuale trasportato, che risulta comunque inferiore alla riduzione indotta dalle attività idroelettriche.

Questo studio suggerisce che i ghiacciai rappresentano una risorsa di sedimento cruciale nelle zone montuose, specialmente sedimento sottile trasportato in sospensione. I risultati dimostrano che è possibile osservare l'impatto climatico sulle dinamiche dei sedimenti anche in bacini molto regolati da attività umane, come il bacino dell'alto Rodano. Inoltre, l'analisi indica che, per esplorare alterazioni delle dinamiche del trasporto in sospensione in regioni montuose, è necessario adottare una prospettiva che includa la comprensione delle fonti di sedimento coinvolte e la loro attivazione idroclimatica. Rispetto a metodi tradizionali, come le curve di taratura, questa prospettiva presenta il vantaggio di poter analizzare cambiamenti del trasporto di sedimenti legati al clima. Abbiamo mostrato che la regolazione del flusso indotta dagli impianti idroelettrici ha effetti sostanziali sul trasporto di sedimenti nel bacino dell'alto Rodano. L'approccio modellistico, su scala di rete fluviale, adottato in questa tesi, ci ha permesso di analizzare gli effetti delle pertur-

bazioni e la loro propagazione lungo i segmenti fluviali. Il modello puo' essere applicato a qualunque altro bacino montuoso per quantificare gli effetti di perturbazioni della capacità di trasporto o della disponibilità di sedimenti. In aggiunta, questo approccio modellistico offre la possibilità di esplorare cambiamenti del trasporto solido in bacini alpini, su scala temporale lunga, ed includendo, per esempio, la quantificazione dell'incertezza legata agli input climatici.

Acknowledgements

I would like to express my gratitude to my PhD advisor Prof. Peter Molnar for giving me the opportunity to conduct my research in the Hydrology Group at ETH Zurich. Thank you Peter for all your help, motivation and support and for guiding me through this PhD. I am also grateful to Professor Burlando for supporting my work and for all the good advices. My PhD wouldn't have been as interesting as it was without the collaboration with the Sedfate Project team. I would like to thank Laura Stutenbecker, Maarten Bakker, Tiago A. Silva, Stuart N. Lane, Jean-Luc Loizeau and Stephanie Girardclose for the inspiring discussions. Special thanks to Fritz Schlunegger for the enlightening insights on the results of my research and for motivating me at the right time.
I would like to thank our secretary Manuela for helping me in many bureaucratic situations and for supporting my German learning process. I want to thank all the PhDs, Postdocs and Master students that have been working in the Hydrology group during these four years. Thanks for sharing coffee breaks, lunches at the Mensa, some afternoon jogs and hikes during the week-end: Alvaro, Pascal, Matteo, Marco, Seba, Chris, Elena, Fede, Gianluca, Giulia, Martina, Scott, Nadav, Silvan, Riccardo, Darcy, Simone. Thank you to my once-in-a-while office mate Ilaria, I truly enjoyed your company. Thank you Daniela for the nice dinners, your hospitality, the help in my research and for transferring me some of your teaching tips. Very special thanks to Theo for the good advices, the nice conversations, the positive and faithful perspectives, the support, the amazing hike in Zermatt, which I will never forget and the cool pictures, including the one of the title page.
Big thanks to Beatrice Keller. Thank you Be for sharing with me many nice evenings, for supporting me in difficult moments, for visiting me in Italy and for cooking such good dinners. Thanks also to your family that made me feeling at home in many occasions.
I would like to thank also other people that made my life in Zurich much nicer: my landlords Mrs and Mr Streiff for their kindness, Mrs Bloch for the interesting insights into naturopathy, and Lisa, the best German-tandem partner ever!
I am deeply grateful to all my friends that supported me from far away. Special thanks to Piero and Sara for your constant support, for the profound and yet fun conversations and for your love. Thank you Silvia for your nice messages and your carefulness. Profound gratitude goes to Lorena for reaching out to me in hard times and for celebrating with me happy moments, for enlightening the way and for being such a generous messenger. A big thank to Claudia for guiding me throughout the discovery of my soul. I want to thank also all the kids that I had around in these years, for showing me how curiosity and lightheartedness are the basis of learning and researching: Pietro, Maria, Antonio, Diego, Oscar, Leonardo, Kira, Elisabetta e Maddalena. Additional thanks to Maddalena

for sharing adventures every time I was back home and for the countless pigiama-parties, you gave me a lot of energy and happiness. I would like to thank my cousins Michela and Elena for all favors and the support.
Special thanks to Nelly and Willi for your hospitality, and for the affection you showed to me from the very first day. I feel incredibly lucky. Thank you, together with Sarah, Livia, Roman, and Michi, also for the warm welcome in your family.
Last but not least, I am extremely thankful to my parents, Santina and Fiorenzo, who always supported me following my passion. Your hard working attitude and never ending energy represent for me a continuous source of inspiration. I am grateful to my two sisters, Francesca and Giovanna, for your understanding, your providential help, your continuous support and love. Thank you, together with Marco and Alberto, also for the enjoyable time when I am back home.
Heartfelt gratitude to my big love Pascal.

Contents

List of Figures

List of Tables

Chapter 1

Introduction

Figure 1.1: View of the Mundbach, tributary of the upper Rhône River (by F. Textor).

1.1 Motivation and aim

Processes of erosion and transport of sediment represent topics of high scientific, environmental, and economic relevance. Sediment transported by rivers has built the world's largest deltas, which host over 500 million people (Milliman and Meade, 1983; Darby et al., 2016). It has been shown that sediment yield from the main Alpine headwater catchments represents a substantial contribution to the continental drainage systems (Hinderer et al., 2013). In agricultural areas, erosion controls the productivity of soil (e.g. Lal, 2001) and is therefore of considerable economic significance. Processes of erosion and sediment transport may also result in a range of natural hazards. Especially in mountainous regions, landslides, rock falls and debris flows threaten populations and infrastructure and cause considerable damage and economic losses every year (e.g. Hilker et al., 2009). In addition, there are several ecological implications connected with sediment. For example, sediment transported along rivers may carry contaminants (e.g. Walling, 2005), together with nutrients, impacting downstream communities. River floodplains built by sedimentation processes are among the most biologically productive and diverse ecosystems on earth, while being at the same time some of the most threatened environments by human activities (Tockner and Stanford, 2002). Sediment is the building block of ecosystem habitat in river floodplains as well as the aquatic environment itself (e.g. Graf, 2006; Braatne et al., 2008; Gabbud and Lane, 2016).

Several factors control erosional processes and sediment dynamics on a river basin scale. The primary ones are geology, glacier inheritance, climate, and human activities. At long time scales, tectonic and seismic activity represent one of the major drivers of erosion and landscape evolution through isostatic uplift, crustal deformation and thickening (e.g. England and Molnar, 1990; Schlunegger and Hinderer, 2001). Glaciers are known to be effective erosional agents (Montgomery, 2002) contributing to shape the topography and maintaining high sediment supply rates. Erosion and sediment transfer are also intimately linked to climatic conditions. For example, Molnar (2004) showed how increased sediment accumulation rates in the late Cenozoic can be associated with enhanced erosion driven by increased climatic variability. Human activities have significantly impacted erosion and sediment transport during the Anthropocene. Mainly, intense agricultural practice has led to soil erosion and degradation (Richards, 1991), and hydropower systems have substantially altered sediment fluxes by trapping sediment behind dams and by flow regulation (e.g. Graf, 2005; Petts and Gurnell, 2006). At a global scale, it has been argued that the increase in river sediment transport due to enhanced erosion by agriculture is exceeded by the decrease due to sediment retention in reservoirs (Syvitsky et al., 2005). Other specific activities like gravel mining for construction material influence the sediment budget of

Alpine rivers (e.g. Stutenbecker et al., 2017). Channelization and other flood protection measures alter hydraulic conditions leading to changes in sediment transport and river morphodynamics (e.g. Habersack and Nachtnebel, 1994). The above human activities and impacts are superimposed on natural sediment dynamics making it difficult to disentangle cause and effect relations.

However, in the context of rapidly increasing human population and changing climatic conditions, significant alterations of sediment fluxes can be expected. Little quantitative information is known on how human pressure and climate will impact sediment dynamics in detail (Arnell et al., 2007), and how these impacts will reflect on the environment and the society at the local and at the global scale. The main aim of this thesis is to gain a better understanding of how hydroclimatic forcing and human action through hydropower control sediment dynamics in Alpine regions.

1.2 Main factors controlling sediment dynamics in Alpine catchments

1.2.1 Climate

Climate plays a major role in sediment dynamics in mountainous environments (e.g. Micheletti and Lane, 2016; Palazon and Navas, 2016). Rainfall is one of the main factors driving hillslope erosion and is a key component of the Universal Soil Loss Equation (USLE; Wischmeier, 1959; Renard et al., 1997) used in early prediction of soil loss from agricultural fields. During precipitation events, raindrops detach soil particles which are subsequently entrained and removed by runoff (e.g. Wischmeier, 1959). Rainfall erosivity is mainly a function of short-term rainfall intensity peaks (e.g. Wischmeier, 1959; Van Dijk et al., 2002). Rainfall also contributes to overland and channel flow and is therefore a primary cause of sediment transporting capacity away from the place of detachment. It has been extensively shown that rainfall is one the main agents triggering landslides and debris flow (e.g. Guzzetti, 2008; Leonarduzzi et al., 2017), which detach and transport large amount of sediment in short amount of time (e.g. Korup et al., 2004; Bennet et al., 2012).

In Alpine regions, precipitation, together with temperature and solar radiation, also drives snow-cover dynamics and snowmelt. While snow-cover protects the soil from erosion, snowmelt may generate runoff, which contributes both to hillslope erosion and to an increase in the sediment transporting capacity along mountainous streams (e.g. Ollesch

et al., 2006; Konz, 2012). In the presence of glaciers, climatic conditions also determine the melting of ice and the contribution of glacial runoff to sediment production. Snow-cover, for example, reduces ice melt by protecting ice from ablation as well as by enhancing albedo. Once sediment is produced at the glacier-bedrock interface through plucking or abrasion (Boulton, 1974), and a connected sub-glacial network of channels exists, it is transported into the proglacial zone. Meltwater discharge is very rich in fine sediment (e.g. Aas and Bogen, 1988; Lawler et al., 1992; Gurnell et al., 1996) and can represent a major contributor to sediment fluxes. The produced fine and coarse sediment may then be transported further downstream, provided the degree of connectivity (e.g. Cavalli et al., 2013) of the proglacial zones and lateral hillslopes (moraines) areas to downstream reaches is guaranteed. In addition, glacier retreat may disclose large amount of sediment and significantly enhance sediment supply of headwater catchments (Bakker et al., 2018), although negative feedbacks can limit the increase in sediment supply which is effectively connected to the fluvial network and transportable downstream (Lane et al., 2016).

Impacts of climate on sediment dynamics take on particular importance in the context of climate change. Future projections under different climate change scenarios show a common tendency for the European Alpine region. Despite large uncertainty, projections foresee a shift from a snow-dominated to a rain-dominated hydrological regime by the end of the 21st century. Decrease in summer precipitation, increase in winter precipitation and reduction of snowfall days projected for the next century, will result in reduced summer discharge and increased winter discharge. At low elevations snow is expected to disappear earlier, whereas at high elevations snow cover duration and snow depth will decrease (Bavay, 2009; Brönnimann et al., 2014). Due to a warmer climate, it is estimated that medium and large glaciers will experience a massive loss of ice volume due to enhanced ice-melt, while the majority of small glaciers will disappear in the next fifty years (Jouvet et al., 2011; Huss, 2016). Future climate-induced alterations of the Alpine hydrological regime are expected to reflect in the sediment dynamics. An initial phase characterized by increasing washload derived from enlarging proglacial areas, may be followed by a second phase in which reduced connectivity (Lane et al., 2016) and lower glacier mass reduce the sediment export from proglacial areas. Alterations of the flow distribution will impact transport capacity, resulting in enhanced or reduced mobilization of coarser grains. Impacts of changing climatic conditions on sediment yield may be highly variable in space and dependent on the degree of the sediment connectivity (Cavalli et al., 2013; Heckmann and Schwanghart, 2013; Bracken et al., 2015). In summary, future projections of sediment fluxes in mountainous region are still characterized by large uncertainty, although much is known about the processes involved. Exploring and quantifying the link

between hydroclimatic forcing and basin-scale sediment dynamics seems to be a necessary step in future research.

1.2.2 Hydropower

Hydroelectric power is a leading source of energy in the Alps. Since the 20th century, many snowmelt- and ice melt-fed rivers in the European Alpine regions are regulated, resulting in 550 large hydropower stations with a power output greater than 10 MW. Two main management systems characterize hydropower in Alpine catchments: (1) water impoundment behind dams, (2) water abstraction at intakes from headwater channels (Fig. 1.2) and transfer to hydropower plants within the same valley or in a lateral valley. These infrastructures and their operation have a substantial impact on both the hydrological and sediment regime. In terms of hydrology, water impoundment, abstraction and regulated water release change the magnitude, timing, frequency and duration of flow. Mostly, a reduction of flood peaks is observed, together with a shift in the timing of the hydrograph with respect to natural conditions. Generally, reduced discharge is observed in the summer, when water is being stored in the reservoirs, and increased discharge is observed in the winter, when water is released for energy production (Magilligan and Nislow, 2005).

Water Impoundment and Water Abstraction

Hydropower regulates not only water flows but also impacts sediment fluxes, disrupting the "sediment continuum" with effects on erosion/deposition, sediment transport, channel grain size, and channel morphology. However, effects of hydropower on sediment highly depend on the specific infrastructure. Dams and barrages commonly reduce sediment availability through trapping in reservoirs. This generally leads to downstream erosion and channel narrowing due to the imbalance between sediment transport capacity and sediment supply (Andrews, 1986; Williams and Wolman, 1984; Schmidt and Wilcock, 2008). Vegetation encroachment further reduces the channel width of the affected streams (e.g. Williams and Wolman, 1984; Petts and Gurnell, 2005). Intakes may also act as sediment barriers (Fig. 1.2), however they are regularly flushed because they are not designed to store sediment over long periods of time. Therefore, in the case of water intakes, sediment is still released to downstream reaches by flushing (Csiki and Rhoads, 2014; Bakker et al., 2018) while sediment transporting capacity of the downstream reaches is reduced due to flow abstraction. Although water intakes are frequent in hydropower schemes of the Alpine region, little attention has been given so far to their impacts on sediment fluxes (e.g. Raymond Pralong et al., 2015; Bakker et al., 2018). Bakker et al. (2018) showed how the effects of water intakes differ from those of classic reservoirs.

Significant aggradation, lateral channel expansion and an increase in bed level elevation have been observed downstream (Bakker et al., 2018).

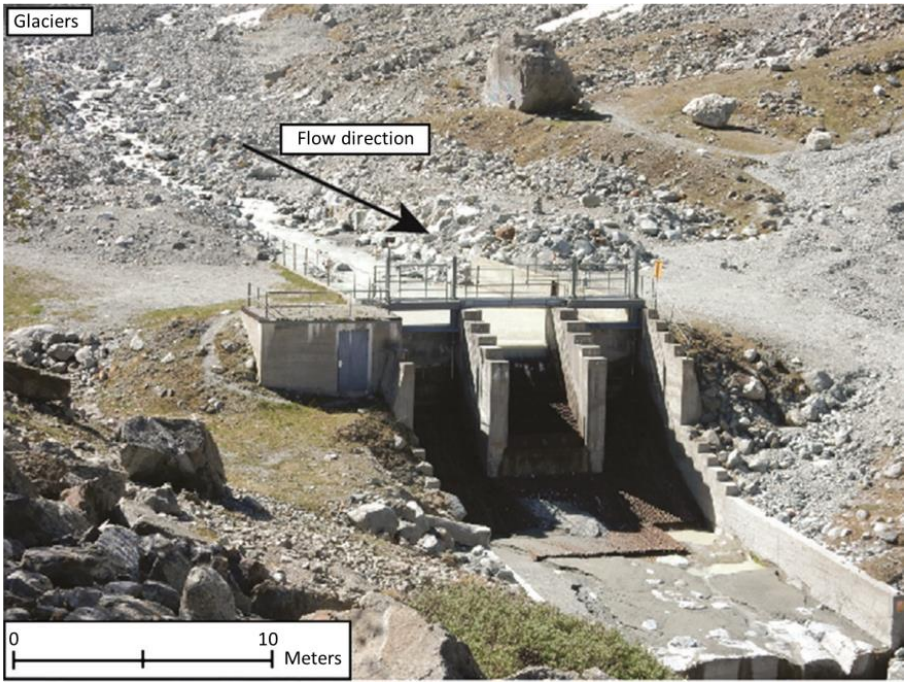

Figure 1.2: Example of water intake (Bas Glacier d'Arolla, Canton of Valais, Switzerland) where the water is extracted and diverted for hydroelectric production and only a residual discharge is released to the river downstream. These types of intakes also serve as sediment traps for sands and gravels. From Gabbud and Lane (2016).

Sediment Storage

Hydropower dams store part of the supplied sediment in the reservoirs. The estimation on the amount of sediment stored behind dams is usually made either through bathymetric surveys (e.g. Anselmetti et al., 2007) or by using empirical equations which are based on the ratio between reservoir capacity and inflow (Brune, 1953), or on particle settling velocity (Camp, 1946; Chen, 1975). However, estimating the effect of reservoirs in terms of sediment trapping efficiency is not straightforward especially for finer fractions. For example, previous studies in Lake Brienz (Central Alps, Switzerland) showed that while the impact of sediment trapping is substantial for coarser grain sizes, finer sediment (< 4 μm) is only very marginally blocked in reservoirs (Finger et al., 2006; Anselmetti et al., 2007).

Flow Regulation

Besides alteration in sediment supply, flow regulation due to hydropower operation has itself a profound impact on sediment transport. Together with sediment trapping, flow regulation leads generally to degradation just downstream of dams, and gradual aggradation further downstream (Williams and Woman, 1984; Petts and Gurnell, 2005; Curtis,

et al., 2010). Erosion right downstream of dams is commonly combined with channel narrowing (e.g. Surian and Rinaldi, 2003), reduction in river sinuosity and consequent decline in ecological quality (Graf, 2006). Observations indicate that in downstream reaches, the grain size distribution is first subject to coarsening, followed by a phase of stabilization and subsequent fining (Williams and Woman, 1984).

However, effects of reservoir operations on sediment transport, are generally very difficult to predict. Due the non-linearity of sediment transport equations (e.g. Rickenmann, 2001) and to the threshold nature of incipient motion conditions for grains (Shields, 1936), estimating the effects on sediment transport is not straightforward, especially at the basin-scale. Changes in hydraulic conditions alter sediment transport capacity and flow competency. However, the transport of sediment is also a function of the supply (e.g. Montgomery and Buffington, 1997; Saletti et al., 2015), which often represents a major source of uncertainty (e.g. Schmitt et al., 2018), and so, effects of hydropower are intimately linked to sediment supply conditions (Schmidt and Wilcock, 2008). In addition, the spatial variability of channel bed grain size distributions, channel morphology, topography and the presence of local inputs of water and sediment, such as tributary junctions, further complicate predictions on the effect of flow regulation. As a result, geomorphic effects driven by hydropower regulation vary both in space and in time in downstream river systems. In terms of first-order predictions, Tealdi et al., (2011) developed a lumped approach to model the long-term longitudinal response of rivers to flow changes. They showed how increasing sediment transport from upstream to downstream results in an initial rapid phase of aggradation, followed by a slow phase of degradation (Tealdi et al., 2011). Curtis et al. (2010) analyzed the effects of tributary junctions on regulated and unregulated rivers. They observed that regulation led to bar growth and channel narrowing downstream of junctions, while upstream they inferred fining of the river bed. In this case flow regulation had a stronger impact on flow competency than on sediment transport capacity (Curtis et al., 2010). In summary, flow regulation may lead to a range of responses, from erosion to deposition, fining to coarsening, depending on local conditions and type of regulation (e.g., Williams and Wolman, 1984; Curtis et al., 2010; Teadi et al., 2010).

1.2.3 Lithology

Lithology is related to rock strength and therefore may exert a major influence on denudation and topography, and indirectly sediment supply. In terms of landslide generation as a mass wasting process supplying sediment to the fluvial system, a recent study has shown that soil erodibility connected to lithology has a strong effect on landslide occurrence

and therefore sediment supply (Leonarduzzi et al., 2017). Softer lithologies are eroded faster than harder lithologies, and the latter can sustain steeper slopes (e.g. Korup and Schlunegger, 2009). Stutenbecker et al. (2017) analyzed the spatial variability of specific landscape properties in several tributary catchments of the upper Rhône River, such as mean elevation, relief, slope, hypsometry and longitudinal profiles of streams. They found evident spatial differences in these landscape metrics, and could relate such differences to the erodibility of the underlying bedrock (Stutenbecker et al., 2017). To summarize, lithology is expected to represent a major controlling factor on erosion and sediment production.

1.2.4 Land use

Together with soil erodibility, land use has an impact on erosion through the way in which the soil is protected or not from rainsplash and overland flow. Root systems enhance mechanical soil strength, vegetation cover attenuates rainfall erosivity. In addition, land use affects erosion by influencing infiltration and runoff generation. The widely used Universal Soil Loss Equation (Wischmeier, 1959; Renard et al., 1997), accounts for land use with the crop management index, representing how much soil erosion is mitigated by vegetation, and the erosion control practice index, expressing the effect on erosion of specific control practices (Renard et al., 1997). At the global scale, it has been estimated that land use changes associated mainly with the development of cropland, increased soil erosion potential by about 17% in the last century (Yang et al., 2003).

During the Holocene, land use changes in northwestern Europe have been mainly tied to deforestation (e.g. Finsinger et al., 2006; Cruise et al., 2009; Giguet-Covex et al., 2011), which exerted substantial impacts on sediment fluxes (e.g. Cruise et al., 2009; Giguet-Covex et al., 2011). Giguet-Covex et al. (2011) could relate increasing sedimentation rates in a subalpine lake to periods of intense soil destabilization attributed to major human-induced activities such as grazing. By analyzing deposits in a small lake in northwestern Italy, Cruise et al. (2009) showed how extensive deforestation and expansion of grassland during the Iron Age and Roman periods has led to enhanced soil erosion (Cruise et al., 2009).

In the more recent past, a decline in land use pressure in the Alpine region has been observed (e.g. Foster et al., 2003; Wick et al., 2003). Wick et al. (2003) could reconstruct phases of intense soil erosion measuring pollen and plant macrofossils at Sägistalsee, a small deep lake in Switzerland. They identified the signal of reforestation during the 20th century (Wick et al., 2003). Reforestation and redistribution of land use pressure may have

resulted in reduced erosion and decreased sediment fluxes, as it has been demonstrated for example in the Lake Annecy (France) by Foster et al. (2003). Although, it is expected that changes in land use in the Alps may be less important than other factors such as climate (Foster et al., 2003) and hydropower, they could partially contribute to the alteration of sediment fluxes.

1.3 Modelling Approaches

Prediction of changes in sediment budgets, fluxes and balances can be made by several different types of sediment transport models, which differ mainly in terms of processes included, description of the spatial distribution, level of complexity, and data requirements (Merritt et al., 2003). Long temporal scale analysis requires the use of landscape evolution models in which climate variables drive the evolution of the landscape itself (e.g. Willgoose et al., 1991; Tucker and Slingerland, 1994; Braun and Sambridge, 1997; Coulthard et al., 2000; Schoorl et al., 2000; Tucker et al., 2001). These models usually pay limited attention to hydrological processes such as rainfall and runoff generation which are highly simplified to allow long term simulation with a reasonable computational effort. A second type of models represents basin scale hydrological processes, flow routing and sediment transport in more details. However, these models, such as for example WEPP (Laflen et al., 1991), KINEROS (Smith et al., 1995), SWAT (Arnold and Fohrer, 2005), and tRIBS-erosion (Francipane et al., 2012), usually neglect changes in topography, i.e. the feedback between sediment transport and landscape evolution. A third category includes non-integrated models, i.e. models that do not account for hydrological processes of the rainfall-runoff transformation but simulate hydraulic variables for given discharge and sediment transport along rivers. In these models, hydraulic variables are often computed by solving the de Saint Venant equations, while sediment transport is estimated with a range of sediment transport formulae. The continuity of mass in the form of the Exner equation is used to update channel bed topography. More advanced versions of this type of models simulate 2-D flow and sediment dynamics and are mostly used to analyze the response of river morphology at small spatial scales, such as in the case of river restoration projects. Examples of such mmodels are SETRAC (Rickenmann et al., 2006; Chiari et al., 2010) designed for steep streams and BASEMENT developed at the Laboratory of Hydraulics, Hydrology and Glaciology at ETH Zurich (Vetsch et al., 2011; Bertoldi et al., 2014).

A fourth modelling approach is applied to simulate sediment transport along rivers at the river network scale. Common features of these models are the 1-D, width-averaged

representation of processes and simplification of flow hydraulics and sediment transport assuming uniform flow and prismatic cross sections. These models have been shown to be very useful when analyzing the effects and propagation of disturbances in sediment dynamics at the river network scale. Because of the modest computational time required, this modelling approach allows testing multiple alternative initial states. This aspect is particularly relevant in applications related to sediment transport because initial and boundary conditions are usually either unknown or highly uncertain. For example, Ferguson et al. (2015) applied such a model to analyze the effects of gold mining on 525 km of the Fraser River (Canada) between 1858 and 1909. The results showed high potential for analyzing the effects of human-induced and natural disturbances on sediment dynamics at the basin-scale. In another approach by Schmitt et al. (2016), the CASCADE river network modeling framework quantifies sediment deliveries between all sediment sources and sinks in large fluvial networks, by describing the transport of sediment from each specific source as an individual cascading process. The model was applied to the Da River system in southeastern Asia and used to demonstrate how patterns and bottlenecks of sediment connectivity and the fate of sediment from manifold sources can be identified (Schmitt et al., 2016). A third example of this fourth modelling type, is the connectivity-based conceptual framework of environmental response for sediment transport by Czuba and Foufoula-Georgiou (2014). This study estimated characteristic velocity for mud, sand and gravel under clearly defined assumptions, based on sediment transport equations in a river network. Velocity is then used to convert the network width function (i.e. the probability of travel distances to the outlet) into geomorphologic instantaneous unit sedimentographs (GIUS) for each class of sediment. GIUS represent the probability distribution of travel times to the outlet of the basin of particles introduced instantaneously and uniformly in the river network. In their application to the Minnesota River Basin, they demonstrated how the effects of two instantaneous inputs of sand completely uncorrelated in time and in space can aggregate and amplify at the outlet of the river network (Czuba and Foufoula-Georgiou, 2014). These types of upstream-downstream effects can only be properly reproduced and predicted with river network models.

Finally, empirical approaches, such as rating curves, are often applied for estimating suspended sediment load. Sediment rating curves, which express suspended sediment concentration as a power function of discharge, have been widely applied (e.g. Campbell and Bauder, 1940; Walling, 1974; 1977; Asselman, 1999; Lenzi and Marchi, 2000; Yang et al., 2007; Wang et al., 2008). Usually the calibration of the rating curve parameters is performed by linear regression after logarithmic transformation of the data. To account for the underestimation of suspended sediment concentration induced by such transformation (Duan, 1983; Ferguson, 1986; Newman 1993), a correction factor is often applied

(e.g. Crawford, 1991; Asselman, 2000; Horowitz, 2003; De Girolamo, 2015). Although they are widely applied, sediment rating curves are usually characterized by large variability in observations around the regression curve, spanning one or more orders of magnitude (e.g. Crawford, 1991; Walling, 1977; Horowitz, 2003; Asselman, 2000). This uncertainty is related to multiple reasons, mainly the fact that sediment supply is not explicitly included. In addition, sediment flux often exhibits a hysteretic behavior with regard to instantaneous flow (Walling, 2005; Sadeghi et al., 2008; Mao and Carrillo, 2016), that such relations cannot account for. If factors such as the type and location of sediment sources and the sediment production and transport processes could be accounted for in rating curve analysis, better predictions of suspended sediment concentration and yield would likely be achieved (Vansickle and Beschta, 1983, Syvitski, 2000; Lenzi et al., 2003; Walling, 2005; De Vente et al., 2006; Warrick, 2015). Moreover, traditional approaches, based on discharge only, are often not capable of capturing the potential causes of alterations in suspended sediment dynamics, whereas an approach accounting for sediment sources would, at least partially, allows exploring potential causes of changes.

1.4 Study Site: the upper Rhône Basin

The center of investigation in this Thesis is the upper Rhône basin, a large Alpine catchment, located in southwestern Switzerland (Fig. 1.3). The "upper" Rhône River refers to the section of the Rhône River that flows from the origin, at the Rhône Glacier, to Lake Geneva (Figs. 1.3a, 1.3b). The "lower" Rhône River, instead, refers to the section that flows through France from Lake Geneva to the Mediterranean Sea. The upper Rhône River originates as a torrential stream at the Rhône Glacier (2200 m a.s.l.), located at the far eastern end of the Swiss canton of Valais. It flows in a western direction along the glacially carved Rhône Valley (Fig. 1.3a), and then turns north until it enters Lake Geneva (372 m a.s.l.). Along its roughly 160 km long course, the upper Rhône River receives the contribution of more than 50 major tributaries. With its 5338 km^2 of surface area, the upper Rhône basin is the largest inner Alpine drainage system. The basin covers a wide elevation range (372 - 4634 m a.s.l.). The dominant land use consists of coniferous forest and agriculture.

The hydrology of the upper Rhône basin is characterized by a pluvio-glacio-nival regime with higher discharge in summer and lower discharge in winter. The mean annual value of discharge is roughly 180 $m^3\ s^{-1}$. Precipitation is characterized by a strong orographic pattern, with more than 3500 mm $year^{-1}$ at the highest elevation, roughly 500 mm $year^{-1}$ along the main valley and mean annual values around 1400 mm $year^{-1}$. Basin-wide mean

annual air temperature is about 1.4 °C, seasonal temperature gradients are quite high with mean values equal to almost 9.5 °C in July and -5.5 °C in January. In the literature it is reported that the Swiss Alpine region has experienced two main periods characterized by rapid warming in the 1940s and in the 1980s (Beniston et al., 1994; Beniston and Rebetez, 1996).

(a) (b)

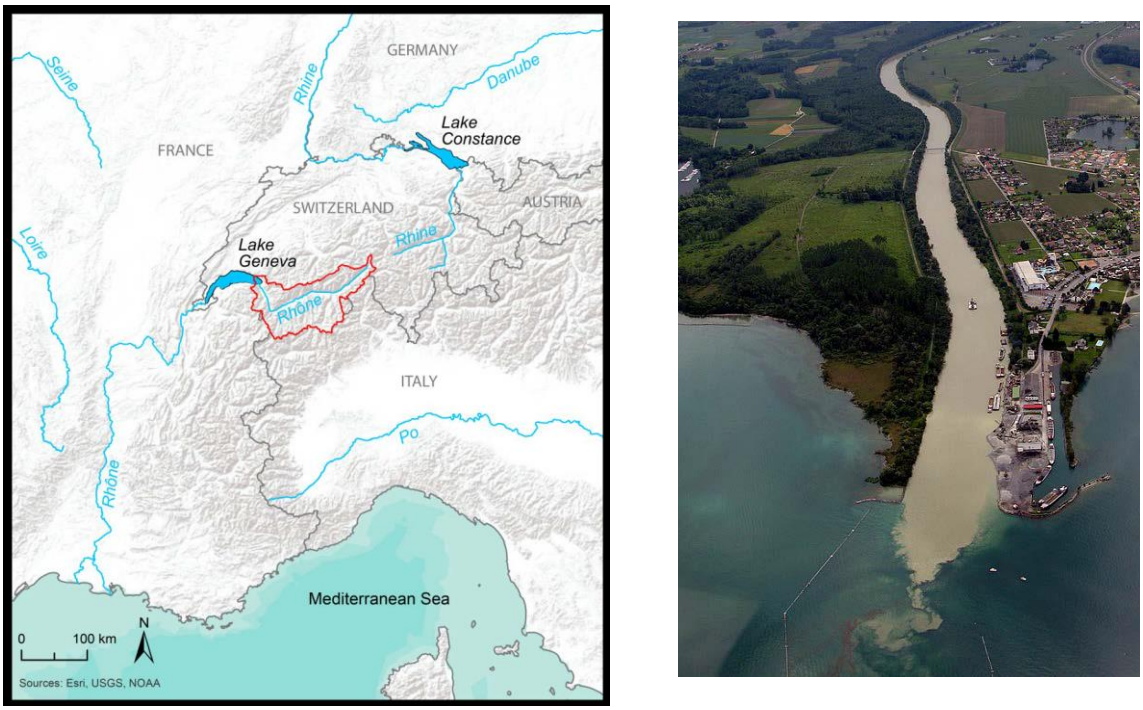

Figure 1.3: (*a*) Location map of the Rhône River system and other major rivers. The catchment of the upper Rhône River is highlighted in red. ©Esri. From Stutenbecker (2017). (*b*) The Rhône River entering Lake Geneva at the village of Bouveret. Photograph by Rama, Wikimedia Commons, CC BY-SA 2.0 FR (2007).

Geology and glaciers

Three main litho-tectonic units can be distinguished in the catchment: the so-called External massifs, comprising autochthonous slices and allochthonous nappes of the European meta-granitoid basement, the Helvetic nappes composed of the mesozoic carbonate sedimentary cover of the European passive continental margin, and Penninic nappes which refer to the Dent Blanche thrust sheet which consists almost exclusively of metagranitoids and gneisses (Stutenbecker et al., 2017). The landscape of the Rhône valley has been shaped by multiple glaciations during the Quaternary (Sutenbecker et al., 2016). At the maximum of the Last Glacial Maximum (LGM), roughly 20000 years ago, the entire basin was covered by an ice sheet of up to 1.5 km thickness (Sutenbecker et al., 2016;

Valla et al., 2011). The presence of U-shaped, deeply carved valleys, hanging tributary rivers and inner gorges reflects the strong glacial inheritance (Sutenbecker et al., 2016; Valla et al., 2011). Nowadays, more than 10% of the surface is covered by glaciers, which are mostly located in the southeastern and eastern part of the catchment (Stutenbecker et al., 2016). The basin hosts some of the largest Alpine glaciers such as the Aletsch Glacier, the largest glacier in the European Alps, roughly 20 km long and approximately 86 km2 in area in 1973 (Haeberli and Holzhauser, 2003). Significant glacier retreat, observed in the catchment during the last century, has intensified during the last 30 years (Paul et al., 2004, 2007) and it is expected that many of the small and mid-size glaciers will disappear by 2050 (Huss and Fischer, 2016).

The upper Rhône River and Lake Geneva

The Rhône River supplies more than 65% of the total input of water and particulate matter into the Lake Geneva (Loizeau et al., 1997). Since 1964, measurements of suspended sediment concentration are collected two times per week at Port du Scex, a measurement station of the Federal Office for the Environment located 5 km upstream of the catchment outlet. Based on these observations and measurements of discharge collected at the same location, the total sediment input to Lake Geneva is estimated to be between 2 and 5 Mt year^{-1}, with a large interannual variability most likely related also to the discontinuity of the sediment sampling. Most of the sediment input from the Rhône River consists of clays to medium-sized silts (Kremer et al., 2015). The Rhône River has a substantial influence on the morphology and ecology of the delta and the lake (Loizeau et al., 1997; Loizeau and Dominik, 2000).

The upper Rhône River mouth consists of a proximal delta front, a sublacustrine canyon and a distal lobe (Silva et al., in review). The delta front is characterized by very high sedimentation rates, around 7.37 cm year^{-1}, while the distal lobe shows lower rates, roughly 2.46 cm year^{-1} (Silva et al., in review). Observations demonstrate that density currents can transfer to the canyon-lobe systems a significant proportion of the sediment input, generating distal sediment accumulation areas. Lake Geneva has a surface area of roughly 580 km^2, and with almost 90 km^3 of water volume, it represents the largest freshwater reservoir in Western Europe. The lake represents an important sediment archive, which records the history of sediment production and paleofloods in the upstream basin. Climatic, hydrological, glacial and geological events can be reconstructed by analyzing the sediment stored in the lake, through bathymetric and seismic surveys, and sedimentological, granulometric, mineralogical and isotopic analyses.

Anthropogenic activities

The upper Rhône basin has been subject to intense anthropogenic influence during the

Anthropocene. Two major interventions of channelization (1^{st} and 2^{nd} Rhône correction projects) took place in 1863-1894 and 1930-1960 for flood protection purposes. River straightening reduced the length of the upper Rhône River from 414 to 251 km, leading to dramatic changes in the riverine ecosystem (Weber et al., 2007). Over fifty sediment mining activities operate in the catchment. The volume of fluvial sediments extracted from the study area is estimated to be between 0.5 and 1.7 x 10^9 kg year^{-1} (Kündig et al., 1997; Stutenbecker et al., 2017).

The upper Rhône basin represents one of the most important regions in Switzerland for hydroelectric energy production. Since 1960s several large dams have been constructed in the catchment. The total storage capacity equals to almost 1.35 km^3 (Fig. 1.4a), and corresponds to about 20% of the total annual volume of water flowing into Lake Geneva from the Rhône River (Loizeau and Dominik, 2000). Besides reservoirs, many water abstraction facilities are active in the catchment: water uptakes, return points and tunnels are part of a complex hydropower scheme (Fig. 1.5). Water from headwater streams is collected at water intakes and transferred to reservoirs (Bakker et al., 2018).

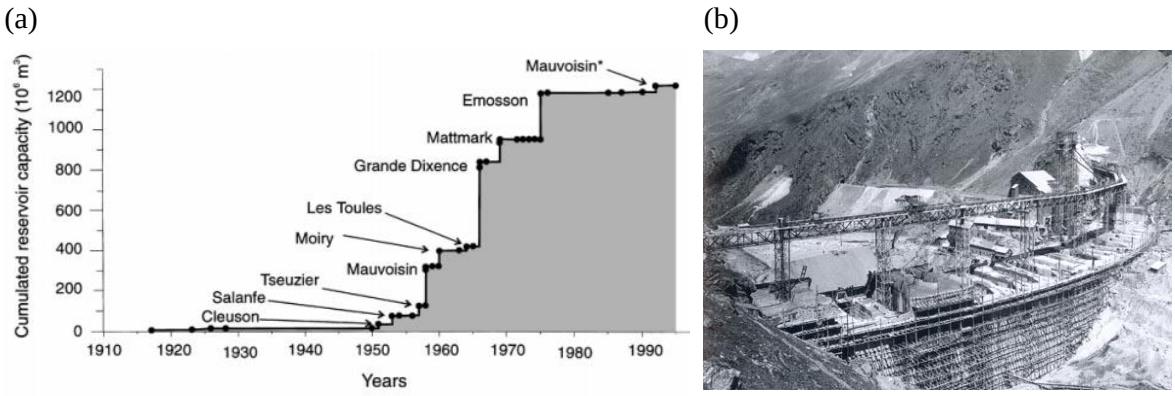

Figure 1.4: (*a*) Evolution of the total capacity of hydropower reservoirs in the upper Rhône basin. From Loizeau and Dominik (2000). (*b*) Construction of the Grande Dixence dam (1951). From HYDROWEB ©2007 v4.2.

Among the major reservoirs of the upper Rhône basin is the Lac de Dix, which has a storage capacity of 400 $106m^3$. The Lac de Dix is part of the Grand Dixence hydropower scheme, constructed in the late 1950s (Fig. 1.3b), which collects water from the headwaters of two tributaries, the Vispa and the Borgne via 75 flow intakes and produces approximately 2 billion kWh of power per year, which corresponds to roughly 20% of Switzerland's energy storage capacity (Bakker et al., 2018).

In summer, water is impounded and reservoirs are filled, while in winter, water is released to produce hydroelectric energy. Consequently, along channels, summer discharge is gen-

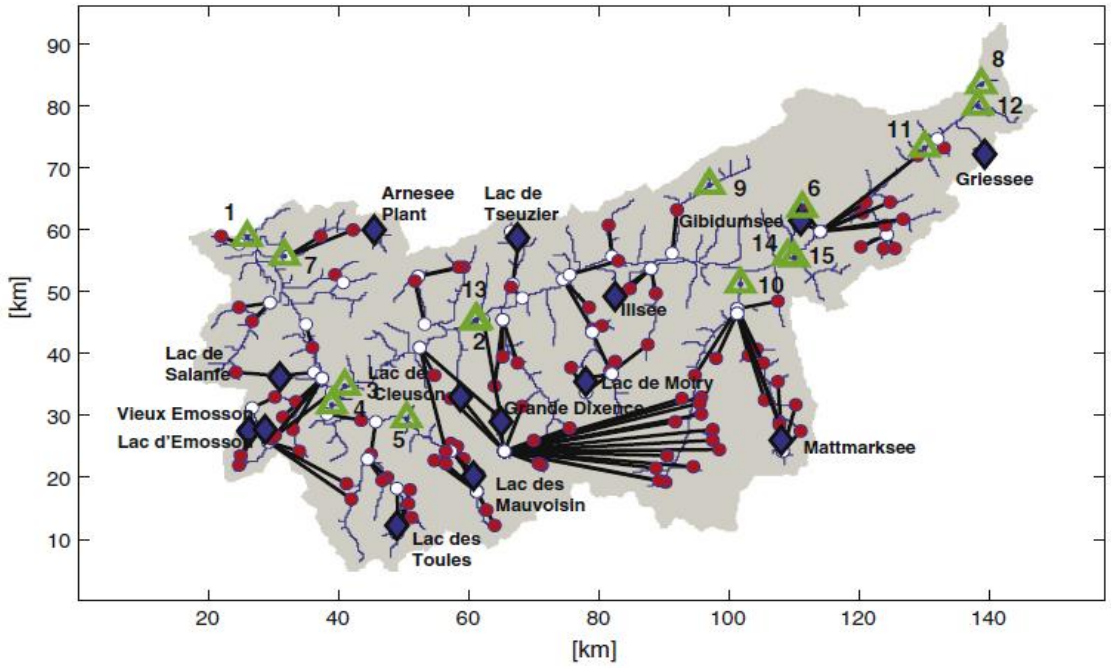

Figure 1.5: Representation of the hydropower scheme operating in the upper Rhône basin. The 14 major reservoirs are represented with blue diamonds and names. Water diversions are represented with black lines, uptake points with red dots, and return points with white dots. Green triangles and numbers indicate the 15 stream gauges managed by the Swiss Federal Office of the Environment. From Fatichi et al. (2015).

erally decreased and winter discharge increased, compared to natural flow conditions, as is typical in all Alpine hydropower systems. However, the effects of flow regulation on streamflow in the Rhône River network vary significantly in space, and river reaches downstream of water abstraction schemes can experience discharge reduction up to 85-90% (Bakker et al., 2018; Fatichi et al., 2015), while others are unaffected. It is clear that hydropower infrastructure must have substantially affected the sediment regime of the upper Rhône basin. In 1997, Loizeau et al. estimated sediment accumulation rates at the Lake Geneva for the periods 1943-1961 and after 1961, by analyzing more than 80 sediment cores collected at the delta of the upper Rhône River. They revealed a substantial decrease in sedimentation rates after 1961 (Fig. 1.6), which they attributed to sediment storage upstream of hydropower barrages (Loizeau et al., 1997). Loizeau and Dominik (2000) estimated daily suspended sediment load entering Lake Geneva based on a rating curve approach, where the coefficients of the rating curve were derived from few sediment samples collected before hydropower was active in the basin. Based on their estimation, they proposed that, due to the reduced summer discharge and increased winter discharge

induced by hydropower operations, a two-fold reduction in annual suspended sediment load is expected (Loizeau et al., 2000).

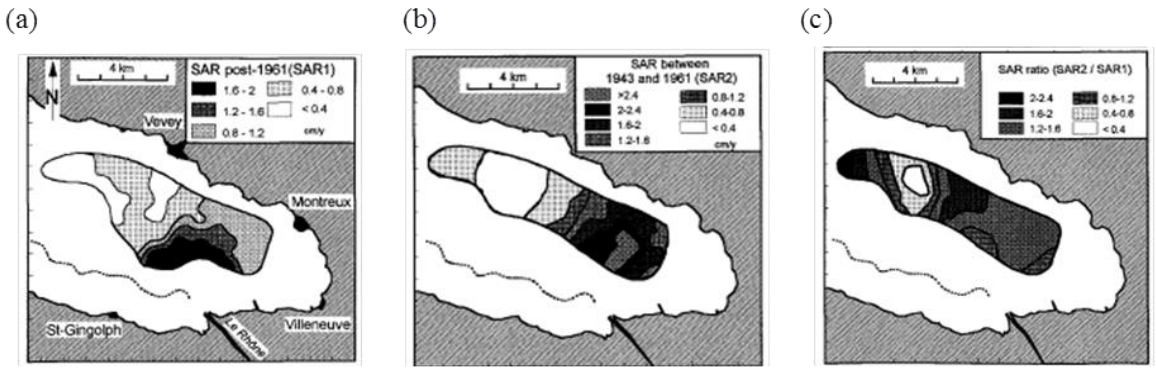

Figure 1.6: Maps of sediment accumulation rates at the delta of the upper Rhône River (Lake Geneva) calculated after 1961, SAR1 (a), between 1943-1961, SAR 2 (b), and ratio between SAR2 and SAR1. From Loizeau et al. (1997).

1.5 Objectives and research questions

This thesis is part of the "Sinergia" project *SedFate*: *Sediment fate in a changing watershed during the Anthropocene* funded by the Swiss National Science Fundation. The main objectives of the project are (1) *to quantitatively explore erosion and sediment transfer in the upper Rhône basin* and (2) *to disentangle the impacts of climatic, geologic, geomorphic and anthropogenic factors on sediment dynamics during the last 100 years.*

This thesis describes the research in which the objective was to *investigate basin-wide sediment dynamics and understand the impacts of hydroclimatic forcing and hydropower within a modelling framework.*

The main research questions addressed in this thesis are:

- Have hydroclimatic conditions changed in the upper Rhône basin in the recent past (40-50 years)? Are these changes reflected on the sediment regime of the catchment? The literature review suggested that fine sediment is a major contributor to total load and Lake Geneva input, at the same time it should not be blocked strongly by hydropower reservoirs. Knowing that the recent period has experienced climate warming, is there statistical evidence of observable changes in sediment concentrations and do these occur in conjunction with changes in hydroclimatology?

- Which are the main hydroclimatic factors controlling sediment fluxes in Alpine environments? The literature review suggested that sediment sources need to be included in predictions of sediment fluxes at the basin scale. Is it possible to separate the effects of different hydroclimatic forcing (rain, snow, icemelt) on fine sediment fluxes and how does this compare with hydropower effects?

- What are the main impacts of hydropower on basin-scale sediment dynamics of Alpine catchments? How does hydropower affect bedload transport at the river network scale? The literature review suggested that a river network perspective needs to be included in particular for coarse sediment load which is affected by flow regulation and can be trapped in hydropower reservoirs. Can we quantify and map the effects of such processes on bedload fluxes and analyse pre- and post-dam scenarios?

The content of this thesis is divided into five chapters. The first chapter outlined the overall motivation of investigating erosion and sediment transport in regulated conditions in Alpine regions, introduced the scientific background, the study site and highlighted the objective and the research questions addressed.

Chapter 2 presents a statistical analysis applied to the time series of suspended sediment concentration and hydroclimatic variables such as discharge, rainfall, ice melt, snowmelt and snow cover, to identify significant changes in the last 40-years in the Rhône Basin. Ice melt, snowmelt and snow cover dynamics are modelled with spatially distributed degree day models calibrated on snow cover maps and discharge from glacierized tributary catchments. The casual link between changes in hydroclimate and changes in suspended sediment concentration is investigated in a conceptual framework which includes the spatial and temporal variability of sediment sources in the catchment and their hydroclimatic activation. This chapter was accepted for publication as: *Costa, A., Molnar, P., Stutenbecker, L., Bakker, M., Silva, T. A., Schlunegger, F., Lane, S. N., Loizeau, J.-L., and Girardclos, S. (2018). Temperature signal in suspended sediment export from an Alpine catchment. Hydrology and Earth System Sciences, 22, 509-528. https://doi.org/10.5194/hess-22-509-2018.*

Chapter 3 investigates the control of hydroclimatic forcing and hydropower on suspended sediment dynamics of the upper Rhône basin. Erosive rainfall, ice melt and snowmelt, modelled as described in chapter 2, together with hydropower releases, modelled with a conceptual approach based on a unique virtual reservoir and target volume functions for water releases, are analyzed. The predictive power of hydroclimatic variables for suspended sediment concentration and their relative contribution to suspended sediment yield are estimated. For this purpose an objective input variable selection algorithm is applied and a multivariate rating curve based on hydroclimatic forcing is calibrated. This chapter

was accepted as a discussion paper and is under review as: *Costa, A., Anghileri, D., and Molnar, P. (2018b). Hydroclimatic control on suspended sediment dynamics of a regulated Alpine catchment: a conceptual approach, Hydrology and Earth System Sciences Discussion. https://doi.org/10.5194/hess-2018-5, in review.*

Chapter 4 presents a new river network bedload model developed in this thesis to simulate bedload transport rates at the river network scale, given the geometric characteristic of the channels and discharge. The model is used to quantify the impacts of hydropower operation on bedload transport rates, channel bed grain size distributions, and spatial erosional and depositional patterns. Discharge is simulated with the spatially-distributed, physically-based hydrological model Topkapi-ETH (Fatichi et al., 2015) both in natural conditions and with hydropower. The chapter contains a detailed description of the model and the results of the simulations for the scenarios before and the after the construction of the reservoirs, and also hypothetical climate change (warming) scenarios. This chapter was submitted to Water Resources Research as: *Costa, A., Molnar P., Schmitt, R. J. P., and Burlando P. (2018). Flow Regulation in Alpine Rivers: a Network-Based Model to Investigate the Impacts on Bedload and Grain Size Distribution.*

The main concluding remarks linked to the results of the individual papers and an outlook of possible future research lines are discussed in the final Chapter 5.

Chapter 2

Temperature signal in suspended sediment export from an Alpine catchment*

** Costa A, Molnar P, Stutenbecker L, Bakker M, Silva TA, Schlunegger F, Lane SN, Loizeau JL and Girardclos S (2018) Temperature signal in suspended sediment export from an Alpine catchment. Hydrology and Earth System Sciences*

Figure 2.1: View of the Matterhorn Mountain in the upper Rhône Basin (by T. Mastrotheodoris).

Abstract

Suspended sediment export from large Alpine catchments (> 1 000 km^2) over decadal timescales is sensitive to a number of factors, including long-term variations in climate, the activation-deactivation of different sediment sources (proglacial areas, hillslopes, etc.), transport through the fluvial system, and potential anthropogenic impacts on the sediment flux (e.g. through impoundments and flow regulation). Here, we report on a marked increase in suspended sediment concentrations observed near the outlet of the upper Rhône River Basin in the mid-1980s. This increase coincides with a statistically significant step-like increase in basin-wide mean air temperature. We explore the possible explanations of the suspended sediment rise in terms of changes in water discharge (transport capacity), and the activation of different potential sources of fine sediment (sediment supply) in the catchment by hydroclimatic forcing. Time series of precipitation and temperature-driven snowmelt, snow cover and icemelt simulated with a spatially distributed degree-day model, together with erosive rainfall on snow-free surfaces, are tested to explore possible reasons for the rise in suspended sediment concentration. We show that the abrupt change in air temperature reduced snow cover and the contribution of snowmelt, and enhanced ice-melt. The results of statistical tests show that the onset of increased icemelt was likely to play a dominant role in the suspended sediment concentration rise in the mid-1980s. Temperature-driven enhanced melting of glaciers, which cover about 10% of the catchment surface, can increase suspended sediment yields through increased contribution of sediment-rich glacial meltwater, increased sediment availability due to glacier recession, and increased runoff from sediment-rich proglacial areas. The reduced extent and duration of snow cover in the catchment are also potential contributors to the rise in suspended sediment concentration through hillslope erosion by rainfall on snow-free surfaces, and increased meltwater production on snow-free glacier surfaces. Despite the rise in air temperature, changes in mean discharge in the mid-1980s were not statistically significant, and their interpretation is complicated by hydropower reservoir management and the flushing operations at intakes. Overall, the results show that to explain changes in suspended sediment transport from large Alpine catchments it is necessary to include an understanding of the multitude of sediment sources involved together with the hydroclimatic conditioning of their activation (e.g. changes in precipitation, runoff, air temperature). In addition, this study points out that climate signals in suspended sediment dynamics may be visible even in highly regulated and human impacted systems. This is particularly relevant for quantifying climate change and hydropower impacts on streamflow and sediment budgets in Alpine catchments.

2.1 Introduction

Erosion processes and sediment dynamics in Alpine catchments are determined by geological, climatic and anthropogenic, factors. Geological forcing is one of the main drivers of sediment production and landscape development, through crustal thickening, deformation and isostatic uplift, and glacier inheritance (e.g. England and Molnar, 1990; Schlunegger and Hinderer, 2001; Vernon et al., 2008). Glacier inheritance influences sediment production and transport as demonstrated by a strong spatial association between sediment yield and past and current glacial cover (Hinderer et al., 2013; Delunel et al., 2014). Almost continuous temperature-driven glacier recession in the European Alps since the late 19th Century (Paul, 2004; 2007; Haeberli, 2007) has maintained large parts of the landscape in early stages of the paraglacial phase where unstable or metastable sediment sources (Ballantyne, 2002; Hornung et al., 2010) can maintain high sediment supply rates. Anthropogenic impacts on sediment yields are more recent, and on a global scale largely related to land cover change through intensified agriculture and the trapping of sediment in reservoirs (e.g. Syvitski et al., 2005). Land use changes impact mainly fine sediment production (e.g. Foster et al. 2003; Wick et al., 2003), while river channelization, flow regulation, water abstraction, and sediment extraction have caused a general reduction in sediment yield and consequently led to sediment-starved rivers world-wide (Kondolf et al., 2014). In Alpine catchments, in addition to trapping in reservoirs, sediment transfer is also disturbed by flow abstraction at hydropower intakes. The reduction of sediment transport capacity downstream of intakes and the periodic flushing of locally trapped sediment has severe impacts on the sediment budget (e.g. Anselmetti et al., 2007) and downstream river ecology (e.g. Gabbud and Lane, 2016).

Here we focus on the dominant role of climate in sediment production and transfer in Alpine environments (e.g. Huggel et al., 2012; Zerathe et al., 2014; Micheletti et al., 2015; Palazon and Navas, 2016; Wood et al., 2016). The premise behind this work is that to explain impacts of changes in climate on Alpine catchment suspended sediment yield, it is necessary to consider both transport capacity and sediment supply. Sediment supply depends on many factors, most importantly the spatial location of sediment sources (e.g. lithology, distance to outlet, connectivity) and the specific processes of sediment production (e.g. hillslope erosion, glacial erosion, release of subglacially stored sediment, channel bed and bank erosion, mass wasting events) and transport (e.g., hysteresis).

In this study we look at specific sediment sources and the hydroclimatic conditioning of their activation (e.g. precipitation, runoff and air temperature) with a process-based perspective with the aim to infer the possible effects of changes in hydroclimate, such as increases in temperature and/or precipitation intensity, on suspended sediment dynamics.

We identify four main sediment sources typical of Alpine environments: glacial erosion, hillslope erosion, channel bed/bank erosion and mass wasting events (e.g. rockfalls, debris flows). Climatic conditions, specifically precipitation and air temperature, contribute to the activation of these four sediment sources through different processes and at different rates. Erosive processes of abrasion, bed-rock fracturing and plucking at the base of glaciers provide proglacial areas with large amounts of sediment (Boulton, 1974). Due to glacial erosion, discharge from subglacial channels has high suspended sediment concentrations (e.g. Aas and Bogen, 1988). Temperature-driven snow and icemelt in spring and summer, as well as intense rainfall on snow-free surfaces, may lead to entrainment from proglacial areas provided they are connected to the river network (Lane et al., 2017). Hillslope erosion driven by overland flow and rainfall erosivity may be exacerbated in Alpine catchments by permanently or partially frozen ground (Quinton and Carey, 2008). In summer and autumn, when Alpine catchments are largely free of snow, intense rainfall may erode large amounts of sediment and transport it in rills and gullies to the river network. Intense rainfall is also responsible for triggering mass wasting events, such as debris flows and landslides, where a large mass of sediment is delivered to the channel network instantaneously (e.g. Bennett et al., 2012). Flow conditions (e.g. shear stress, stream power) then determine the sediment transport capacity and in-stream sediment mobilization along rivers, and hence its transfer to downstream locations.

The close link between precipitation, air temperature, runoff and the activation-deactivation of sediment sources in Alpine catchments becomes critical in the context of climate change. Alpine regions represent a sensitive environment in relation to current rapid warming. In Switzerland, together with glacier recession, a reduction in snow cover duration and mean snow depth has been observed during the last thirty years (e.g. Beniston, 1997; Laternser and Schneebeli, 2003; Scherrer et al., 2004; Marty, 2008; Scherrer et al., 2006). Although current effects of climate change are less clear for precipitation (Brönnimann et al., 2014) than for temperature, a sharp reduction in the number of snowfall days has been observed at many meteorological stations in Switzerland (Serquet et al. 2011).

The upper Rhône River Basin draining into Lake Geneva in Switzerland is at the center of our investigation. The basin has experienced a rise in air temperature that coincided with a rise in suspended sediment concentrations in the mid-1980s. Our main objective is to explore the presence of the signal of a warmer climate in the suspended sediment dynamics of this regulated and human-impacted Alpine catchment. In this work, we refer to fine sediment as the sediment transported in suspension. To investigate the potential causes of the observed increase in suspended sediment concentration, we conceptualize the upper Rhône Basin as a series of spatially distributed sediment sources that are activated or deactivated by hydroclimatic forcing. In addition to discharge (transport

capacity), we consider four main hydroclimatic variables: (a) icemelt runoff (IM) which evacuates accumulated fine sediment, the product of glacial erosion, through subglacial channels (e.g. Swift et al., 2005); (b) snow cover fraction (SCF) which influences icemelting onset, impacts icemelt efficiency through albedo and may result in more rapid erosion and sediment production through an increased glacier basal velocity (e.g. Herman et al., 2015); (c) snowmelt runoff (SM) from snow-covered areas which may generate downstream hillslope erosion and channel erosion (e.g. Lenzi et al., 2003); and (d) effective rainfall (ER), defined as liquid precipitation over snow-free areas, which lead to hillslope erosion, mass wasting and, due to enhanced discharge, also channel erosion (e.g. Bennet et al., 2012; Meusburger and Alewell, 2014). Our aims are: (a) to estimate daily basin-wide icemelt, snow cover fraction, snowmelt and effective rainfall over the Rhône Basin for the last 40 years; and (b) to analyze these variables with the goal to provide statistical evidence for possible reasons for the rise in suspended sediment concentrations in the mid-1980s.

2.2 Study Site Description

The upper Rhône Basin is located in the southwestern part of Switzerland, in the Central Swiss Alps (Fig. 2.2). It has a total surface area of 5 338 km^2, and an altitudinal range of 372 to 4 634 m a.s.l. About 10% of the surface is covered by glaciers, which are mostly located in the eastern and southeastern part of the catchment (Stutenbecker et al., 2016). The Rhône River originates at the Rhône Glacier and flows for about 160 km through the Rhône valley before entering Lake Geneva, a few kilometers downstream of the gauging station located at la Porte-du-Scex (Fig. 2.2). Basin-wide mean annual precipitation is about 1 400 mm year^{-1} and shows strong spatial variability driven mostly by orography and the orientation of the main valley. The hydrological regime of the catchment, typical of Alpine environments, is strongly influenced by snow and icemelt with highest discharge in summer and lowest in winter. Mean annual discharge is 180 m^3 s^{-1}, which corresponds to about 1 060 mm year^{-1} and an annual runoff coefficient of 75%.

The catchment has been strongly affected by anthropogenic impacts during the last century. The main course of the Rhône River has been extensively channelized for the purposes of flood protection: levees were constructed and the channel was narrowed and deepened in the periods 1863-1894 and 1930-1960 (First and Second Rhône Corrections). Due to the residual flood risk that affects the main valley, a third project was started in 2009 with the main objectives to increase channel conveyance capacity and river ecological rehabilitation (Oliver et al., 2009). In addition, significant gravel mining operations are

carried out along the main channel and many tributaries. Since the 1960s, several large hydropower dams have been built in the main tributaries of the Rhône River. The total storage capacity of these reservoirs corresponds to about 20% of the mean annual streamflow (Loizeau and Dominik, 2000). Flow impoundment, water abstraction and diversion through complex networks of intakes, tunnels and pumping stations, have significantly impacted the flow and sediment regime of the catchment. Flow regulation due to hydropower production has resulted in a considerable decrease of discharge in summer and increase in winter (Loizeau and Dominik, 2000). That said, the construction of dams and start of hydropower operation has coincided with a drop in the suspended sediment load of the main Rhône River measured at la Porte-du-Scex in the 1960s (Loizeau et al., 1997; Loizeau and Dominik, 2000).

Two sub-catchments of the Upper Rhône basin are used for the calibration/validation of the icemelt model: the Massa and the Lonza (Fig. 2.2). The Massa is a medium-sized basin (195 km^2) with a mean elevation of 2 945 m a.s.l. More than 60% of the surface is glacierized, and the remaining surface is classified mostly as rock and firn (Boscarello et al., 2014). The basin includes the Aletsch Glacier, which is the largest glacier in the European Alps with a length (1973) of around 23.2 km and a surface area (1973) of approximately 86 km^2 (Haeberli and Holzhauser, 2003). The Lonza is a relatively small basin located to the west of the Massa with an average elevation of 2 630 m a.s.l. It has a total drainage area of roughly 77.8 km^2 and almost 36% of its surface (1991) is covered by glaciers.

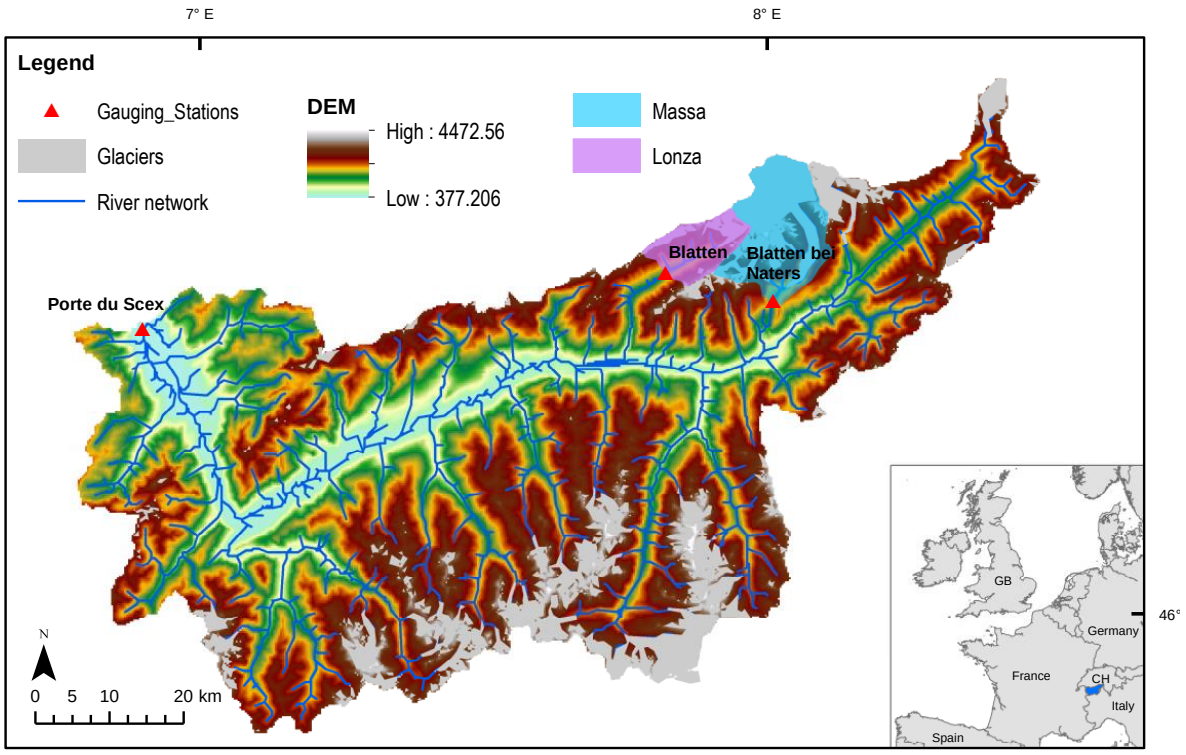

Figure 2.2: Map of the upper Rhône Basin with topography, glacierized areas and river network. Inset shows the position of the upper Rhône Basin in Europe (blue). Locations of gauging stations used in this analysis are shown as triangles. Massa and Lonza sub-basins used in the calibration and validation of the ice melting component are highlighted.

2.3 Methods

Our objective is to explore the potential effect of climate on suspended sediment dynamics of the upper Rhône Basin in the period 1975-2015. To this end, we analyze observed and simulated hydroclimatic and sediment transport variables, as listed in Table 2.1: mean daily temperature T, total daily precipitation P, mean daily discharge Q, suspended sediment concentration SSC, daily snow cover fraction SCF, snowmelt SM, icemelt IM, and effective rainfall over snow-free areas (ER). Some variables originate from observations (Q, SSC) or spatial interpolation of observations (T, P), others from simulations by spatially distributed snow and icemelt models (SCF, SM, IM), or from a combination thereof (ER). The snowmelt model is described in Sect. 2.3.1, the icemelt model in Sect. 2.3.2, and their calibration in Sect. 2.3.3. We first interpolate the input datasets of precipitation and temperature on a 250x250 m grid resolution by the nearest-neighbor interpolation method. Second we run the snow and icemelt model at the daily timescale over the period 1975-2015. In a third step, we analyze the variables (Table 2.1) as mean monthly and mean annual values averaged over the basin area. To quantify changes in the hydroclimatic variables and in suspended sediment concentration, we apply standard statistical tests for change detection described in Sect. 2.3.4. A description of all datasets used in this analysis is reported in more details in Sect. 2.4.

2.3.1 Snowmelt Model

We use a snowmelt model to predict SM and SCF over the entire basin, because snow station measurements are sparsely and irregularly distributed and a physical consistency between precipitation and air temperature as climatic driving forces and snowmelt and snow cover as response variables are needed. The spatially distributed temperature index method (degree-day model) was used due to its simplicity, low data requirements, and demonstrated success at daily temporal scales over large basins (e.g. Hock, 2003; Boscarello et al., 2014). The degree-day approach also matches the coarse spatial (250x250 m) and temporal (daily) resolution of our analysis and the areal averaging at the basin scale. Models based on energy balance, or enhancements of the degree-day approach, represent physical processes better and could be used when higher spatial and temporal resolution and accuracy is needed (e.g. Pellicciotti et al., 2005).

The snowmelt model includes snow accumulation and melt. At the grid scale, precipitation P [mm day-1] is first partitioned into solid and liquid form based on (a) daily minimum T_{min} [°C] and maximum air temperature T_{max} [°C] and (b) a rain-snow threshold temperature T_{RS} [°C]. If minimum air temperature T_{min} is above the threshold temperature

Table 2.1: List of the variables analysed: observed SSC, and hydroclimatic variables originating from measurements (Q) or spatial interpolation of measurements (T, P), from simulations of the snow and icemelt model (SCF, SM, IM), or a combination thereof (ER). Information on the source and the spatial and temporal resolution are reported for each variable.

Variable	Data Source	Resolution
T	Daily mean temperature [° C] on a ∼2x2 km grid provided by MeteoSwiss	basin-averaged, daily, 1975-2015
P	Daily total precipitation [mm day^{-1}] on a ∼2x2 km grid provided by MeteoSwiss	basin-averaged, daily 1975-2015
Q	Daily mean discharge [m^3 s^{-1}] at three stations (Porte du Scex, Blatten, Blatten bei Naters) provided by FOEN	daily, 1975-2015
SSC	Suspended sediment concentration [mg l^{-1}] at la Porte du Scex provided by FOEN	2 times per week, 1975-2012
SCF	Snow cover fraction [0-1] simulated by the Snowmelt Model on a 250x250 m grid, and calibrated with MODIS satellite data for the period 2000-2009	basin-averaged, daily, 1975-2015
SM	Snowmelt rate [mm day^{-1}] simulated by the Snowmelt model on a 250x250 m grid	basin-averaged, daily, 1975-2015
IM	Icemelt rate [mm day^{-1}] simulated by the Icemelt model on a 250x250 m grid, and calibrated at Blatten and Blatten bei Naters	basin-averaged, daily, 1975-2015
ER	Effective rainfall [mm day^{-1}] (rainfall on snow-free pixels), estimated from P, T and SCF on a 250x250 m grid	basin-averaged, daily, 1975-2015

T_{RS}, all precipitation falls as rainfall R; if the maximum air temperature T_{max} is below the threshold temperature T_{RS}, all precipitation falls as snow S; otherwise precipitation is a mixture of liquid and solid form, partitioned proportionally to the temperature difference:

$$\begin{cases} R = c_p P \\ S = (1 - c_p) P' \,, \end{cases} \tag{2.1}$$

where

$$\begin{cases} c_p = 1 & T_{min} > T_{RS} \\ c_p = 0 & T_{max} \leq T_{RS} \\ c_p = \frac{T_{max} - T_{RS}}{T_{max} - T_{min}} & T_{min} \leq T_{RS} < T_{max} \end{cases}, \tag{2.2}$$

The daily snowmelt rate $SM_i[mmday^{-1}]$ is estimated from a linear relation with air temperature:

$$\begin{cases} SM_i = k_{snow}(T_{mean} - T_{SM}) & T_{mean} > T_{SM} \\ SM_i = 0 & T_{mean} \leq T_{SM} \,, \end{cases} \tag{2.3}$$

where T_{mean} [°C] is the mean daily air temperature, T_{SM} [°C] is a threshold temperature for the onset of melt, and k_{snow} is a melt factor [mm day^{-1} °C^{-1}]. Snow depth (SD), in mm snow water equivalent, for time t is then simulated from a balance between accumulation and melt at every grid cell i:

$$SD_i(t) = SD_i(t-1) + S_i(t) - SM_i(t) \,. \tag{2.4}$$

The snow cover fraction SCF for a chosen area containing i = 1,..., N grids, is:

$$SCF(t) = \frac{1}{N} \sum_{i=1}^{N} H[SD_i(t)] \tag{2.5}$$

where H is a unit step function: H=0 when SD=0 and H=1 when SD>0. The area of integration N can be the entire catchment, sub-basins, elevation bands, etc. For the entire catchment, we estimate mean daily snowmelt SM [mm day^{-1}] as the arithmetic average over all grid melt rates:

$$SM(t) = \frac{1}{N}\sum_{i=1}^{N} SM_i(t)\ . \tag{2.6}$$

The threshold temperatures for defining the precipitation type T_{RS} and the onset of melt T_{SM} depend on many factors such as atmospheric boundary layer conditions, temperature, humidity, among others. Different parametrizations and temperature values are available in the literature (Wen et al., 2013). Depending on region, altitude and modelling approach, rain-snow temperature thresholds show a range of variability from -5 °C (Collins et al., 2004) to more than 6 °C (Auer, 1974). For the upper Rhône Basin we assume a constant rain-snow temperature threshold T_{RS}=1°C, resulting from a calibration and validation of the physically-based fully distributed hydrological model Topkapi-ETH in the catchment (Fatichi et al., 2015). To reduce degrees of freedom, the threshold temperature for the onset of melt T_{SM} is set equal to 0°C, which is a typical value for Alpine regions (e.g. Schaefli et al. 2005; Corbari et al., 2009; Boscarello et al., 2014). The calibration of the snowmelt model consists of estimating only the melt factor k_{snow} with methods described in Sect. 2.3.3. In addition, we apply a sensitivity analysis on the three parameters k_{snow}, T_{RS}, T_{SM}, as described in the Supplementary Material, Sect. 2.8.

2.3.2 Icemelt Model

Similar to snowmelt, icemelt is also simulated with a temperature index (degree-day) model on grid cells that are identified as glacier-covered. The daily icemelt IM_i [mm day^{-1}] on glacier surfaces that are snow-free is estimated as:

$$\begin{cases} IM_i = k_{ice}(T_{mean} - T_{IM}) & T_{mean} > T_{SM} \\ IM_i = 0 & T_{mean} \leq T_{IM}\ , \end{cases} \tag{2.7}$$

where T_{mean} [°C] is mean daily air temperature, T_{IM} [°C] is a threshold temperature for the onset of icemelt, and k_{ice} [mm day^{-1} °C^{-1}] is the icemelt factor. For the entire catchment, we estimate mean daily icemelt IM [mm day^{-1}] as the arithmetic average over all ice-covered grid cells:

$$IM(t) = \frac{1}{N}\sum_{i=1}^{N} IM_i(t)\ . \tag{2.8}$$

The threshold temperature for glacier melting T_{IM} is set equal to 0°C. Icemelt occurs only if the glacier cell is snow-free. The snow cover simulated by the snowmelt model in

Sect. 2.3.1 is thus essential for estimating icemelt. The calibration of the icemelt model consists of estimating only the melt factor k_{ice} as described in Sect. 2.3.3.

2.3.3 Calibration and Validation of Snowmelt and Icemelt Model

We perform the calibration and validation of the snow and icemelt model parameters in sequence, since the snow-covered surface is required for icemelt estimation on glaciers. The snowmelt factor k_{snow} is calibrated based on comparisons with snow cover maps. Snow cover observations are split into two periods: 1 October 2000 - 30 September 2005 for calibration and 1 October 2005 - 31 December 2008 for validation, for a total number of 217 calibration and 143 validation days. Snow cover maps at 500x500 m resolution are distributed by proximal interpolation to the snowmelt model 250x250m computational grid. Maps of snow depth simulated with Eq. 2.4 are first transformed into simulated snow cover fraction SCF^{sim} with Eq. 2.5 and are afterwards compared with snow cover fraction SCF^{obs} derived from the observations. The objective function for calibration is based on a combination of mean absolute error and true skill statistic. The mean absolute error MAE is estimated as:

$$MAE(t) = \frac{1}{n}\sum_{j=1}^{n}|SCF_j^{obs} - SCF_j^{sim}|\,, \tag{2.9}$$

where n is the number of MODIS image maps. MAE captures the overall ability of the model to reproduce the snow cover fraction accurately. The true skill statistic TSS is a spatial statistic that measures the grid-to-grid performance of the model in capturing snow-no snow presence. It is computed as the sum of sensitivity SE (correct snow predictions) and specificity SP (correct no-snow predictions) computed from contingency tables (e.g. Wilks, 1995; Mason and Graham, 1999; Corbari, 2009) in each image j and averaged over the n MODIS maps in the simulation period:

$$TSS = \frac{1}{n}\sum_{j=1}^{n}TSS_j = \frac{1}{n}\sum_{j=1}^{n}(SE_j + SP_j - 1)\,. \tag{2.10}$$

Because TSS includes both sensitivity and specificity, it captures both predictions of snow-covered and snow-free areas. It takes on values between 0 and 1, where 0 indicates a random model with SE = 1 - SP, and 1 indicates perfect performance. TSS is a widely applied metric for assessing spatial model performance (e.g. Begueria, 2006; Allouche et al., 2006). We combine both goodness-of-fit measures (MAE and TSS) into an objective function OF, by giving more weight to MAE. Finally, we evaluate the objective function

OF over b=5 different elevation bands in order to better capture the topographic gradients in snowmelt distribution in the Rhône Basin:

$$OF = \sum_{b=1}^{5} OF_b = \sum_{b=1}^{5} -0.6MAE_b + 0.4TSS_b \,. \tag{2.11}$$

This objective function is maximized in calibration. The rationale of using both MAE and TSS in evaluating performance is to give weight to both basin-integrated snow cover as well as to grid-based predictions. Indeed, the same value of snow cover fraction can result in two different spatial arrangements of snow-covered pixels, and a correct spatial distribution of snow-covered and snow-free areas is relevant for this analysis insofar as it affects the activation and deactivation of specific sediment sources. The weights assigned to MAE and TSS in Eq. 2.11 are the outcome of sensitivity tests with the model. After calibration, we also estimate the Nash-Sutcliffe efficiency NS (Nash and Sutcliffe, 1970) and the mean square error MSE to quantify the performance of the model:

$$NS = 1 - \frac{\sum_{j=1}^{n}(SCF_j^{obs} - SCF_j^{sim})^2}{\sum_{j=1}^{n}(SCF_j^{obs} - \overline{SCF})^2} \,, \tag{2.12}$$

$$MSE = \frac{1}{n}\sum_{j=1}^{n}(SCF_j^{obs} - SCF_j^{sim})^2 \,, \tag{2.13}$$

where $\overline{SCF}$ is the average observed snow cover fraction during the calibration-validation period. We calibrate the icemelt factor k_{ice} on the sub-basin of the river Massa (Fig. 2.2), on the basis of daily discharge measurements, and focusing only on months when the icemelt contribution is not negligible (June-October). The gauging station is located upstream of the Gebidem dam, therefore discharge is not influenced by reservoir regulation and represents undisturbed natural flow. Calibration is performed on the period 1 January 1975 - 31 December 2005, while validation covers the remaining ten years of available data, i.e. the period 1 January 2006 - 31 December 2015. We then validate the model on the Lonza sub-basin with the same procedures and goodness of fit measures. The optimal value of k_{ice} is found by minimizing the mass balance error MBE_s computed for the period June-October:

$$MBE_s = 100\frac{\sum_{i=1}^{ny}(V_i^{obs} - V_i^{sim})}{\sum_{i=1}^{ny} V_i^{obs}} \,, \tag{2.14}$$

where ny is the number of calibration years, V_i^{obs} and V_i^{sim} [mm year^{-1}] are the observed and simulated discharge volumes per unit area reaching the outlet of the catchment during the period June-October of each calibration year i:

$$V^{obs} = \sum_{j=1}^{nd} Q_i^{obs} \,, \tag{2.15}$$

$$V^{sim} = \sum_{j=1}^{nd} Q_i^{sim} = \sum_{j=1}^{nd} (R_j + SM_j + IM_j) \,. \tag{2.16}$$

Here, nd is the number of observation days from June to October, Q_j^{obs} [mm day^{-1}] is the daily discharge per unit area observed at Blatten bei Naters (Blatten), R_j, SM_j, IM_j are respectively the total daily rainfall, snowmelt and icemelt aggregated over the Massa (Lonza) basin. Rainfall (R) and snowmelt (SM) are simulated with the snow accumulation and melt model in Sect. 2.3.1, while icemelt (IM) is simulated with the icemelt model in Sect. 2.3.2.

It should be noted that in this study we do not consider glacier evolution, i.e. changes in ice thickness due to accumulation and melt, as well as glacier ice flow. Neglecting glacier retreat rises the possibility that we overestimate the icemelt contribution over the study period. To quantify the potential effect of glacier retreat, we compare our simulations with time series produced from the Global Glacier Evolution Model (GloGEM), a model accounting for both the mass balance and glacier evolution (Huss and Hock, 2015). For comparison, we use total monthly runoff generated from glacierized surfaces of the upper Rhône basin, simulated with GloGEM for the period 1980-2010. GloGEM computes the mass balance for every 10-m elevation band of each glacier, by estimating snow accumulation, snow and ice melt, and refreezing of rain and melt water. The response of glaciers to changes in mass balance is modelled on the basis of an empirical equation between ice thickness changes and normalized elevation range parametrized as proposed by Huss (2010). Normalized surface elevation changes δh_r are derived for each elevation band from mass balance changes (mass conservation). Starting from initial values derived by the method of Huss and Farinotti (2012), ice thickness is updated at the end of each hydrological year by applying the relation between normalized elevation range h_r and normalized surface elevation change δh_r. The area of each glacier is finally adjusted by a parabolic cross-sectional shape of the glacier bed (Huss and Hock, 2015). GloGEM is calibrated and validated over the period 1980-2010 with estimates of glacier mass changes by Gardner et al. (2013) and in situ measurements provided by the World Glacier Monitoring Service.

2.3.4 Statistical Testing for Change

We use the non-parametric Pettitt test (Pettitt, 1979) for the detection of the time of change (year-of-change) in the air temperature data. We then test the other variables (SSC, P, Q, SM, SCF, IM and ER) for changes in the mean (and variance) by splitting the time series into two periods before and after the identified year-of-change, and by applying two-sample two-sided t-tests for the equality of the means (and variances). The null hypothesis of no change is tested at the 5% significance level. The t-test is a parametric test commonly used in hydrology to assess the validity of the null hypothesis of two samples having equal means and unknown unequal variances. We apply the t-test to all hydroclimatic variables averaged at the annual and monthly timescales with the same year-of-change to determine which hydroclimatic variables, and therefore the activation or deactivation of which sediment sources, are possibly responsible for the observed changes in suspended sediment concentration.

In our catchment, SSC is sampled intermittently (twice per week). This might have an effect on the change detection analysis of the hydroclimatic variables. We estimate this potential effect by considering the hydroclimatic variables SM, IM, ER and Q only on days corresponding to SSC-measurement days. We compare these new time series with the original ones by estimating the cumulative distribution functions of the variables and by testing changes of mean monthly and annual values over time. We consider only the positive (non-zero) part of the distributions. Results are reported in Sect. 2.5.4.

2.4 Data Description

2.4.1 Precipitation and Air Temperature

For precipitation and air temperature we use spatially distributed datasets provided by the Swiss Federal Office of Meteorology and Climatology (MeteoSwiss). Total daily precipitation, mean, minimum and maximum daily air temperature are available on a $\sim$ 2x2 km resolution grid for Switzerland (MeteoSwiss, 2013). All four datasets are developed by spatial interpolation of quality-checked data collected at MeteoSwiss meteorological stations (Frei et al., 2006; Frei, 2014). We apply the statistical analysis of change to basin-averaged values of precipitation and temperature and not to individual grid point values, which might be potentially affected by substantial interpolation errors. Moreover, the variability in time of the number of stations involved in the spatial interpolation may induce non-homogeneities in the datasets. This is particularly relevant when analyzing

long-term changes as in the case of this study. Therefore, we verify the effects of potential non-homogeneities by using an experimental dataset developed by MeteoSwiss specifically for this research, based on a constant number of stations (294 for precipitation and 48 for temperature) for the period 1971-2013. We applied the statistical tests for detecting changes both on the original and the experimental datasets of P and T. Results of the statistical tests on the two datasets coincide. This confirms that temporally variable number of meteorological stations employed to build the product does not influence the changes detected in the original dataset.

2.4.2 Discharge and Suspended Sediment Concentration

We use daily discharge data measured by the Swiss Federal Office for the Environment (FOEN) at three gauging stations: la Porte-du-Scex (available since 1905), Blatten Bei Naters (available since 1931) and Blatten (available since 1956) (Fig. 2.2). For suspended sediment concentration, two in-stream samples per week collected by FOEN at la Porte-du-Scex are available since October 1964 (Grasso et al., 2012). In this work, we focus on sediment transported in suspension. Previous analysis on the grain size distribution of suspended sediment at the outlet of the upper Rhône River reports a bimodal distribution, with mode diameters equal to 13.7 μm (silt) for the finer fraction and 39.6 μm (silt) for the coarser grains (Santiago et al., 1992). The composition of grains cover a wide range of values, including clay (16.9%), silt (64.7%) and sand (18.4%). The mean suspended sediment size is reported to be equal to 17.7 μm (silt), and the largest grains transported in suspension during summer high flow conditions are in the range of coarse sand (>500 μm) (Santiago et al., 1992).

2.4.3 Snow Cover and Glacier Data

We use snow cover maps derived from satellite imagery for the upper Rhône Basin over the period 2000-2008 processed in previous research (Fatichi et al., 2015). We use the 8-day snow cover product MOD10A2 retrieved from the Moderate Resolution Imaging Spectroradiometer (MODIS) (Dedieu et al., 2010) for the calibration and validation of the snowmelt model. MOD10A2 is provided at a 500x500 m spatial resolution, where cells are classified as snow-covered, snow-free, inland water or cloud-covered. In order to reduce the impacts of clouds in estimating snow cover fraction, maps with cloud cover greater than 30% are excluded from the dataset, resulting in a total number of usable images equal to 360, i.e. on the average 40 days per year.

The surface covered by glaciers is assigned based on the GLIMS (Global Land Ice Measurements from Space) Glacier Database (Fig. 2.2). Ice-covered cells identified based on the GLIMS data of 1991 give more than 10% of the upper Rhône Basin as covered by ice with a total glacier surface of almost 620 km^2.

2.4.4 Digital Terrain Model

We use a digital terrain model (DTM) with 250x250 m resolution (85409 cells in total, Fig. 2.2), obtained by resampling a finer model (25x25 m) provided by SwissTopo in the ETH geodata portal (GeoVITe). The DTM is used as a mask for extracting climatic inputs and for elevation information in the snowmelt modelling.

2.5 Results

2.5.1 Calibration of Snowmelt and Icemelt Models

The snowmelt factor, calibrated following the procedure described in Sect. 2.3.3, is k_{snow}=3.6 mm day^{-1} $°C^{-1}$. The snowmelt model reproduces well the seasonal fluctuations of snow cover fraction (SCF) in the basin, with Nash-Sutcliffe efficiencies (NS) close to 0.90 and low mean square errors (MSE). The model maintains good performances also in the validation period showing slight reduction in the goodness of fit measures (Table 2.2). The temporal variability of SCF is also well simulated at the basin scale. Although the comparison between observed and simulated SCF is affected by the discontinuous nature of the MODIS data (8-day resolution), Fig. 2.3 shows that the model with a single constant k_{snow} for the entire catchment reproduces the snow cover dynamics reasonably well for all of the studied elevation bands. At lower elevations, the model tends to slightly underestimate SCF in autumn and overestimate it in winter. The model performs better at higher elevation bands, even at the very highest elevations with permanent snow cover (Fig. 2.3 bottom). The spatial distribution of snow cover is satisfactory, with average values of sensitivity and specificity greater than 0.7 (Table 2.2). Goodness of fit measures indicate that, on average, more than 70% of snow-covered and snow-free pixels are correctly identified. The true skill score, which combines both metrics, results in values around 0.5 (Table 2.2). Snow cover duration maps averaged over the period 2000-2008 for MODIS observations and simulations show a good spatial coherence (Fig. 2.4). In summary, we conclude that the snowmelt model represents the spatial and temporal dynamics of snow

cover in the Rhône Basin satisfactorily. Results of the sensitivity analysis on k_{snow}, T_{RS}, T_{SM} are reported in the Supplementary Material (Sect. 2.8).

The icemelt factor, calibrated following the procedure described in Sect. 2.3.3, is k_{ice}=6.1 mm day^{-1} °C^{-1}. Calibration and validation results are summarized in Table 2.2. In Fig. 2.5 we show the seasonal pattern of basin-averaged IM, SM, and R simulated with the calibrated snow and icemelt model, together with discharge Q observed at the outlet of the two highly glacierized sub-catchments Massa (Fig. 2.5a) and Lonza (Fig. 2.5b). The fit of the simulated (computed as IM+SM+R) to the observed discharge is good, with mass balance errors about 7% for the Massa and 8% for the Lonza.

Although in our hydrological model we do not include glacier evolution, the annual runoff volumes (SM+IM+R) from glacierized areas during the period 1980-2010 correlates well with the results of GloGEM (Fig. 2.6a). Measures of performance confirm the agreement between the two models: the correlation coefficient is equal to 0.86 and the Nash-Sutcliffe efficiency is equal to 0.67. We also capture quite well the seasonal pattern of runoff generated from glacierized areas (Fig. 2.6b). Perhaps most importantly, GloGEM simulations show that total annual runoff is increasing throughout the period and there is no evidence for decreasing icemelt rates. This confirms that, although glaciers of the upper Rhône basin are retreating, melt-water discharges from glacierized and proglacial areas are increasing during the 1980-2010 period. As expected, total runoff from glacierized surfaces and icemelt is highly correlated (Fig. 2.6a, correlation coefficient = 0.95), thus indicating that the increase in total runoff is due to an increase of the icemelt component. Indeed, non-parametric Mann-Kendall tests indicate an increasing trend with 5% significant level. Trend slopes, estimated with the Theil-Sen estimator, confirm the agreement between the two models: we find a total runoff of ∼27.65 mio m^3 year^{-2} with GloGEM and ∼21.71 mio m^3 year^{-2} with our model. We also computed the basin-averaged mass balance accounting for snow accumulation and snow and icemelt for each hydrological year. The mean mass balance over the period 1980-2010 is equal to -0.78 ± 0.22 m w.e. year^{-1} which is within the uncertainty range of recent studies (Fischer et al., 2015). In summary: although we do not account for glacier retreat, our model results agree well with state-of the art glaciological models that include glacier evolution. Both comparisons with GloGEM and our basin-averaged mass balance indicate that we are not significantly overestimating icemelt during the period 1975-2015.

Table 2.2: (top) Calibrated snowmelt factor k_{snow} and goodness of fit measures for validation and calibration period: Nash-Sutcliffe efficiency (NS), mean square error (MSE), true skill statistic (TSS), sensitivity (SE) and specificity (SP) for the entire upper Rhône Basin; (bottom) calibrated icemelt factor k_{ice} and goodness of fit measures: mass balance error computed on June-October months (MBES) and on the entire year (MBEA) for Massa and Lonza sub-basins.

	k_{snow} = 3.6 mm day^{-1} °C^{-1}	
	Calibration	Validation
NS	0.88	0.86
MSE	0.01	0.01
TSS	0.54	0.46
SE	0.77	0.76
SP	0.73	0.70

	k_{ice} = 6.1 mm day^{-1} °C^{-1}	
	MBES [%]	MBEA [%]
Calibration Massa	6.10	7.22
Validation Massa	6.77	9.19
Validation Lonza	11.35	10.09

2.5.2 Temperature, Precipitation, Discharge and SSC in the Rhône Basin

Mean annual air temperature shows a clear and statistically significant increase in 1987 (p-value < 0.01). A two-sample t-test for equal means (p-value < 0.01) confirms an increase in mean daily temperature greater than 1 °C (Fig. 2.7a). Statistical tests on monthly means reveal that the 1987 temperature jump is mainly in spring and summer months from March to August, while changes in the autumn and winter months are not statistically significant (Fig. 2.8a). For the period March-August, mean monthly temperatures have risen by about 1.2 °C on the average.

The change in air temperature around 1987 coincides with statistically significant changes in mean annual suspended sediment concentration (Fig. 2.7c). After the abrupt warming, mean annual suspended sediment concentrations are roughly 40% larger than before: average values have risen from 172 ± 6.86 mg l^{-1} before 1987 up to 242 ± 14.45 mg l^{-1} after 1987, where the ranges express the standard error of the mean. This change can be ascribed to statistically significant (p-value < 0.01) increases in summer (July-August) concentrations (Fig. 2.8c). Suspended sediment concentration is also characterized by much larger inter-annual variability after 1987 than before: the standard deviation of

mean annual SSC increases from $\sim$ 32 mg l^{-1} before 1987 up to $\sim$ 78 mg l^{-1} after (Fig. 2.7c). A statistically significant increase in the variance is confirmed with a two-sample F-test at 5% significant level.

While the upper Rhône Basin underwent an abrupt warming around 1987, mean annual precipitation (Fig. 2.7b) and mean monthly precipitation (Fig. 2.8b) do not change significantly in time. Likewise, mean annual discharge does not show any statistically significant change in 1987 (Fig. 2.7d). Mean monthly discharge (Fig. 2.8d) is characterized by a small statistically significant increase in winter (November-February) runoff, most likely due to increased snowmelt and possibly changes in hydropower generation.

2.5.3 Hydroclimatic Activation of Sediment Sources

Mean annual simulated snowmelt (SM) shows a decreasing tendency during the last thirty years (Fig. 2.9a). The reduction in snowmelt after 1987 occurs mostly in summer and early autumn (Fig. 2.10a) mainly due to poor snow cover (Fig. 2.10b). However, except July and September, the changes in all months are within the 95% confidence interval. The increase of snowmelt in March and April is due to warmer temperatures in spring. Results are coherent with the temporal evolution of simulated snow cover fraction, which is also gradually decreasing (Fig. 2.9b), especially in spring and summer (Fig. 2.10b). Statistical analysis reveals a step-like reduction of more than 10% for mean annual values of snow cover fraction in 1987 (p-value < 0.01).

Although mean annual and monthly precipitation were shown not to change significantly in the mid-1980s, effective rainfall (ER) on snow-free areas has increased, especially in early summer (Fig. 2.9d, Fig. 2.10d). Effective rainfall increases in conjunction with decreases in snow cover fraction, and a statistically significant jump is identified in 1987 (p-value < 0.01) (Fig. 2.9d). However, although snow cover fraction is significantly lower throughout the entire melting season, only June and especially July show statistically significant increases in ER after 1987 (Fig. 2.10d).

Our results show that the temporal evolution of icemelt is consistent with suspended sediment concentration rise. Although the change is rather gradual at the annual scale (Fig. 2.9c), the step-like increase in icemelt is evident in the ice-melting season (May-September) and reaches highest magnitudes in July and August (Fig. 2.10c) in conjunction with rises in suspended sediment concentration in those months (Fig. 2.8c).

The simultaneous increase in icemelt and decrease in snowmelt suggests that the abrupt warming has led to important alterations of the hydrological regime. To quantify this

alteration, we compute the relative contribution of rainfall, snow and icemelt on the sum of these three components in July and August. The average relative contribution of icemelt has almost doubled after 1987 (from ∼12% to ∼22%, Fig. 2.12), while the relative contribution of snowmelt has reduced by more than 30% (from ∼52.5% to ∼35%, Fig. 2.12). This indicates the substantial effect of the sharp temperature rise on the basin hydrology.

2.5.4 Effect of Intermittent SSC sampling

The empirical cumulative distribution functions of total daily basin-averaged SM, IM, ER and Q, computed on all days ("all non-zero days") and only on days corresponding to SSC-measurements ("SSC-measurement non-zero days") is shown in Fig. 2.12. Although extremely high and low values may indeed be missed by the non-continuous sampling, cumulative distributions of SM, IM, ER and Q on "SSC-measurement non-zero days" and on "all non-zero days" are similar. This indicates that, although SSC is measured at a fixed interval, the sampling captures accurately the process variability. In addition, results of the statistical tests on mean monthly and mean annual values of all analyzed hydroclimatic variables are unchanged. We therefore conclude that our results are not significantly influenced by the discontinuous nature of the SSC sampling.

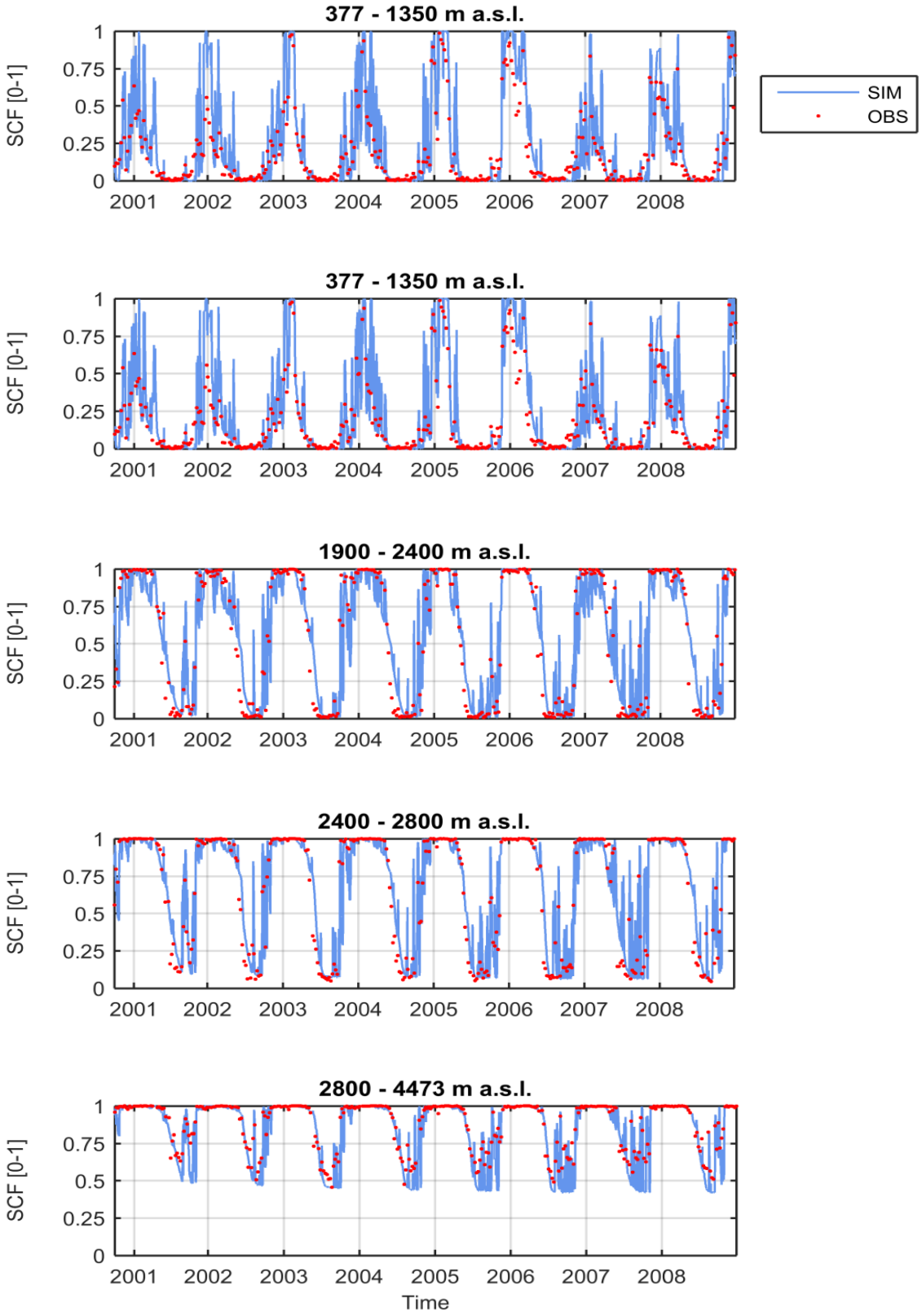

Figure 2.3: Comparison between observed (red circles) and simulated (light blue lines) snow cover fraction (SCF) of the upper Rhône Basin for five different elevation bands. Simulations are computed with calibrated snowmelt factor $k_{snow} = 3.6$ mm day^{-1} °C^{-1}.

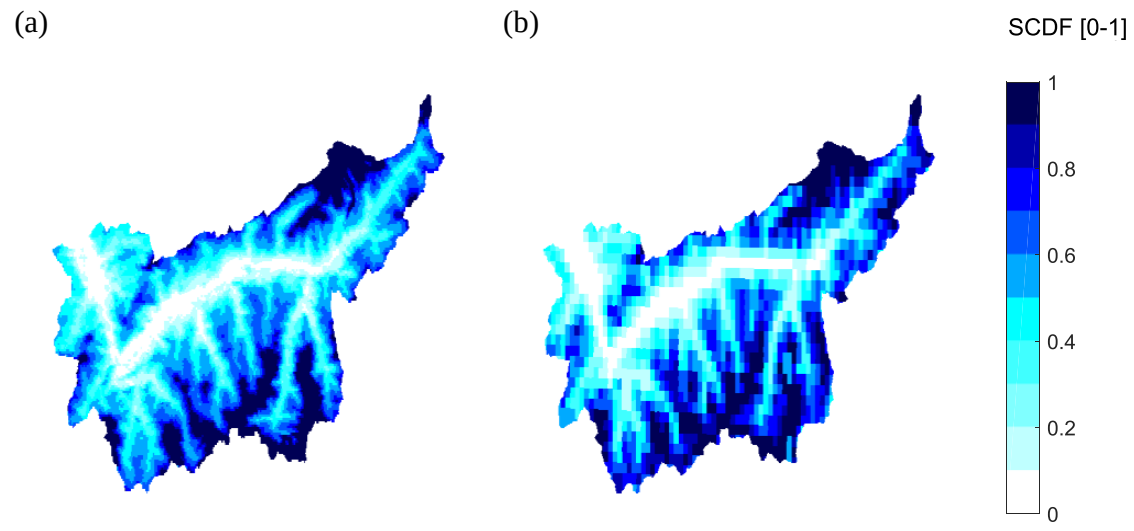

Figure 2.4: Map of average snow permanence over the period 2000-2008, expressed as fraction of time in which pixels are snow-covered (SCDF [0 - 1]): (a) observations (MODIS) and (b) simulations.

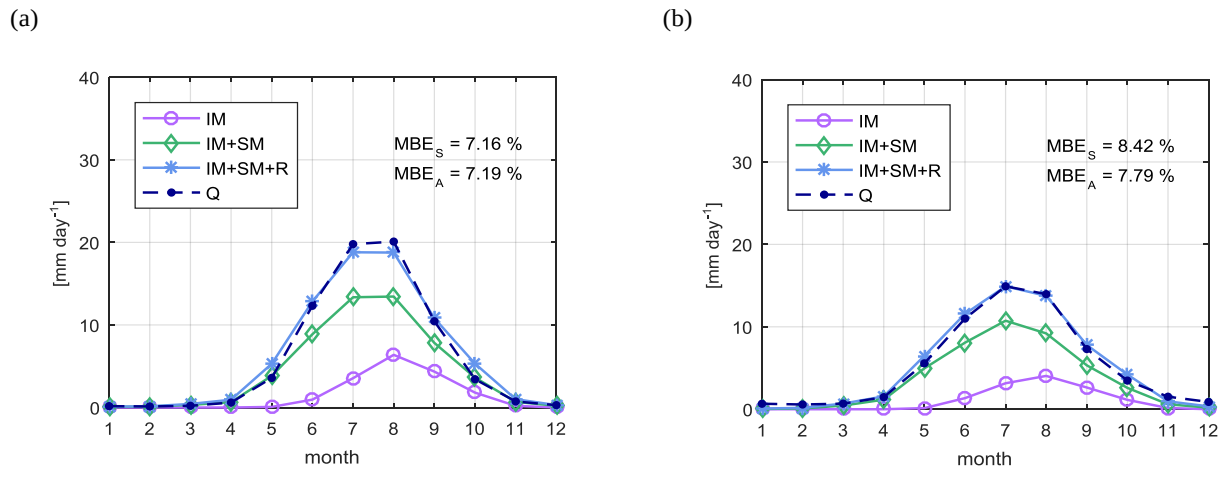

Figure 2.5: Comparison of mean monthly observed (dark blue) and simulated discharge (light blue) for the period 1975-2015: (a) Massa basin and (b) Lonza basin. Simulated discharge is the sum of three components: icemelt (IM), snowmelt (SM) and rainfall (R).

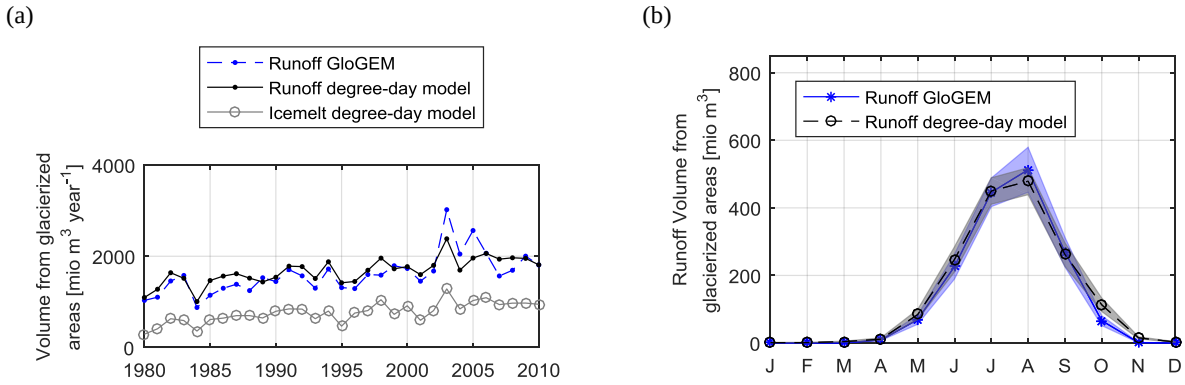

Figure 2.6: Runoff (snowmelt + icemelt + rainfall) generated from glacierized areas within the upper Rhône basin, simulated with GloGEM and with the snowmelt and icemelt models (degree-day) for the period 1980-2010: (a) total annual values; (b) mean monthly values. Fig. 2.6a also depicts the time series of total annual icemelt simulated with the icemelt model.

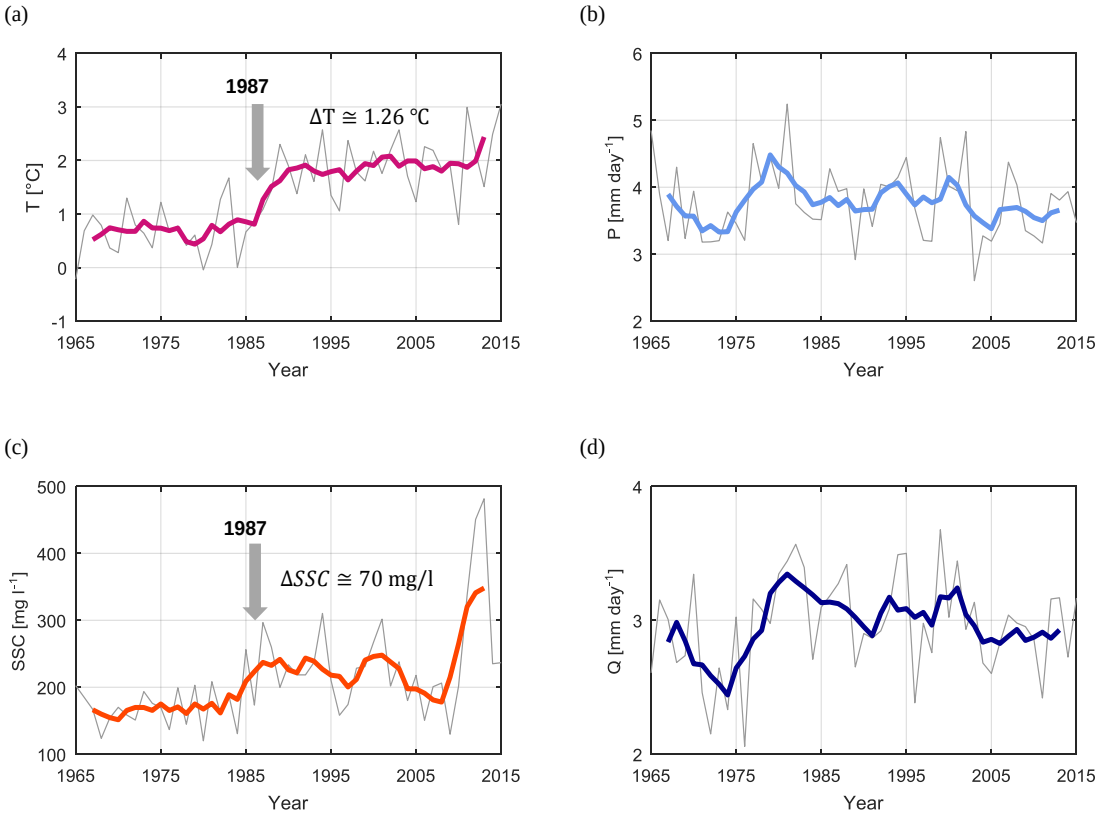

Figure 2.7: Observations for the period 1965-2015 of: (a) basin-averaged air temperature; (b) basin-averaged daily precipitation; (c) suspended sediment concentration measured at the outlet of the basin; (d) daily discharge per unit area measured at the outlet of the basin. Mean annual values are shown in grey and the 5-years moving average is shown with a bold line.

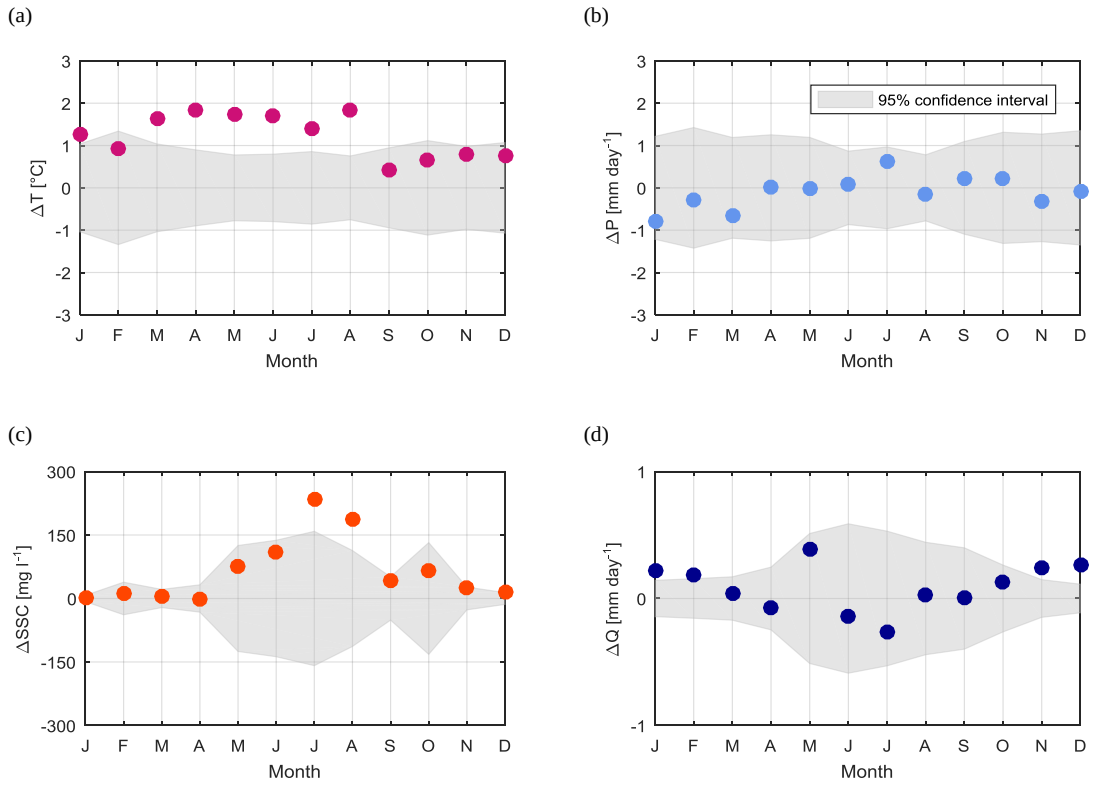

Figure 2.8: Monthly differences between the period after and before the year-of-change (1987-2015 and 1965-1986) of: (a) basin-averaged air temperature; (b) basin-averaged daily precipitation; (c) mean suspended sediment concentration measured at the outlet of the basin; (d) daily discharge per unit area measured at the outlet of the basin. Points outside the confidence interval (grey shaded area) represent statistically significant (5% significance level) changes in the monthly mean.

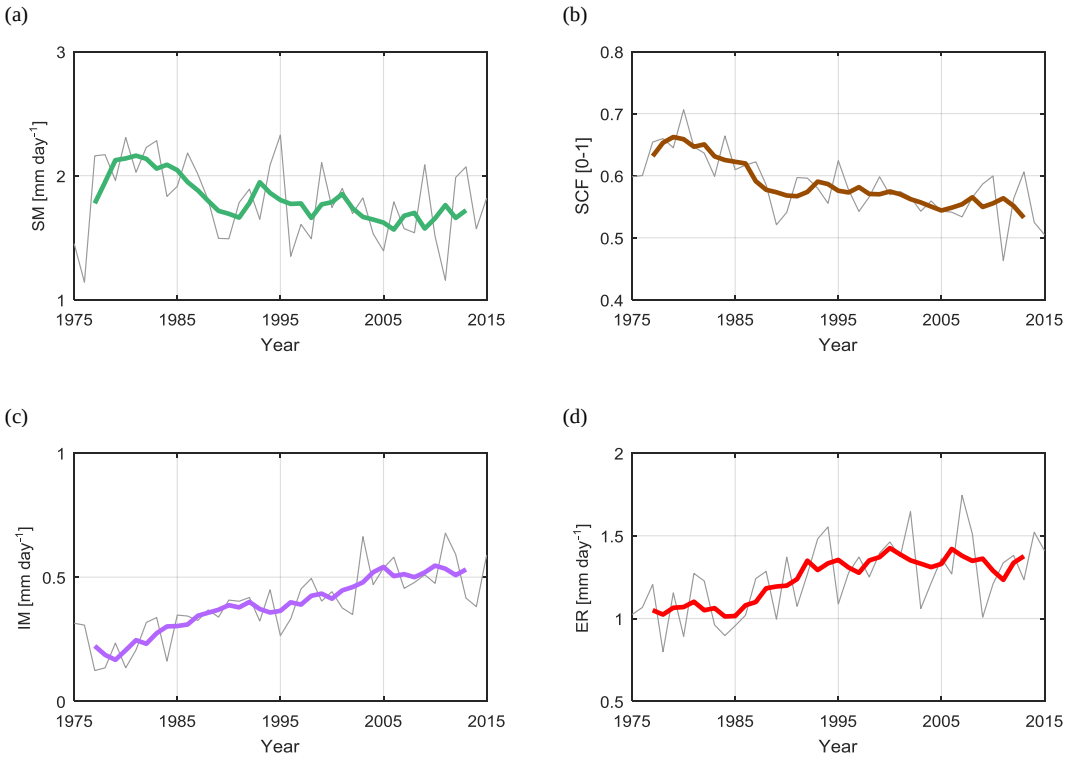

Figure 2.9: Simulations for the period 1975-2015 of mean annual: (a) snowmelt SM; (b) snow cover fraction SCF; (c) icemelt IM; (d) effective rainfall ER. Mean annual values are shown in grey and a 5-year moving average is shown with a thick line.

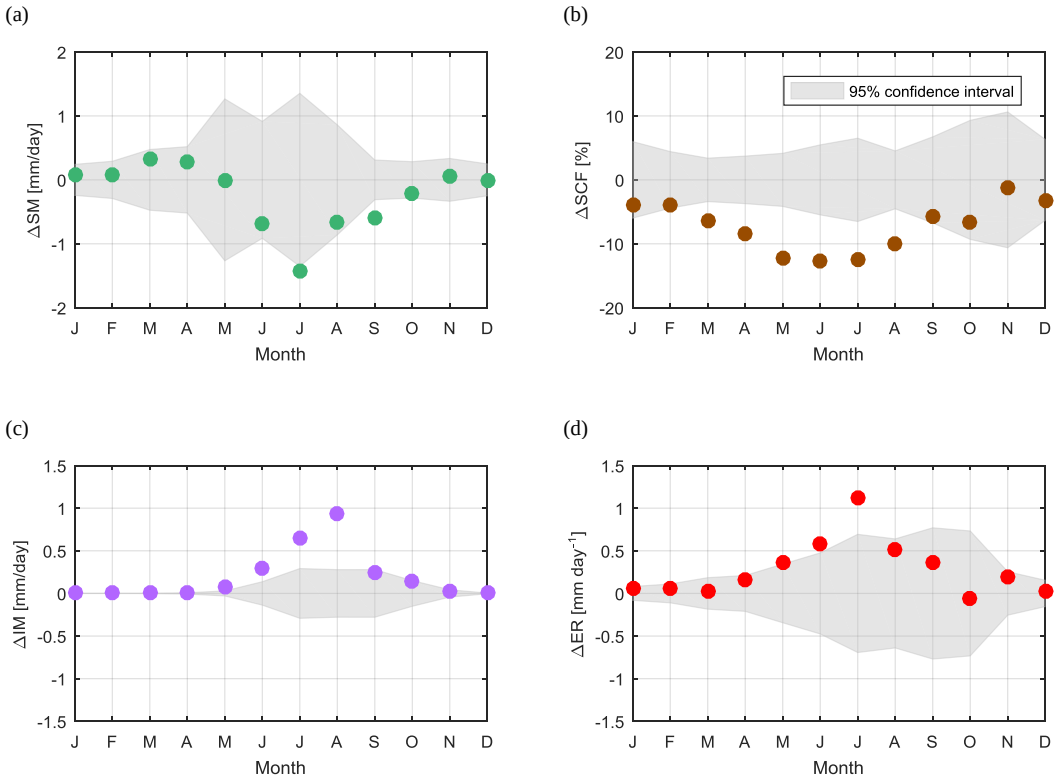

Figure 2.10: Mean monthly differences (between 1987-2015 and 1975-1986) in: (a) snowmelt SM; (b) snow cover fraction SCF; (c) icemelt IM; (d) effective rainfall ER. Points outside the confidence interval (grey shaded area) represent statistically significant (5% significance level) changes in the monthly mean.

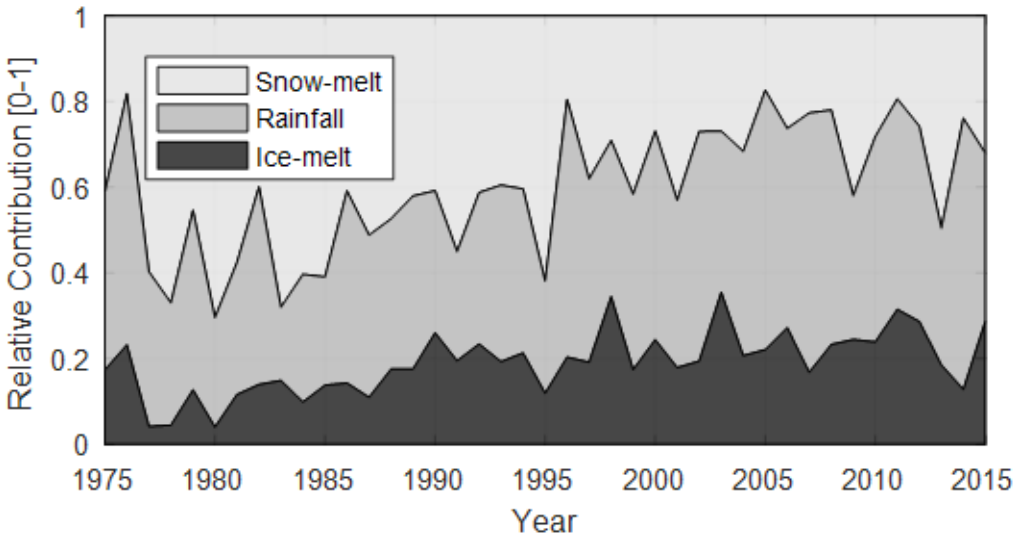

Figure 2.11: Relative contribution of snowmelt (SM), rainfall (R), and icemelt (IM) for the summer months July-August, computed as the ratio between each component and their sum. Rainfall is extracted from observed precipitation by using a rain-snow temperature threshold, snow and icemelt are simulated with spatially distributed temperature-index models.

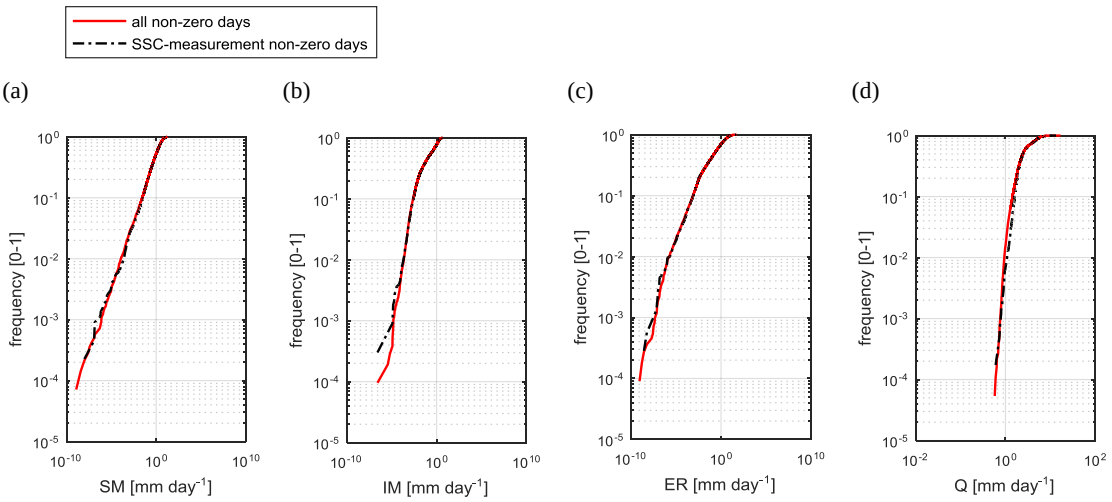

Figure 2.12: Empirical cumulative distribution functions of total daily basin-averaged SM (a), IM (b), ER (c) and Q (d), computed on all days and only on days corresponding to SSC-measurements. Only positive values of SM, IM and ER are included.

2.6 Discussion

2.6.1 Snowmelt and Icemelt Models

The value of the snowmelt factor k_{snow} (3.6 mm day^{-1} °C^{-1}) is in agreement with previous studies carried out in this region. In the upper Rhône Basin, Boscarello et al. (2014) found a snowmelt factor equal to 4.3 mm day^{-1} °C^{-1} based on previous studies on the Toce Basin in Italy (Corbari et al., 2009). Calibration of a semi-lumped conceptual model for the three tributary catchments of the upper Rhône Basin - Lonza, Drance and Rhône at Gletsch - led to snowmelt factors equal to 6.1, 4.5 and 6.6 mm day^{-1} °C^{-1}, respectively (Schaefli et al. 2005). Differences in k_{snow} between this and previous studies are attributable to different temporal resolution of models, lengths of calibration datasets, type and thresholds of precipitation partitioning, climatic inputs, threshold temperature for melt, and others. We highlight that the higher performance of the model in simulating snow cover at the highest elevation in our study, where most of the glaciers are located, is a prerequisite for successful icemelt estimation. The underestimation of SCF in autumn and the overestimation in winter at lower elevations are likely related to errors in partitioning precipitation into solid and liquid form. One of the main problems of degree-day models is related to their poor performance in reproducing the spatial distribution of snow accumulation and melt in complex topography. The temperature-index approach does not take into account features that affect melting, such as topographic slope, aspect, surface roughness and albedo (Pellicciotti et al., 2005). However, in our case, the spatial distribution of snow cover is satisfactory. Sensitivity and specificity are characterized by a strong seasonal signal. In summer, when a large part of the basin is snow-free, it is much easier for the model to capture snow-free pixels correctly than snow-covered pixels. In winter, when the basin is largely snow-covered, the situation is reversed. We account for this by computing the true skill score which combines both sensitivity and specificity into a better representation of overall model performance. Despite the large regional and temporal variability that characterizes icemelt factors, comparison with previous studies confirms that the calibrated value (7.1 mm day-1°C^{-1}) is reasonable for the Alpine environment (e.g. Schaefli et al., 2005; Boscarello et al., 2014). A range from 5 to 20 mm day^{-1} °C^{-1} has been reported in the literature (e.g. Hock, 2003; Schaefli, 2005). It should be noted that, when calibrating the icemelt factor, we neglect evaporation (evapotranspiration). However, evaporation plays indeed a secondary role in the long-term water balance in Alpine environments compared to precipitation and snowmelt (Braun et al., 1994; Huss et al., 2008), especially at high elevation such as in the case of the Massa and Lonza sub-catchments.

Considering that the aim of this study is to evaluate long-term changes in hydroclimatology and sediment dynamics of the upper Rhône Basin and not the short-term variability of icemelt at the daily scale, we consider the Snowmelt and Icemelt model performances as satisfactory. In addition, we show that although our model does not account for glacier retreat, it does not overestimate the icemelt contribution during the period 1975-2015. However, considering climate projections further into the future, and glaciers that continue to retreat, the issue of future icemelt contribution will need to be revised. Under climate change, even the largest glacier in the basin, the Aletsch Glacier, is expected to shrink at a rate where its icemelt contribution would start decreasing before 2050 (Farinotti et al., 2012; FOEN, 2012; Brönnimann et al., 2014).

2.6.2 Changes in Hydroclimatolology and SSC

Abrupt temperature jumps, such as the one we observed in the upper Rhône basin, rather than gradual changes in air temperature have been observed globally (e.g. Jones and Moberg, 2003; Rebetez and Reinhard, 2008). Observations indicate that Switzerland has experienced two main rapid warming periods in the past, with the 1940s and 1980s being the warmest decades of the last century (Beniston et al., 1994; Beniston and Rebetez, 1996). The simultaneous increase in temperature and suspended sediment concentration indicates that changes in climatic conditions may effectively impact sediment dynamics, especially in Alpine environments where temperature-driven processes, like snow and icemelt, have a strong influence on the basin hydrology. The statistically significant change in the SSC variance supports the finding that processes related to fine sediment regime of the upper Rhône Basin have been altered by changing climatic conditions, resulting in greater concentrations and higher variability of suspended sediment reaching the outlet of the basin. Conversely, differences in precipitation before and after 1987 are within the 95% confidence interval and are not statistically significant. Differences in discharge are also not statistically significant except in winter, when the suspended sediment concentration does not show changes. Therefore, it is very unlikely that the abrupt increase in suspended sediment concentration around mid-1980s in July and August is caused by changes in mean precipitation and/or discharge.

2.6.3 Hydroclimatic Activation of Sediment Sources

Our simulations of snowcover and melt are in agreement with snow observations across Switzerland. The decreasing tendency in snow cover after mid or late 1980s has been demonstrated for the Swiss Alps (Beniston, 1997; Laternser and Schneebeli, 2003; Scherrer

et al., 2004; Marty, 2008; Scherrer et al., 2006). Snow depth, number of snowfall days, and snow cover show similar patterns during the last century: a gradual increase until the early 1980s, interrupted in late 1950s and early 1970s, and a statistically significant decrease afterwards (Beniston, 1997; Laternser and Schneebeli, 2003). Previous analyses also state that the reduction in snow cover after mid-1980s is characterized more by an abrupt shift than by a gradual decrease (Marty, 2008), in agreement with our simulations. The reduction in snow cover duration, which is observed to be stronger at lower and mid altitudes than at higher elevations, is mainly the result of earlier snow melting in spring due to warmer temperatures (Beniston, 1997; Laternser and Schneebeli, 2003; Marty, 2008). Moreover, by analysing 76 meteorological stations in Switzerland, Serquet et al. (2011) demonstrated a sharp decline in snowfall days relative to precipitation days, both for winter and early spring, showing the impact of higher temperature on reduced snowfall, independently of variability in precipitation frequency and intensity. Therefore, despite the high complexity that characterizes snow dynamics in the Alps (Scherrer et al., 2006; 2013), the dominant effect of temperature rise on snow cover decline after late 1980s has been clearly shown (Beniston, 1997; Marty, 2008; Serquet et al. 2011; Scherrer et al., 2004; 2006).

The increase in potentially erosive rainfall, is partially confirmed by recent observations. Rainfall erosivity, expressed by the R-factor of the Revised Soil Loss Equation (Wischmeier and Smith, 1978; Brown and Foster, 1987), computed on the basis of 10 min resolution precipitation data, was recently analysed for Switzerland. Although, the upper Rhône Basin together with the Eastern part of Switzerland was found to have relatively low rainfall erosivity (low R-factor) compared to the rest of the country due to a lower frequency of thunderstorms and convective events (Schmidt et al., 2016), there is evidence of an increasing trend for the R-factor from May to October during the last 22 years (1989-2010) (Meusburger et al., 2012). This suggests that the increase in effective rainfall on snow-free surfaces may have contributed to suspended sediment concentration rise, through a combination of reduced snow cover fraction, increased rainfall-snowfall ratio and possible increases in rainfall intensity at sub-daily scale. However, simulations show a statistically significant jump in effective rainfall in June and July, while SSC is significantly larger in July and August. Therefore, we argue that erosive rainfall alone is unlikely to explain the abrupt jump in suspended sediment concentration observed around mid-1980s.

Enhanced icemelt is coherent with the observed acceleration of Alpine glacier retreat after mid-1980s. Ground-based and satellite observations, combined with mass balance analysis, reveal that current rates of glacier retreat are consistently greater than long-term averages (Paul, 2004; 2007; Haeberli, 2007). Estimations of glacier area reduction rates indicate a

loss rate for the period 1985-1999, which is seven times greater than the decadal loss rate for the period 1850-1973 (Paul, 2004). Investigations with satellite data and in-situ observations suggest that the volume loss of Alpine glaciers during the last thirty years is more attributable to a remarkable down-wasting rather than to a dynamic response to changed climatic conditions (Paul, 2004; 2007). Haeberli et al. (2007) estimated that glaciers in the European Alps lost about half of their total volume (roughly 0.5% year^{-1}) between 1850-1975, another 25% (1% year^{-1}) between 1975-2000, and an additional 10-15% (2-3% year^{-1}) in the period 2001-2005. The appearance of proglacial lakes and rock outcrops with lower albedo and high thermal inertia, separation of glaciers from the accumulation area, and general albedo lowering in European Alps (Paul, 2005), are among the main positive feedbacks that accelerate glacier disintegration and make it unlikely to stop in the near future (Paul, 2007). Although glacier dynamics are quite complex and involve many variables and feedbacks, the dominant role played by temperature rise in glacier wasting has been clearly demonstrated (e.g. Oerlemans, 2000). The major volume loss in the recent past in Swiss Alpine glaciers is attributable to negative mass balances during the ablation season rather than to a lower accumulation by precipitation (Huss, 2008). For small high altitude Alpine glaciers, Micheletti and Lane (2016) showed negligible ice melt contributions to runoff between the mid-1960s and mid-1980s, after which contributions increased markedly.

Most importantly, runoff coming from glaciers is notoriously rich in sediments. Very fine silt-sized sediment resulting from glacier erosion is transported in suspension most often as wash load (Aas and Bogen, 1988). Proglacial areas generally represent rich sources of sediment due to active glacier erosive processes of abrasion, bed-rock fracturing and plucking (Boulton, 1974; Hallet et al., 1996). Glacier retreat discloses large amount of sediments available to be transported by proglacial streams. Moreover, change in climatic conditions and specifically temperature-driven glacier recession and permafrost wasting may initiate specific erosional processes that consequently enhance sediment supply in proglacial environments (Micheletti et al., 2015; Micheletti and Lane, 2016; Lane et al. 2016).

As shown in Sect. 2.5.3, icemelt increase is highest in July and August (Fig. 2.10c), in agreement with the jump in suspended sediment concentration (Fig. 2.8c), while ER rise occurred mainly in June and July (Fig. 2.10d). We then conclude that the significant increase in icemelt detected in the mid-1980s (Fig. 2.9c, 2.10c, 2.11) is likely to be the main cause of the sharp rise in suspended sediment concentration entering Lake Geneva, through a combination of: (1) increased discharge originated in proglacial environments, which implies higher suspended sediment concentration; (2) larger relative contribution of sediment-rich icemelt compared to snowmelt and precipitation fluxes; and (3) intensified

sediment production and augmented sediment supply in proglacial areas due to rapid ice recession.

2.6.4 Anthropogenic Factors and Climate Signals

The interpretation of increases in suspended sediment concentration may be complicated by anthropogenic drivers and changes in the mid-1980s. Three main anthropogenic activities may have potentially influenced the suspended sediment regime of the upper Rhône basin: river channelization, construction of reservoirs and hydropower operations, and gravel extraction along the main stream and tributaries. However, the second and last large channelization project was completed in 1960 (Oliver et al., 2009), much earlier than the observed increase in SSC. Likewise, the largest reservoirs in the catchment have been in operation since 1975 (Loizeau and Dominik, 2000). Therefore, it is unlikely that these two anthropogenic factors have contributed to the SSC rise detected in mid-1980s. The same holds for gravel mining activities. Annual volumes of gravel extracted from the Rhône, provided by the Cantonal Authorities as differences from the average over the period 1989-2014, do not show any significant correlation with mean annual suspended sediment concentration ($R^2 = 0.08$). Although gravel mining operation may perturb SSC for short periods after river bed disturbance by causing local pulses of fine sediments, this process does not affect significantly the suspended sediment load at the outlet of the basin over seasonal and annual timescales. A possibility still remains that changes in the hydropower operation itself, i.e. the distribution of flow responding to electricity demand, and the flushing of dams have increased SSC concentrations. We currently do not have any evidence for such changes , however we think it is unlikely that they would have long-term effects on SSC.

Our results show that even in highly human impacted and regulated catchments such as the Rhône Basin, a strong climatic signal in hydrological and sediment dynamics can persist. This also suggests that the decrease in fine sediment load at the outlet of the upper Rhône Basin observed in the 1960s on the basis of sediment cores recovered in the Rhône delta region and reported by Loizeau et al. (1997), could be the result of a combined effect of hydropower system development, as it has been hypothesized (Loizeau et al., 1997; Loizeau and Dominik, 2000), but also reduced icemelt loads due to colder temperatures at the time. The cooling period, which occurred between 1950s and late 1970s (e.g. Beniston et al., 1994) was characterized by colder and snowy winters (e.g. Laternser and Schneebeli, 2003) and has been accompanied by reduced icemelt rates, glacier advance and positive glacier mass balances (Zemp et al., 2008; VAW-ETH, 2015).

The climate signal in sediment dynamics takes on particular importance in the context of climate change projections into the future. Despite the large uncertainty, future projections under different climate change scenarios show a common tendency for Switzerland, characterized by a shift from snow-dominated to rain-dominated hydrological regime, reduced summer discharge, increased winter discharge, reduced snow cover, and enhanced glacier retreat (Bavay, 2009; Jouvet et al., 2011; Brönnimann et al., 2014; Fatichi et al., 2015; Huss, 2016). In contrast to these hydrological predictions, changes in sediment fluxes are highly uncertain due to the complexity and feedbacks of the processes involved, inherent stochasticity in sediment mobilization and transport, and large regional variability in sediment connectivity across the Alpine landscape (Cavalli et al., 2013; Heckmann and Schwanghart, 2013; Bracken et al., 2015; Lane et al., 2017).

2.7 Conclusion

The aim of this research was to analyze changes in the hydroclimatic and suspended sediment regimes of the upper Rhône Basin during the period 1975-2015. We show an abrupt increase in basin-wide mean air temperature in the mid-1980s. The simultaneous step-like increase in suspended sediment concentration at the outlet of the catchment, detected in July and August, suggests a causal link between fine sediment dynamics and climatic conditions. Two main factors link warmer climate and enhanced SSC: increased transport capacity and increased sediment supply resulting from spatial and/or temporal activation-deactivation of sediment sources. Our results show that transport capacity, through discharge, is not likely to explain the increases in SSC, because no statistically significant changes in the mid-1980s are present in Rhône Basin discharge, neither at the annual nor monthly timescales. The suggestion is that the impact of warmer climatic conditions acts on fine sediment dynamics through the activation and deactivation of different sediment sources and different sediment production and transport processes.

To understand sediment supply conditions we analyze the temporal evolution of three main sediment fluxes: (1) sediments sourced and transported by snowmelt along hillslopes and channels; (2) sediments entrained and transported by erosive rainfall events over snow-free surfaces, including hillslope and channel bank erosion, and mass wasting events; (3) fine sediment fluxes generated by glacier ice-melt. The fluxes of snow and icemelt together with snow cover fraction and rainfall are analyzed to detect changes in time and their coherence with changes in SSC.

Our results show that while mean annual precipitation does not show any evident change between the periods before and after the SSC jump in mid-1980s, potentially erosive rain-

fall clearly increases over time especially in June and July, but not in August. On the other hand, icemelt has significantly increased due to temperature-driven enhanced ablation. Statistically significant shifts in icemelt were identified for summer, with highest increases in July and August, in accordance with the rise in SSC. Concurrently to the temperature and SSC rise, the relative contribution of icemelt to total annual runoff (sum of rainfall, snow and ice-melt) presents a significant increase in mid-1980s, substantially altering the hydrological regime of the Rhône Basin. Based on these results we propose that climate has an effect on fine sediment dynamics by altering the three main fluxes of suspended sediment in the Rhône Basin, and that icemelt plays a dominant role in the suspended sediment concentration rise in the mid-1980s through: (1) increased flow derived from sediment-rich subglacial and proglacial areas; (2) larger relative contribution of sediment-rich icemelt compared to snowmelt and precipitation; and (3) increased sediment supply in hydrologically connected proglacial areas due to glacier recession. While snowmelt has decreased, the reduced extent and duration of snow cover may also have contributed to the suspended sediment concentration rise through enhanced erosion by heavy rainfall events over snow-free surfaces.

Because changes in SSC are not consistent with changes in discharge and transport capacity, our work emphasizes how the inclusion of sediment sources and their activation through different processes of production and transport is necessary for attributing change. This analysis also demonstrates that climate-driven changes of suspended sediment dynamics may be significantly strong even in highly regulated and human impacted catchments such as the Upper Rhône basin, where sediment fluxes are affected by flow regulation due to hydropower production and by grain-size dependent trapping in reservoirs. This has consequences for climate change impact assessments and projections for Alpine catchments with hydropower systems, where climate change signals are sometimes thought to be secondary to human regulation. Although at this stage we cannot reliably conclude in which direction sediment fluxes will change in the future, our paper clearly shows that a more process-based understanding of the connections between hydrological change and the activation of sediment sources will provide us with a better framework for analysing and attributing changes in sediment yields in Alpine catchments in the future.

Author contribution A. Costa and P. Molnar designed the methodology. A. Costa developed the code and carried out simulations and computations. A. Costa prepared the manuscript with contributions from all co-authors. The authors declare that they have no conflict of interest.

Acknowledgments We thank Christoph Frei (Federal Office of Meteorology and Climatology MeteoSwiss) for providing us with experimental temperature and precipitation

datasets and for suggestions on the right use of MeteoSwiss gridded data and the application of statistical tests. We also thank Daniel Farinotti (Swiss Federal Institute for Forest, Snow and Landscape Research WSL, Department of Civil, Environmental and Geomatic Engineering ETH Zurich) for providing us with GloGEM simulations, for the fruitful discussion on glaciers retreat and glacier dynamics and for kindly revising the manuscript. The Federal Office of the Environment (FOEN) provided discharge and suspended sediment concentration data. We thank Alessandro Grasso (FOEN) for the explanation on the SSC data collection procedures. Finally, we would like to thank the Valais Cantonal Authorities for supplying information on gravel mining extraction. This research was supported by the Swiss National Science Foundation Sinergia grant 147689 (SEDFATE).

2.8 Supplementary Material

2.8.1 Sensitivity Analysis on Snow Model parameters

We apply a sensitivity analysis on the three main parameters of our Snowmelt model: snowmelt factor k_{snow} [mm day^{-1} °C^{-1}], threshold temperature for the onset of snow melt T_{SM} [°C], and the rain-snow threshold temperature T_{RS} [°C]. We analyze the impact of the parameters on the model results by perturbing one single parameter at the time. We compute some of the goodness of fit measures adopted during the calibration (TSS, NS RMSE) and analyze their relative change as function of the parameter perturbation (Fig. 2.13). As expected, the snowmelt factor k_{snow} is the most sensitive parameter (Fig. 2.13). For k_{snow} between 1.6 and 5.6 mm day^{-1} °C^{-1}, the relative reduction of TSS and NS results respectively lower than 10% and 15% (Fig. 2.13). Although reducing the snowmelt factor k_{snow} below 2.6 mm day^{-1} °C^{-1} increases RMSE by almost 40%, it results in incrementing RMSE only by 0.06 units (SCF [0-1]). For T_{SM} varying within the range of -2 ± 2 °C, TSS and NS decrease less than 10%. While the change in RMSE results larger similarly to the case of k_{snow} (Fig. 2.13). The effect of T_{RS} is even more negligible, with relative changes of goodness of fit measures within 5.5% (Fig. 2.13). We also estimated the influence of these three parameters on the trends and the jumps that we identified over the period 1975-2015 for the hydroclimatic variables simulated with the model: SM, IM, ER, SCF. For this purpose, we applied statistical tests for equality of mean annual and monthly values before and after mid-1980s after perturbing one parameter at the time within physically reasonable ranges of values. In agreement with the results of our analysis (Sect. 2.5.3), a statistically significant increase of mean annual IM and ER and a statistically significant decrease of mean annual SCF after mid-1980s are detected for all selected parameter values. Similarly, mean annual SM shows a decreasing tendency after mid-1980s for all parameter selections, and in about 50% of all the parameters selections statistical tests even show a statistically significant drop in mean annual SM. The increases in mean monthly ER in June and July are identified respectively in more than 90% and in 100% of the cases. Similarly, all parameters sets show an abrupt rise of IM after mid-1980s for all spring and summer months (May-August). This confirms that by perturbing the parameters of the snow model within reasonable ranges, the overall results of our analysis do not change. This is also depicted in Fig. 2.14. The differences in mean monthly values of IM and ER between the period after and before mid-1980s are shown for multiple values of each of the three parameters. The confidence interval depicted in Fig. 2.14 is built by selecting, for each month, the highest and the lowest values of the confidence interval (5% significance level) among all parameter sets. The comparison between Fig. 2.14 and Fig.

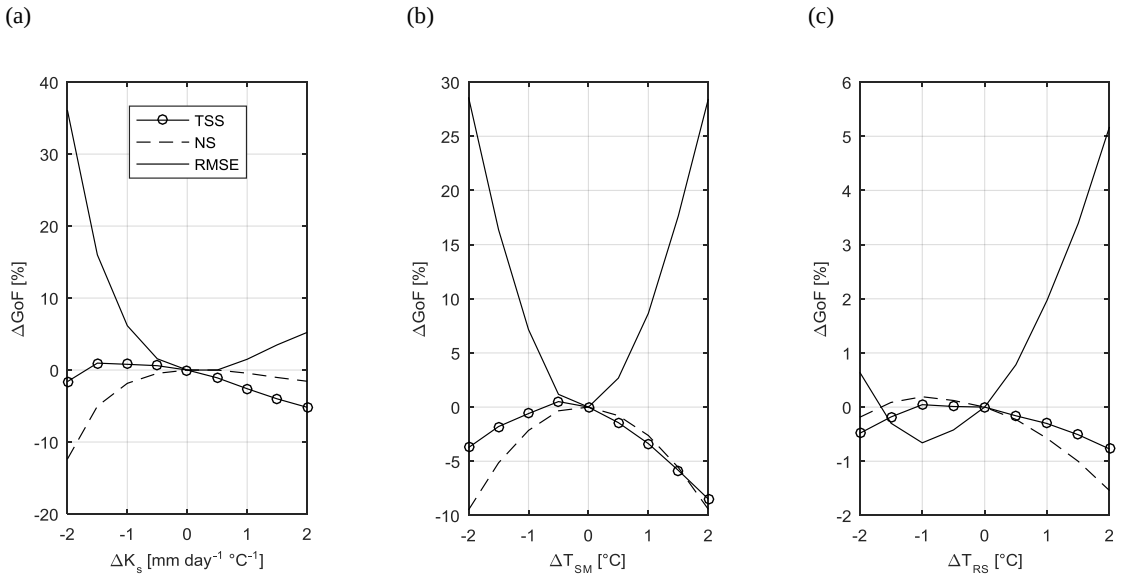

Figure 2.13: Parameter perturbation analysis on: (a) snowmelt factor k_{snow} , (b) threshold temperature for the onset of melt T_{SM}, (c) rain-snow threshold temperature T_{RS}. The relative change [%] of TSS, NS and RMSE are shown for each parameter.

2.9c and Fig. 2.9d, shows that changing parameters within reasonable ranges would not substantially change the results of our analysis.

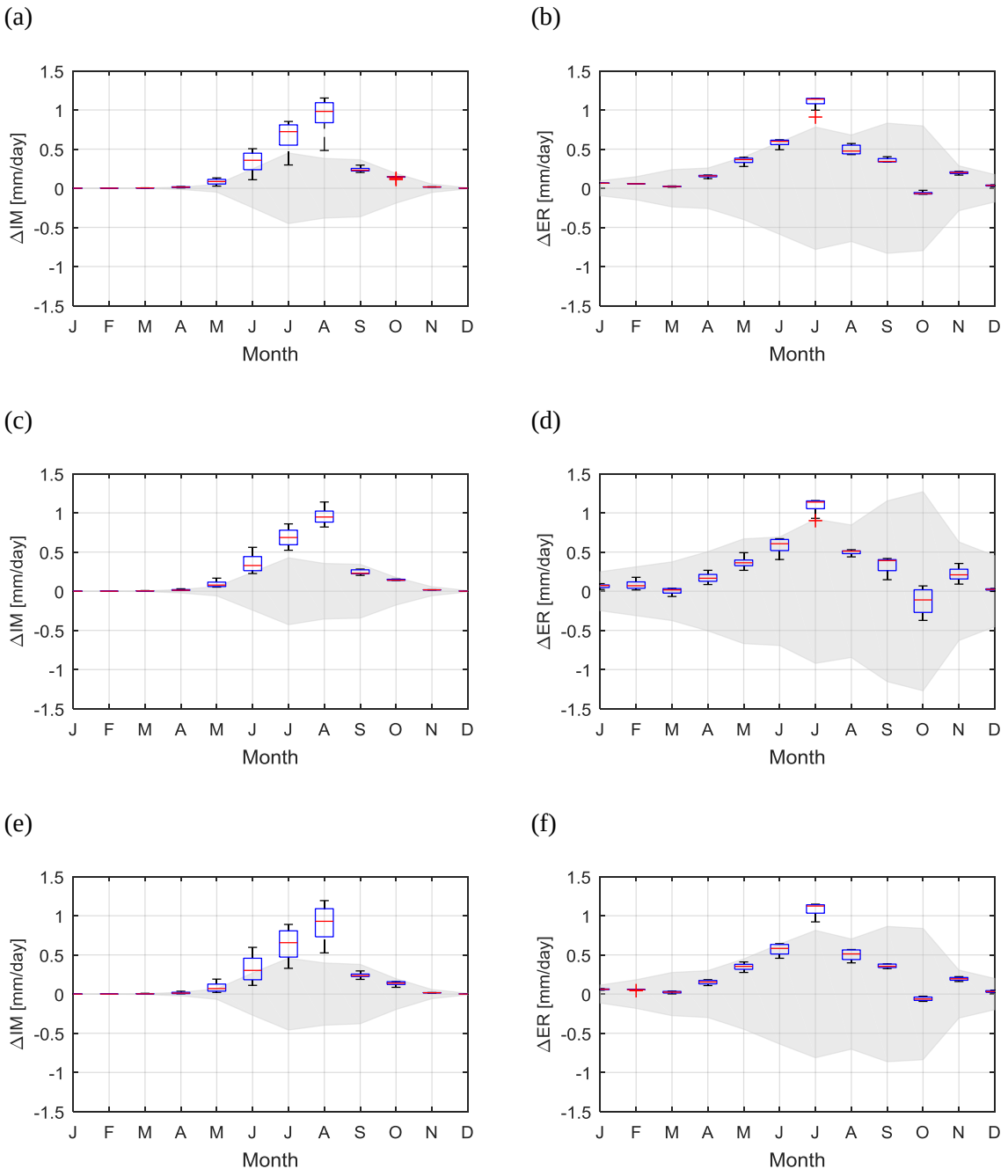

Figure 2.14: Sensitivity analysis on monthly differences between the periods after and before the year-of-change (1987-2015 and 1975-1986) for IM (left) and ER (right). Box plots represent monthly differences for all selections of parameters within given ranges of values: 1.6 mm day^{-1} °C^{-1} $\leq$ k$_{snow}$ $\leq$ 5.6 mm day^{-1} °C^{-1} (a,b); -2°C $\leq$ T$_{SM}$ $\leq$ 2 °C (e,f); -1 °C $\leq$ T$_{RS}$ $\leq$ 3 °C (c,d). Grey shaded areas represent the widest confidence interval among all selections of the parameters.

Chapter 3

Hydroclimatic control on suspended sediment dynamics of a regulated Alpine catchment: a conceptual approach*

** Costa A, Anghileri D and Molnar P (2018) Hydroclimatic control on suspended sediment dynamics of a regulated Alpine catchment: a conceptual approach. Hydrology and Earth System Sciences Discussion*

Figure 3.1: View of the Haut Glacier d'Arolla in the upper Rhône Basin (by C. Dutoit).

Abstract

We analyse the control of hydroclimatic factors on suspended sediment concentration (SSC) in Alpine catchments by differentiating among the potential contributions of erosion and suspended sediment transport driven by erosive rainfall, defined as liquid precipitation over snow free surfaces, icemelt from glacierized areas, and snowmelt on hillslopes. We account for the potential impact of hydropower by intercepting sediment fluxes originated in areas diverted to hydropower reservoirs, and by considering the contribution of hydropower releases to SSC. We obtain the hydroclimatic variables from daily gridded datasets of precipitation and temperature, implementing a degree-day model to simulate spatially distributed snow accumulation and snow-ice melt. We estimate hydropower releases by a conceptual approach with a unique virtual reservoir regulated on the basis of a target-volume function, representing normal reservoir operating conditions throughout a hydrological year. An Iterative Input Selection algorithm is used to identify the variables with the highest predictive power for SSC, their explained variance, and characteristic time lags. On this basis, we develop a hydroclimatic multivariate rating curve (HMRC) which accounts for the contributions of the most relevant hydroclimatic input variables mentioned above. We calibrate the HMRC with a gradient-based nonlinear optimization method and we compare its performance with a traditional discharge-based rating curve. We apply the approach in the upper Rhône Basin, a large Swiss Alpine catchment, heavily regulated by hydropower. Our results show that the three hydroclimatic processes - erosive rainfall, icemelt, and snowmelt - are significant predictors of mean daily SSC, while hydropower release does not have a significant explanatory power for SSC. The characteristic time lags of the hydroclimatic variables correspond to the typical flow concentration times of the basin. Despite not including discharge, the HMRC performs better than the traditional rating curve in reproducing SSC seasonality, especially during validation at the daily scale. While erosive rainfall determines the daily variability of SSC and extremes, icemelt generates the highest SSC per unit of runoff, and represents the largest contribution to total suspended sediment yield. Finally, we show that the HMRC is capable of simulating climate-driven changes in fine sediment dynamics in Alpine catchments. In fact, HMRC can reproduce the changes in SSC in the past 40 years in the Rhône Basin connected to air temperature rise, even though the simulated changes are more gradual than those observed. The approach presented is this paper, based on the analysis of the hydroclimatic control on suspended sediment concentration, allows the exploration of climate-driven changes in fine sediment dynamics in Alpine catchments. The approach can be applied to any Alpine catchment with a pluvio-glacio-nival hydrological regime and adequate hydroclimatic datasets.

3.1 Introduction

Climate plays a dominant role in erosional and sediment transfer processes in Alpine catchments (e.g. Huggel et al., 2012; Micheletti and Lane, 2016; Palazón and Navas, 2016). In such environments, three main hydroclimatic forcings drive the processes that contribute to suspended sediment concentration (SSC) along channels: erosive rainfall, glacial melt, and snowmelt. Erosive rainfall (ER), defined here as liquid precipitation over snow free surfaces, is responsible for soil detachment and erosion along hillslopes (Wischmeier, 1959; 1978), triggering of mass wasting events, such as debris flows and landslides (e.g. Caine, 1980; Dhakal and Sidle, 2004; Guzzetti, 2008; Leonarduzzi et al., 2017), which can mobilize large amounts of fine sediment (e.g. Korup et al., 2004; Bennett et al., 2012) resulting in very high suspended sediment concentrations in the receiving streams. Together with erosional processes along hillslopes, which are strongly related to rainfall intensity (e.g. Van Dijk et al., 2002), precipitation events may also enhance channel and bank erosion through increased discharge. Icemelt (IM) is responsible for high concentrations of fine sediment produced with a variety of glacial erosion processes (Boulton, 1974). Icemelt may substantially increase suspended sediment concentration in glacially-fed streams by entraining and transporting fine sediment previously stored in subglacial networks and paraglacial environments (Aas and Bogen, 1988; Gurnell et al., 1996; Lawler et al., 1992). Snowmelt-driven overland flow (SM) generates hillslope erosion and potentially affects channel and bank erosion by contributing to streamflow. This hydroclimatic forcing is important in Alpine environments where snowmelt can produce high hillslope runoff and be a major contributor to channel discharge (e.g. Grønsten and Lundekvam, 2006; Ollesch et al., 2006; Konz, 2012). Due to the diversity of the erosion and transport processes (e.g. erosion driven by overland flow, mass wasting events) and the variety of sediment sources involved (e.g. hillslopes, channels, glaciers), sediment fluxes generated by these three hydroclimatic variables are expected to contribute to suspended sediment dynamics in a complementary way, both in terms of magnitude and timing.

In addition to natural hydroclimatic forcings, human activities potentially contribute to alter sediment dynamics, e.g. by changes in land use (e.g. Foster et al., 2003) and sediment storage in reservoirs (e.g. Syvitsky et al. 2005). In Alpine environments, it is especially water impoundment and flow regulation due to hydropower production which may substantially influence the suspended sediment regime (e.g. Anselmetti et al., 2007). The impacts of hydropower operations on suspended sediment dynamics may vary substantially between catchments, depending on the specific features of the hydropower system (e.g. reservoir trapping efficiency, hydropower operations), and on the catchment characteristics (e.g. amount and grain size distribution of the eroded sediment, seasonal pattern

of sediment production). Here, we focus on two main effects of hydropower operations: sediment trapping in reservoirs, and temporary sediment storage behind water diversion infrastructures (intakes), which may substantially reduce the amount of sediment delivered to downstream reaches and/or significantly alter the timing of sediment release to the river network (e.g. Vörösmarty et al., 2003; Finger et al., 2006; Gabbud and Lane, 2016; Bakker et al., 2017). Despite sediment trapping, water released from hydropower reservoirs (HP) may carry suspended sediment either previously stored in the reservoirs or entrained along the downstream channels.

In the context of environmental change, it is important to understand how the sediment regime has changed and what the relative role of different hydroclimatic forcings may have been. There are examples of studies which demonstrated alterations in suspended sediment yields driven by changes in land use, climate, or by disturbances such as wildfires, earthquakes and flow impoundments (e.g. Loizeau and Dominik, 2000; Foster et al., 2003; Dadson et al., 2004; Yang et al., 2007; Horowitz, 2010; Costa et al., 2017). These changes are normally addressed by calibrating different sediment rating curves models, which express suspended sediment concentration as a power function of discharge, for different sediment supply regimes and by making the parameters of the rating curves time dependent (e.g. Syvitski, 2000; Yang, 2007; Hu, 2011; Huang and Montgomery, 2013; Warrick, 2015). However these approaches do not explicitly address the sources of sediment and their activation by different hydroclimatic forcings and are limited to using discharge as a predictor. As a result the hydroclimatic causality of changes in suspended sediment concentration in such analyses remains elusive. The approach proposed in this paper accounts explicitly for the hydroclimatic and hydropower activation/deactivation of different sediment sources, with the aim to identify their predictive power in estimating suspended concentration even without using discharge.

Our main objectives are: (1) to explore the role played by the hydroclimatic variables erosive rainfall ER, ice-melt IM, snow-melt SM, and the hydropower release HP, in controlling suspended sediment concentration of an Alpine catchment; and (2) to analyse long-term, climate-driven changes in suspended sediment concentration on the basis of a conceptual, data-driven approach accounting separately for the contribution of ER, IM, SM and HP. The upper Rhône Basin in southern Switzerland is used as the study catchment. The upper Rhône River contributes more than 65% of the total input of particulate matter into Lake Geneva, the largest lake in the Alps (Loizeau et al., 1997), substantially influencing the morphology and ecology of the river delta and the lake (Loizeau and Dominik, 2000; Loizeau et al., 1997). The catchment is heavily regulated by hydropower infrastructure. Several large hydropower reservoirs have been in operation since 1960s, leading to a total retention capacity equal to roughly 20% of the total annual discharge of the catchment

(Loizeau and Dominik, 2000; Fatichi et al., 2015). In addition to reservoirs, a complex network of water intakes and diversions extracts water from headwater streams and delivers it either to the major reservoirs or directly to the hydropower plants. From a detailed map of the hydropower scheme, including reservoirs and water diversions (Fatichi et al., 2015), it is estimated that roughly 25% of the catchment is affected by hydropower: 8% flowing directly into the reservoirs, and 17% diverted through tunnels and pumping stations. Sediment fingerprinting conducted in the catchment in a recent study from Stutenbecker et al. (2017) indicates that sediment originated in the lithological unit more affected by hydropower is underrepresented at the outlet of the catchment, suggesting the impact of water impoundment on the sediment budget of the basin. In addition, alterations of suspended sediment concentration entering Lake Geneva have been observed in the recent past and attributed to human impacts (Loizeau and Dominik, 2000; Loizeau et al., 1997) and changes in climatic conditions (Costa et al., 2017).

The paper is organized as follows: Sect. 3.2 describes the data pre-processing, the hydrological modelling procedure to obtain the hydroclimatic variables (ER, IM, SM), the approach to obtain the hydropower releases (HP), and the analysis performed to infer their link to suspended sediment concentration; Sect. 3.3 presents the upper Rhône basin and the data used in our analysis; Sect. 3.4 reports the main results which are discussed in Sect. 3.5; and Sect. 3.6 concludes the manuscript by summarizing the main findings.

3.2 Methods

To analyse the role of hydroclimate on the suspended sediment regime of a catchment regulated by hydropower reservoirs, we first divide the catchment into two distinct areas: (1) the area which contributes to the runoff accumulated in hydropower reservoirs (regulated area), including the fraction of the catchment draining directly into the reservoirs and the fraction connected to the reservoirs through tunnels and pumping stations, and (2) the remaining area, which naturally flows to the river network (unregulated area).We assume that the sediment fluxes originated in the unregulated area contribute directly to SSC at the outlet of the catchment, while sediment fluxes generated in the regulated area are diverted into the reservoirs and later totally or partially released according to hydropower operations. Finally, we estimate the contribution to SSC at the outlet of the catchment of sediment fluxes originated in the unregulated area by ER, IM and SM, and of sediment fluxes carried by water released from the reservoirs during hydropower operations HP.

Our methodology consists of four main steps: (1) the derivation of mean daily SSC_t and ER_t, SM_t, IM_t, HP_t datasets - mean daily SSC_t at the outlet of the catchment is

derived from continuous measurements of turbidity (Sect. 3.2.1), the hydroclimatic input variables mean daily ER_t, SM_t, IM_t are derived from spatially distributed snow and icemelt models, and the mean daily water releases from hydropower reservoirs HP_t is derived by a conceptual approach based on a unique virtual reservoir, which is intended to model the cumulative effect of multiple reservoirs, when present in the catchment, and a target volume function (Sect. 3.2.2); (2) we use an Input Variable Selection algorithm to identify the variables with the highest predictive power for SSC_t and we estimate their characteristic time lags (Sect. 3.2.3); (3) we calibrate and validate a rating curve accounting for the variables identified in the previous step (Hydroclimatic Multivariate Rating Curve - HMRC), and we evaluate the contribution of each hydroclimatic and hydropower component to SSC_t (Sect. 3.2.4); (4) we apply the HMRC to simulate 40-year long time series of SSC_t at the outlet of the catchment to investigate the impact of changes in climatic conditions on suspended sediment dynamics, and we compare simulated values with observations obtained with a traditional rating curve (RC) based on discharge only (Sect. 3.2.5).

3.2.1 Estimate of daily suspended sediment concentration

The specific operations described in this and the following paragraphs strongly depend on the data availability for the case study under consideration. In the following, we describe the operations we carried on for the upper Rhône Basin, but we also comment about the applicability of these and alternative operations to other catchments.

SSC sampling has been historically conducted manually, usually with low frequency (e.g. a few samples a week) and fixed intervals, because manual measurements are costly and time consuming (e.g. Gippel, 1995; Pavanelli and Pagliarani, 2002). This results in long but intermittent SSC datasets, which are not suitable for data-driven modelling, because they might not be representative of the entire range of possible suspended sediment concentrations. On the other hand, automatic gauging stations with optical turbidity sensors produce turbidity datasets which are continuous but usually shorter, because of the recent wide-spread availability and installation of such sensors. Because turbidity is strongly related to suspended sediment concentration (e.g. Gippel, 1995; Lewis, 1996; Pavanelli and Pagliarani, 2002; Holliday et al., 2003; Lacour et al., 2009; Métadier and Bertrand-Krajewski, 2012), the two datasets, when available at the same location, can be combined to obtain a high frequency SSC dataset. In our case, punctual manual measurements of SSC are collected twice per week at the outlet of the Rhône Basin and continuous measurements of Nephelometric Turbidity Units (NTU) are available for an overlapping period

in 2013-2017 at the same location. To build a SSC-NTU relationship, we consider simultaneous measurements of NTU and SSC (i.e. with a maximum time lag of five minutes), after removing observations greater than the 90th percentile (corresponding to 2000 mg l^{-1} and 1000 NTU respectively) because we are concerned about errors in observed high sediment concentration pulses due to the punctual bottle-sampling procedure and known measurement errors at high NTUs, and the fact that SSC and NTU measurements are not taken exactly at the same location in space (and time) in the cross-section. We use least squares regression to fit the model after a logarithmic transformation of the variables:

$$SSC = a_0 \cdot NTU^{b_0} \, . \tag{3.1}$$

For the back-transformation from the logarithmic to the linear scale, we applied the correction factor proposed by Duan (1983). Finally, we compute mean daily NTU values from continuous measurements of turbidity, and we use the SSC-NTU relation (Eq. 3.1) to estimate mean daily SSC.

3.2.2 Hydroclimatic Data Modelling

Datasets of the hydroclimatic variables ER, IM and SM need to be derived by hydrological modelling. The choice of the model should be driven by the data availability for calibration and the required accuracy of the simulated outputs. In our case, we use a conceptual and spatially distributed model of snow and icemelt driven by spatially distributed precipitation and temperature (Costa et al., 2017). We use gridded datasets of mean daily precipitation and mean, maximum, and minimum daily air temperature to divide precipitation into rainfall and snowfall on the basis of a temperature threshold. We model ice and snow accumulation and melting with a degree-day approach (e.g. Hock, 2003). Icemelt occurs only on glacier cells that are snow-free. Likewise, erosive rainfall occurs only on snow-free hillslope cells. We set temperature thresholds for snow/rain division (1°C) and for snow and icemelt initiation (0°C) based on the literature and on previous studies (e.g. Fatichi et al., 2015; Costa et al., 2017), while we calibrate melt factors with satellite-derived snow cover (MODIS) and with discharge measured at different locations in the catchment. We first calibrate the snowmelt rate from snow cover maps by spatial statistics that measure the grid-to-grid matching of the model. Second, we calibrate the icemelt rate on the basis of discharge measured at the outlet of two highly glaciated sub-catchments. For more details on the hydrological model description and calibration see Costa et al. (2017). Finally, we sum the spatially distributed hydroclimatic variables over the regulated and unregulated areas and we obtain respectively mean daily ER_t^{HP},

IM_t^{HP}, SM_t^{HP} and ER_t, SM_t, and IM_t. We represent all the hydropower reservoirs operating in the catchment with a unique virtual reservoir, because data of water releases from individual reservoirs are seldom available. The release from the virtual reservoir is estimated on the basis of a target-volume function which represents the reservoir operations in normal conditions. For each day of the year, the hydropower release from the virtual reservoir HP_{t+1} within the interval from day t to day t+1 is estimated as the difference of the reservoir storage and the target volume, when positive, zero otherwise. The reservoir storage $V_(t+1)$ is finally computed on the basis of the mass balance:

$$V_{t+1} = V_t + I_{t+1} - HP_{t+1} \,, \tag{3.2}$$

where I_{t+1} represents the inflow into the virtual reservoir within the interval from day t to day t+1. To derive the capacity of the virtual reservoir, we consider the 13 largest reservoirs operating in the Rhône catchment. A list of the reservoirs with their retention capacity is reported in Table 3.2 of the Supplementary Material, while their spatial location is shown in Fig. 3.2. We compute the target-volume functions of each individual reservoir by averaging observed storage time series for reservoirs when observations are available and by adopting normalized reference curves within the individual reservoir regulation range otherwise (see Fatichi et al., 2015 for the full details). We then compute the target-volume function of the virtual reservoir by adding the target-volume functions of each individual reservoir and by scaling the sum to the total annual inflow. We compute the daily inflow I_t in Eq. (3.2) as the sum of the three hydroclimatic fluxes, erosive rainfall, icemelt and snowmelt generated over the regulated area:

$$I_t = ER_t^{HP} + IM_t^{HP} + SM_t^{HP} \,. \tag{3.3}$$

It has to be noted that I_t represents direct potential runoff from the regulated area without accounting for evapotranspiration and infiltration losses. We therefore scale the capacity of the virtual reservoir, to obtain reservoir seasonal dynamic resembling the available observations. For the scaling, we assume the minimum volume of the virtual reservoir equal to zero, and the maximum volume equal to 70% of the total annual inflow into the reservoirs, which roughly corresponds to the average ratio between storage capacity and total annual inflow. The procedure described above implies that all reservoirs of the catchment are regulated following the same operational rule driven by the seasonality of inflow, i.e. an annual cycle of drawdown during winter and refill during spring and summer. Due to their geographical proximity, the similar elevation, and the available observations, this assumption can be considered realistic. We validate the hydropower operations model

by comparing the mean daily normalized values of simulated hydropower releases of the virtual reservoir and observations from Mattmark, a reservoir with a volume capacity of 108 m^3 located in the upper part of the catchment. Although our hydropower operations model is relatively simple, the comparison shows a good agreement with the observations (Fig. 3.10 of the Supplementary Material).

3.2.3 Input Variable Selection Algorithm

We apply the Iterative Input Selection (IIS) algorithm (Galelli and Castelletti, 2013) to (1) select which variables play a significant role in predicting SSC_t, (2) quantify their relative importance, and (3) identify the time lags of the sediment flux associated with each selected variable. The IIS algorithm selects the most relevant input variables, among a set of candidate input variables (in our case mean daily ER_{t-l}, SM_{t-l}, IM_{t-l}, HP_{t-l} at different time lags l), to predict a specific output variable (in our case mean daily SSC_t). It calibrates and validates a series of regression models considering different sets of input variables and selecting the ones that display the best model performances. The algorithm adopts Extremely Randomized Trees, or Extra-Trees, (Geurts et al., 2006) as regression models, because they allow dealing with non-linear relations between input and output variables in a computationally efficient way. The Extra-Trees regression is based on a recursive splitting procedure, which partitions the dataset into sub-samples containing a specified number of elements. This splitting procedure is performed several times by randomizing both the input variable and the cut-point used to split the sample, in order to minimize the bias of the final regression (for more details see Geurts et al., 2006).

The IIS algorithm is based on an iterative procedure, which allows for the ranking of the candidate input variables according to their significance in explaining the output variable on the basis of the coefficient of determination R^2 of the underlying regression model. At the first iteration, regression models are identified and the candidate variable leading to the best model performance is selected. At subsequent iterations, the original output variable (i.e. SSC_t) is substituted with the residual of the model computed at the previous iteration. This ensures that candidate input variables that are highly correlated with the selected one are discarded and, thus, reinforces the ability of the IIS algorithm against the selection of redundant and cross-correlated input variables (Galelli and Castelletti, 2013). Because of the relatively short duration of our dataset and the marked seasonal pattern that characterizes the considered candidate input variables and output variable, we randomly shuffle the dataset 100 times before running the IIS algorithm to ensure the consistency of the selection. The shuffling is done on lagged variables and, therefore, it does not affect the serial correlation in the variables. Among the 100 runs of the algorithm,

we choose the most frequently selected model and the most frequently selected model including hydropower releases, if the two do not correspond. We then analyse the selected input variables, their characteristic time lags and the fraction of variance explained by each selected variable.

3.2.4 Relative contribution of hydroclimatic forcing to SSC

To further investigate the contribution of hydroclimatic forcing to suspended sediment dynamics, we propose a non-linear multivariate rating curve (Hydroclimate Multivariate Rating Curve, HMRC), which relates SSC_t to the hydroclimatic variables described above, representing the main drivers for the suspended sediment regime of an Alpine catchment:

$$SSC_t = a_1 \cdot ER_{t-l_1}^{b_1} + a_2 \cdot IM_{t-l_2}^{b_2} + a_3 \cdot SM_{t-l_3}^{b_3} + a_4 \cdot HP_{t-l_4}^{b_4} \,, \tag{3.4}$$

where ER_{t-l_1}, IM_{t-l_2}, SM_{t-l_3} are mean daily erosive rainfall, icemelt, and snowmeltover unregulated areas, computed at time $t-l_1$, $t-l_2$, and $t-l_3$ respectively, and $HP_{t-l_4}$is the daily release of water from the virtual hydropower reservoir at time t-l_4.SSC_t is expressed in dg l^{-1} while ER_{t-l_1}, IM_{t-l_2}, SM_{t-l_3} and HP_{t-l_4} are expressed as mean values over the catchment in mm day^{-1}. The time lags, l_1, l_2, l_3 and l_4, identified with the Input Variable Selection Algorithm (Sect. 3.2.3), represent the time necessary for sediment produced at a given location in the catchment to reach the outlet. In principle, the travel time depends on the sediment source location (i.e. distance from the outlet) and the velocity of the transport (which is a function of runoff, topography, and flow resistance). Here, we assume a characteristic travel time for each hydroclimatic/hydropower component, i.e. l_i (with i = 1, 2, 3, 4), which represents an average travel time in space (i.e., over the catchment) and time (i.e., over the hydrological year). We also assume that coefficients a_i and b_i (with i = 1, 2, 3, 4) may vary between the hydroclimatic/hydropower variables, because they express sediment availability as well as the nonlinearity of SSC_t production by each variable. The HMRC does not use discharge in the estimation of SSC_t. We calibrate the parameters of the non-linear multivariate HMRC a_i and b_i in Eq. 3.4, by minimizing the mean squared error (MSE) between observed and simulated SSC with a gradient-based optimization approach. We assume that each sediment flux originates under supply-unlimited conditions, i.e. there is a positive relation between sediment transport capacity and the load of sediment mobilized and transported. Accordingly, the optimization is subject to the following constraints: b_i>-1 (with i = 1, 2, 3, 4); coefficients a_i, (with i = 1,2,3,4) are instead not constrained, which allows for dilution when $a_i < 0$; and

simulated $SSC_t \geq 0$. We repeat the optimization procedure 100 times, starting from randomly generated initial values to reduce the risk of detecting sub-optimal parameter configurations.

We evaluate the ability of the HMRC in reproducing mean daily SSC_t time series observed at the outlet of upper Rhône Basin, and we compare its performance with a traditional rating curve (RC) which relates suspended sediment concentration to mean daily discharge Q_t only:

$$SSC_t = a_{RC} \cdot Q_t^{b_{RC}} \ . \tag{3.5}$$

We calibrate the parameters of the RC (Eq. 3.5) a_{RC} and b_{RC} by least squares regression applied to the logarithm of SSC_t and Q_t. As for the SSC-NTU relation, we apply the smearing estimator of Duan (1973) to the back-transformed values of SSC_t to correct for the bias (e.g. De Girolamo et al., 2015). The performance of the HMRC and RC models are evaluated by computing goodness of fit measures such as coefficient of determination R^2, Nash-Sutcliffe efficiency NSE, and root mean squared error RMSE, over the calibration and validation periods. We compare the simulated and observed seasonal patterns of SSC_t by analysing mean monthly values.

3.2.5 Long-term changes in SSC

Simultaneously with an abrupt rise in air temperature, the upper Rhône basin has experienced a statistically significant jump in mean annual SSC in mid-1980s, which has been attributed to an increase of icemelt and rainfall over snow free surfaces (Costa et al., 2017). To analyze the impact of changing climatic conditions on the long-term dynamics of suspended sediment, we apply the rating curve based on hydroclimatic variables, HMRC, to simulate the time series of mean daily SSC_t at the outlet of the upper Rhône basin for the 40-year period 1975-2015. We compare HMRC simulations both to the twice-a-week observations of SSC and to the values simulated with the traditional RC. We compare the three time series (observed, simulated with HMRC and with traditional RC) on the basis of mean annual values, computed by considering only simulations corresponding to SSC measurement days to allow for a fair comparison with observations. We apply statistical tests for equality of the means on time series of mean annual SSC, simulated with the HMRC and the traditional RC, to test if the models can reproduce the shift of SSC detected in the observations.

3.3 Upper Rhône Basin: description and data availability

We apply our approach to the upper Rhône Basin in the Swiss Alps (Fig. 3.2). The total drainage area of the catchment is equal to 5338 km^2 and about 10% of the surface is covered by glaciers. The topography of the basin which has been heavily preconditioned by uplift and glaciations (Stutenbecker et al., 2016) is characterized by a wide elevation range (from 372 to 4634 m a.s.l.). The Rhône River originates at the Rhône Glacier and flows for roughly 170 km before entering Lake Geneva. The hydrological regime of the catchment is dominated by snow and ice melt with peak flows in summer and low flows in winter. Mean discharge is equal to about 320 m^3s^{-1} in summer and 120 m^3s^{-1} in winter, while the mean annual discharge is around 180 m^3s^{-1}.

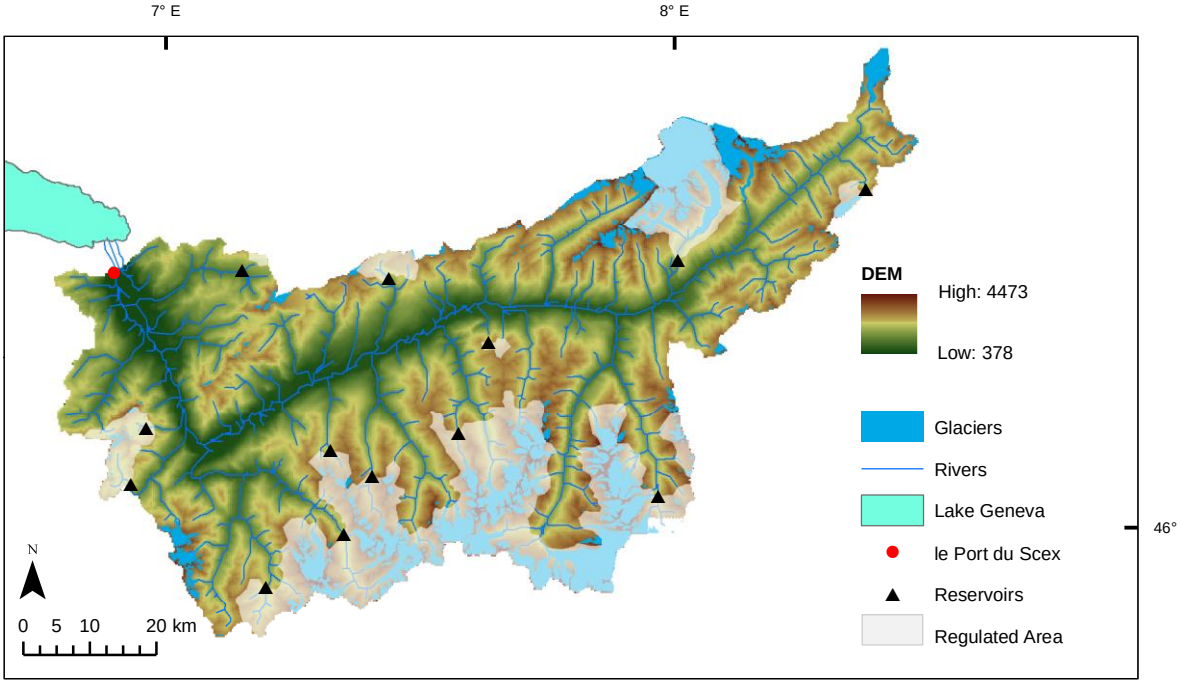

Figure 3.2: Map of the upper Rhône Basin with topography, glacierized areas and river network. The measurement station le Port-du-Scex, located just upstream the Rhône River enters the Lake Geneva, is indicated with a red marker. The main 13 reservoirs considered in this study are represented with black triangles and the regulated fraction of the catchment is highlighted with light grey shaded area.

Basin-wide mean annual precipitation is about 1400 mm yr^{-1} and mean annual temperature is about 1.4 °C estimated at basin mean elevation. Porte-du-Scex is the measurement station at the outlet of the Rhône River into Lake Geneva (Fig. 3.2), where the Swiss Federal Office of the Environment (FOEN) collects discharge, SSC and turbidity data. Mean daily discharge is available since 1905, while SSC is measured twice per week since Oc-

tober 1964. Quality-checked continuous measurements of NTU are available since May 2013 (Grasso et al., 2012). SSC at the outlet is characterized by a seasonal pattern typical of Alpine catchments (Fig. 3.3a). During winter (December-March) sediment sources are limited because a large fraction of the catchment is covered by snow and precipitation occurs in solid form. Streamflow is mainly determined by baseflow and hydropower releases (Loizeau and Dominik, 2000; Fatichi et al., 2015), and SSC assumes its minimum values. In spring, SSC increases when snowmelt-driven-runoff mobilizes sediments along hillslopes and in channels. Simultaneously, snow cover decreases and rainfall events over gradually increasing snow free surfaces erode and transport sediment downstream, resulting in SSC peaks. In July, SSC reaches its highest values in conjunction with streamflow (Fig. 3.3a).

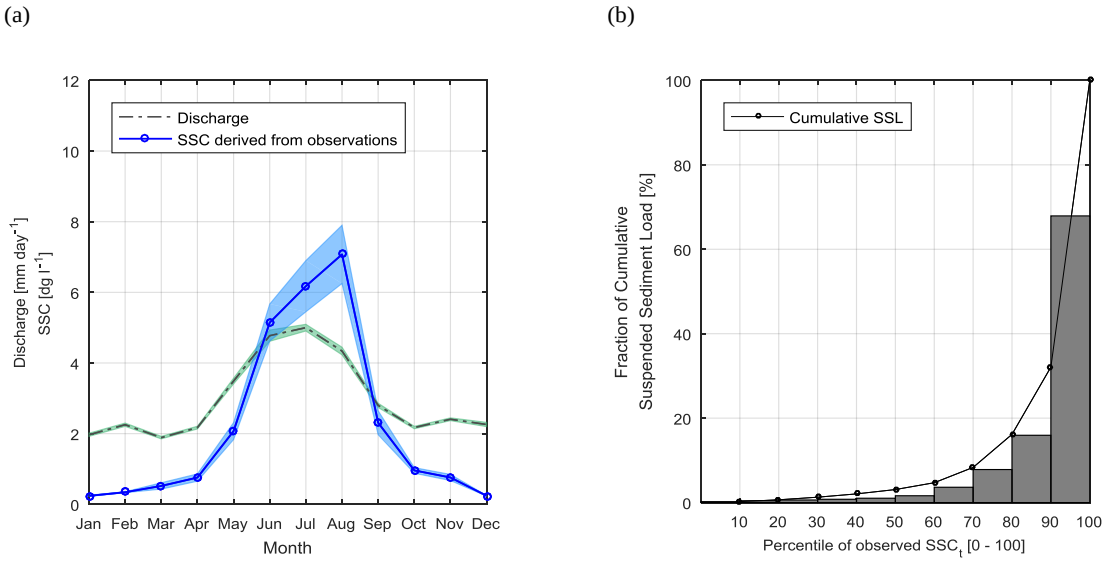

Figure 3.3: (*a*) Mean monthly values of: discharge measured at the outlet of the catchment (dash-dot grey line), SSC_t derived from observations of NTU (solid blue line with circles). Coloured shaded areas represent the range corresponding to ± standard error. Mean values and standard errors are computed over the entire observation period. (b) Cumulative suspended sediment load (SSL) transported at the outlet of the upper Rhône basin during the observation period as function of different percentiles of SSC_t (black line with circles). Bars represent the fraction of the total SSL transported by the different percentiles of SSC_t (e.g.: more than 66% of total SSL is transported with $SSC_t > 90^{th}$ percentile).

In late summer (August and September), when icemelt dominates, sediment rich fluxes coming from proglacial areas maintain high values of SSC although discharge is decreasing (Fig. 3.3a). In terms of suspended sediment yield, low SSC conditions do not play a relevant role compared to moderate and high SSC conditions: more than 66% of the total

suspended sediment load entering Lake Geneva during the 4-year period May 2013 - April 2017 is estimated to be due to SSC values greater than the 90^{th} percentile (Fig. 3.3b). The linear relationship between the logarithm of NTU and SSC for the overlapping period of measurement is statistically significant with a coefficient of determination $R^2 = 0.94$ (Fig. 3.4). After applying the correction factor for back-transforming from logarithmic to linear scale, the calibrated parameters of the relation in Eq. (3.1) are a_0= 0.56 and b_0 = 1.25. This relation was used to convert NTU observations to mean daily SSC. We are aware that the relation between SSC and turbidity: (1) is site-specific, (2) may vary seasonally as function of discharge and transported grain sizes, and (3) depends on sediment sources, because the size, the shape, and the composition of suspended material may influence values of turbidity (Gippel, 1995).

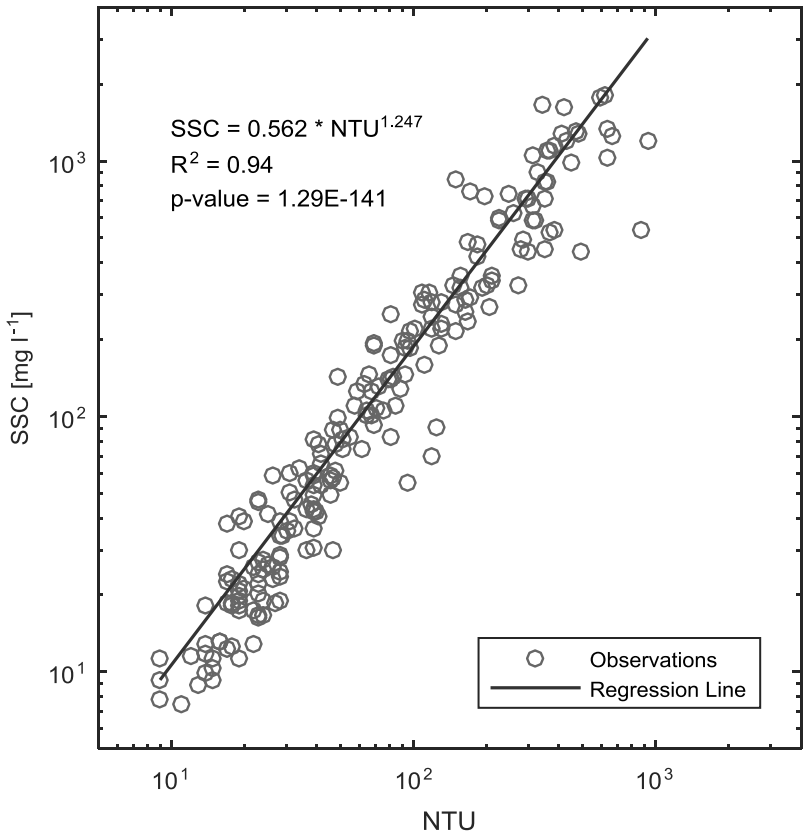

Figure 3.4: Scatterplot of NTU and SSC observed simultaneously (i.e. with a maximum lag of 5 minutes) at the outlet of the catchment (grey circles), and calibrated regression line of Eq. 3.1 (black line).

For this reason, in this analysis: (1) we apply a site-specific SSC-NTU relation, (2) we calibrate the relation over a wide range of NTUs and discharge conditions to account for the seasonal variability in grain sizes transported by the flow, and (3) we derive the SSC-NTU relation based on a relatively short period of time, in which there is not evidence

of changes in sediment sources. In addition, by allowing a non-linear relation between SSC and NTU, we take partially into account the variability of turbidity with grain size. Higher suspended sediment concentrations are expected to transport proportionally larger grains, and the exponent in the SSC-NTU relation was expected to be greater than 1.

We estimate the hydroclimatic variables for the forty year period 1975-2015 with the spatially distributed degree-day model of snow and icemelt. The model is implemented using a DEM with a spatial resolution of 250x250 m (Federal Office of Topography - Swisstopo). For the climatic dataset, we use gridded mean daily precipitation, mean, maximum and minimum daily air temperature at $\sim$ 2x2 km resolution provided by the Swiss Federal Office of Meteorology and Climatology (MeteoSwiss). These datasets are produced by spatial interpolation of quality-checked measurements collected at meteorological stations (Frei et al., 2006; Frei, 2014). Snow cover maps used for the calibration of the snowmelt rate were derived for the period 2000-2008 in a previous study (Fatichi et al., 2015) from the 8-day snow cover product MOD10A2 retrieved from the Moderate Resolution Imaging Spectroradiometer (MODIS) (Dedieu et al., 2010). We consider the GLIMS Glacier Database of 1991 to define the initial configuration of the ice covered cells. To calibrate the icemelt rate, we use mean daily discharge data measured at the outlet of two highly glacierized tributary catchments: the Massa and the Lonza (Costa et al., 2017).

To separate sediment fluxes originated in regulated and unregulated areas of the catchment (Fig. 3.2), we used a detailed map of the main hydropower reservoirs and water uptakes and diversions, available from previous work of Fatichi et al. (2015) and based on information included in the product "Restwasserkarte" available from the Swiss Federal Office for the Environment (BAFU).

When applying the IIS algorithm (Sect. 3.2.3), we consider mean daily ER_{t-l}, SM_{t-l}, IM_{t-l} and HP_{t-l} at time lags l from 0 day to 7 days. This choice is driven by the size of the basin and the expected flow concentration times in the basin. We calibrate the HMRC on data from the period 1 May 2013 - 30 April 2015 (730 days) and validate it over the period 1 May 2015 - 30 April 2017 (731 days). For the sake of comparison, calibration and validation periods are the same also when considering the RC.

3.4 Results

3.4.1 Control of Hydroclimatic Forcing on SSC

The IIS algorithm selects most frequently (56% of the runs) a model with erosive rainfall, icemelt, and snowmelt generated over the unregulated area of the catchment at 1-day lag, ER_{t-1}, IM_{t-1}, and SM_{t-1}, as the most relevant variables to predict mean daily SSC_t (Fig. 3.5a). We consider only the first 3 selected variables because the cumulative explained variance, expressed as the coefficient of determination R2, is greater than 0.9 (Fig. 3.5a) and the contribution of additional variables is negligible (the fourth selected variable ER_{t-2} explains roughly 1%). Pair-wise correlation coefficients between the selected input variables are significantly low, equal to -0.006 between IM_{t-1} and SM_{t-1}, 0.2 between IM_{t-1} and ER_{t-1}, and 0.02 between ER_{t-1} and SM_{t-1} respectively. This confirms that cross-correlation and redundancy are minimized. The IIS result is interesting for several reasons. (1) It confirms our hypothesis that erosion and transport processes driven by all 3 hydroclimatic variables ER, IM and SM play a role in determining the suspended sediment dynamics of the Rhône Basin, and likely in most Alpine basins with pluvio-glacio-nival hydrological regimes. (2) It gives an indication of the relative importance of the different processes. In fact, the contribution of each hydroclimatic variable to the overall R^2 differs quite significantly. While ER_{t-1} explains almost 75% of the variability of SSC_t, the melting components IM_{t-1} and SM_{t-1} are responsible for a much lower fraction of the variance, i.e. 12% and 4% respectively (Fig. 3.5a). (3) The time lags selected for ER, IM and SM, which represent basin-averaged mean travel times of sediment from source to outlet, including also the time required to produce runoff sufficient to entrain sediment, are equal to 1 day, in agreement with the typical concentration time of the catchment. (4) The most selected model does not include hydropower releases, HP, (Fig. 3.5a) indicating that fluxes released from hydropower reservoirs do not play a significant role in determining the variability of the SSC_t signal at the outlet of the basin.

When models including hydropower releases are considered (8% of the runs), the first three explanatory variables selected by the IIS algorithm and their explained variance correspond to the ones of the most selected model described above, while hydropower releases are selected at time lag equal to 0 and represent less than 1.5% of the variability of SSC_t (Fig. 3.5b). This indicates the characteristic time lag at which the variable HP is considered in the next steps and confirms that it explains only a minor fraction of the variance of SSC.

Nevertheless, we include HP in the Hydroclimate Multivariate Rating Curve, HMRC, to assess its contribution to SSC in terms of magnitude and seasonality. After the calibration

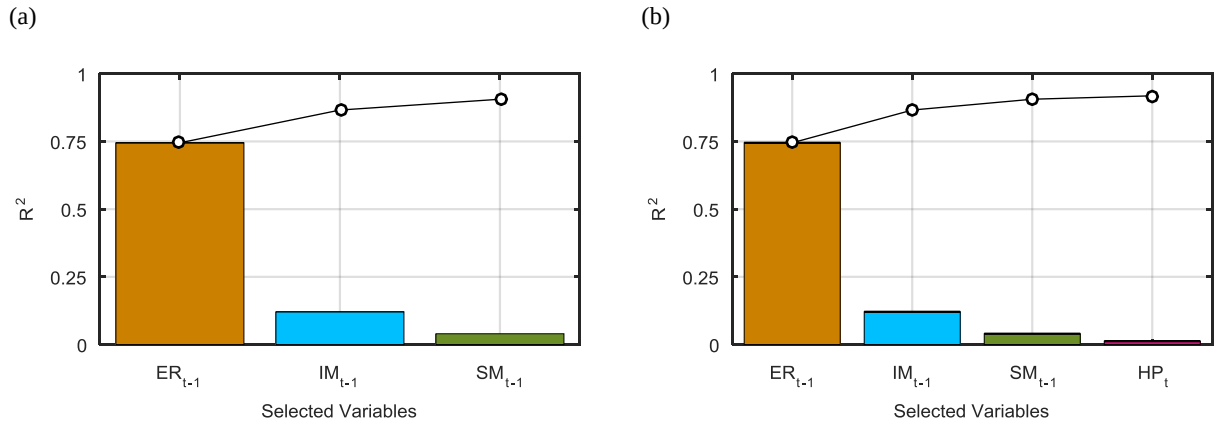

Figure 3.5: Results of the IIS algorithm: fraction of the variance of SSC_t explained by the selected explanatory variables, and cumulative explained variance (black line with circles) of (a) the most frequently selected model (ER_{t-1}, IM_{t-1}, SM_{t-1}) and (b) the most frequently selected model including hydropower releases (ER_{t-1}, IM_{t-1}, SM_{t-1}, HP_t).

Table 3.1: Goodness of fit measures for the HMRC and the traditional RC in calibration (left) and validation (right): coefficient of determination (R^2), Nash−Sutcliffe efficiency (NSE), root mean squared error (RMSE).

	Calibration 01.05.13 - 30.04.15		Validation 01.05.15 - 30.04.17	
	HMRC	RC	HMRC	RC
R^2	0.59	0.6	0.61	0.42
NSE	0.54	0.6	0.61	0.42
RMSE [dg l^{-1}]	3.25	3.02	2.66	3.23

of the parameters (Sect. 3.2.4), the rating curve based on hydroclimatic variables HMRC and the traditional RC result respectively in the following forms:

$$SSC_t = max[0.70 \cdot ER_{t-1}^{1.14} + 11.21 \cdot IM_{t-1}^{1.22} + 0.12 \cdot SM_{t-1}^{2.14} - 1.93 \cdot HP_t^{0.47}, 0] \,, \quad (3.6)$$

$$SSC_t = 0.08 \cdot Q_t^{2.63} \,, \quad (3.7)$$

where SSC_t is measured in dg l^{-1}, the hydroclimatic variables ER_{t-1}, IM_{t-1}, SM_{t-1} and HP_t are expressed in mm day^{-1}, and mean daily discharge Q_t is expressed in mm day^{-1}. The values of the parameters of the traditional RC are in agreement with a previous study on the upper Rhône basin (Loizeau and Dominik. 2000).

Table 3.1 compares the performances of the HMRC and RC in reproducing mean daily observed SSC_t as measured by the coefficient of determination R^2, Nash−Sutcliffe efficiency NSE, and root mean squared error RMSE, over the calibration and validation periods. The HMRC and the RC both show satisfactory performance over the calibration period, e.g. NSE close to 0.6 in both cases, despite the fact that the HMRC does not use observed discharge in the estimation of SSC_t. While the performance of the RC drops in the validation period (e.g. NSE equal to 0.42), the HMRC retains satisfactory performance (e.g. NSE equal to 0.61 and lower RMSE). Fig. 3.6 contrasts the HMRC and the RC estimates of mean monthly SSC with SSC derived from observations of NTU from Eq. (3.1).

It is evident that HMRC is better capable to reproduce the seasonal sediment dynamics in all seasons except early spring (February-April). The traditional RC follows discharge seasonality and significantly overestimates SSC in winter and June, generates an early SSC peak, and underestimates SSC in summer (July-September). Perhaps most importantly, mean monthly values of SSC predicted by HMRC in summer, when the amount of sediment transported in suspension is at its highest, are satisfactorily similar to observations.

The values of the parameters indicate that IM generates by far the greatest contribution to SSC_t per unit volume of water, followed by ER and SM. The coefficient of the hydropower releases is negative, i.e. water fluxes released from hydropower reservoirs poor in sediment reduce SSC_t in the downstream river by dilution. Over the observation period, IM represents the largest contribution to SSC_t with a mean annual relative contribution equal to almost 40%, followed by ER and SM contributing on average respectively 34%

and 26% of SSC_t. Fig. 3.7 shows the mean monthly contribution to SSC_t of ER, IM and SM averaged over the observations period. As expected, while IM contributes to SSC_t especially during summer months (July-September), the fraction of SSC_t carried by SM is higher in spring during the snowmelt season (April-June). The effect of erosive rainfall is more evenly distributed throughout the year, and intensified in summer (July-August) when the fraction of the catchment free from snow is at its maximum and rain intensities are high.

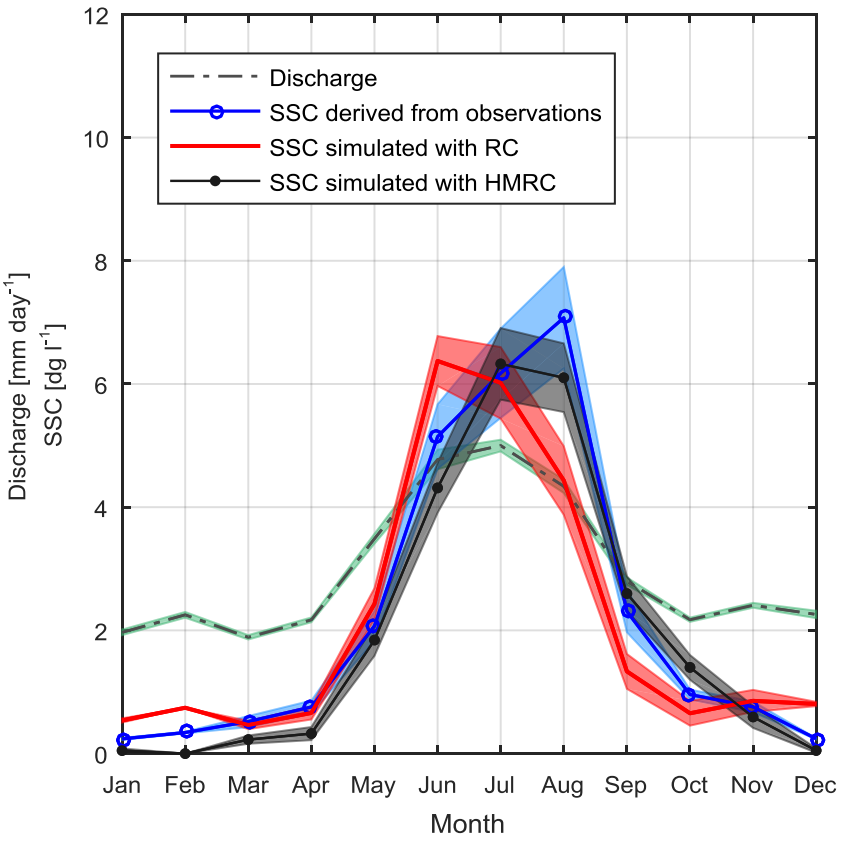

Figure 3.6: Mean monthly values of discharge measured at the outlet of the catchment (dash-dot grey line), SSC_t derived from observations of NTU (solid blue line with circles), SSC_t simulated with the traditional RC (solid red line), and with the HMRC (solid black line with dots). Coloured shaded areas represent the range corresponding to ± standard error. Mean values and standard errors are computed over the entire observation period.

3.4.2 Long-term changes in SSC

We simulate the HMRC and the traditional RC over the 40-year period 1975-2015 at a daily resolution and compare the two simulations with observations over the same period.

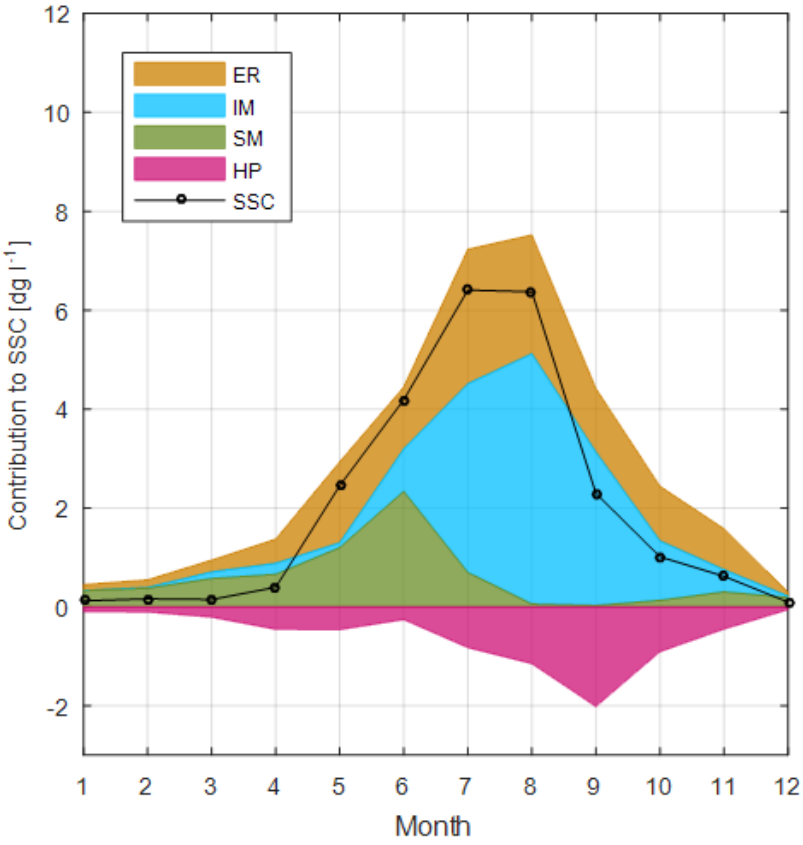

Figure 3.7: Mean monthly values of SSC_t computed with HMRC (black line with circles). Coloured areas represent the mean monthly contribution to SSC_t of ER_{t-1}, IM_{t-1} and SM_{t-1} and HP_t (dilution) averaged over the observation period.

We sample only SSC values on days when real twice-a-week observations were taken, to make a fair comparison with observed values which exhibited a jump in 1987. A two-sample two-sided t-test for equality of the mean around this point does reveal a statistically significant jump (5% significance level) only in mean annual SSC values simulated with HMRC and not with RC, if the actual time of the change is known a priori. Also, if we assume that the time of change is not exactly known, and we compute the probability distribution functions of SSC in two separated periods before and after the observed rise in SSC (namely 1975-1990 and 2000-2015), we conclude that the observations show different distributions in the two periods (Fig. 3.8a) and that only the HMRC simulation reproduce similar distributions (Fig. 3.8b) but not the traditional RC (Fig. 3.8c).

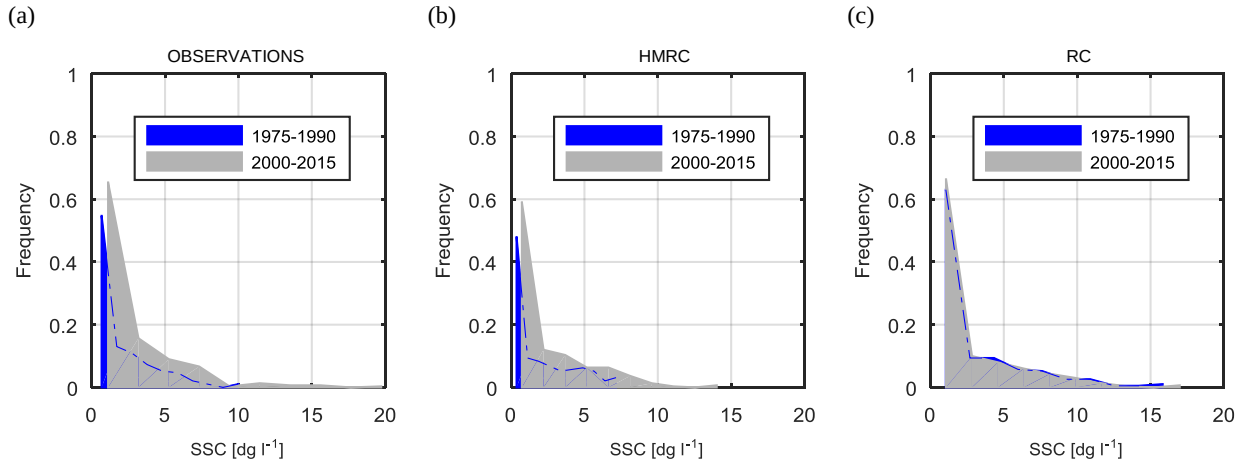

Figure 3.8: Empirical probability density functions of mean monthly SSC computed on twice-a-week samples: (a) observed, (b) simulated with HMRC, and (c) with traditional RC for two 15-year periods 1975 - 1990 (blue) and 2000 - 2015 (grey).

3.5 Discussion

The robustness of the hydroclimatic predictors of SSC in this work depends on the hypothesis that the hydroclimatic variables are independent drivers which activate different sediment sources in Alpine catchments. Indeed the high fraction of the daily SSC_t variance explained by the first three hydroclimatic variables selected by the IIS algorithm, ER_{t-1}, IM_{t-1}, and SM_{t-1}, is in accordance with the physical processes underlying the erosion and sediment transport dynamics in such environments. The higher intensity that characterizes rainfall events in comparison to the melting components is more likely to generate peaks of SSC during heavy rainfall and floods. In accordance, ER is responsible for a large fraction of the process variability (75%). Indeed, intense rainfall events can

detach and mobilize large amounts of sediment (Wischmeier, 1959; 1978; Meusburger et al., 2012). The sharp rise in streamflow, which typically follows a precipitation event, results in an increase in sediment transport capacity that may further entrain sediment previously stored along channels. Precipitation is also one of the main triggering factors of mass wasting events, like landslides and debris flow (e.g. Caine, 1980; Dhakal and Sidle, 2004; Guzzetti, 2008, Leonarduzzi et al., 2017), in which large quantities of sediment may be instantly released to the river network (e.g. Korup et al., 2004; Bennet et al., 2012). Conversely, the physical processes of icemelt-driven erosion and sediment transport are more gradual and continuous. Similarly, the slow and continuous effect of snowmelt-driven runoff on hillslope and channel erosion contributes to the seasonal pattern of SSC and plays a secondary role in explaining its daily variability and peaks in SSC. Interestingly, hydropower releases do not influence significantly the variance of SSC at the daily scale, despite the fact that the Rhône Basin is heavily regulated by hydropower reservoirs. This is most likely related to the fact that water fluxes downstream of Alpine hydropower dams have lower concentrations of suspended sediment compared to fluxes entering the reservoirs, due to sediment trapping in the reservoirs (Loizeau and Dominik. 2000; Anselmetti et al., 2007). This is in agreement with results of the sediment fingerprinting analysis recently performed in the catchment, which suggests the underrepresentation of sediments originated in the most highly regulated lithological unit (Stutenbecker et al., 2017). This is also indicated by the negative coefficient of HP, which suggests that hydropower releases dilute suspended sediment in the HMRC model and therefore leads to a reduction of SSC_t compared to natural flow. It should also be noted that the effect of hydropower reservoirs on sediment storage is grain size dependent (e.g. Anselmetti et al., 2007) and may be substantially different for coarser grains transported as bedload. Moreover, it is necessary to consider that this analysis focuses on the effects of hydropower on daily suspended sediment dynamics at the basin scale, and neglects potential effects at sub-daily scale and localized in tributary catchments. For example, the instantaneous and intermittent flushing of sediment downstream of water diversions infrastructures, located at the most upstream headwater streams, may have substantial effects locally.

We calibrate and validate a rating curve based on the hydroclimatic variables selected by the IIS algorithm and hydropower releases (HMRC) and a traditional rating curve (RC) based on discharge only. While both the HMRC and the traditional RC show similar performance in calibration, the HMRC by taking into account the physical processes which govern SSC in a more direct way, performs better in validation, simulates more accurately the seasonal pattern of SSC, especially in summer when melting of snow and ice are active and a large fraction of the catchment is snow free and subject to erosion by rainfall. The traditional RC overestimates SSC in winter because it relies on streamflow

only and does not account for the low concentration of sediment coming from hydropower reservoirs.

On the basis of the HMRC parameters, we find that although ER is responsible for the peaks of SSC and therefore, contributes the most to the variance of SSC, IM fluxes generate the highest SSC per unit volume of water. This is in agreement with the fact that meltwater originated in glaciated areas is characterized by very high sediment concentrations (Gurnell et al., 1996; Lawler et al., 1992). For a catchment significantly glacierized such as the upper Rhône basin (roughly 10% of the surface is covered by glaciers) this implies also that among the hydroclimatic variables, IM represents the greatest contribution to SSC and suspended sediment yield from this Alpine catchment (as shown in Fig. 3.7). This supports the findings of Costa et al. (2017) where the authors show that the increase in SSC observed at the outlet of the Rhône Basin in mid-1980s is most likely due to a significant rise in icemelt fluxes due to the enhanced glacier retreat associated with warmer temperatures. In concurrence with increasing icemelt, the mean annual SSC at the outlet of the catchment generated by IM, as simulated by the HMRC, increases after mid-1980s (Fig. 3.9). This explains why the HMRC is capable of simulating the observed shift in SSC, although the simulation resembles more a gradual increase than a sudden jump. The results show that a more process based rating curve accounting for the different hydroclimatic forcing can not only separate the relative effects of the different forcings on SSC, but also explain climate-driven changes in suspended sediment dynamics, which is not possible by adopting a traditional rating curve based on discharge alone.

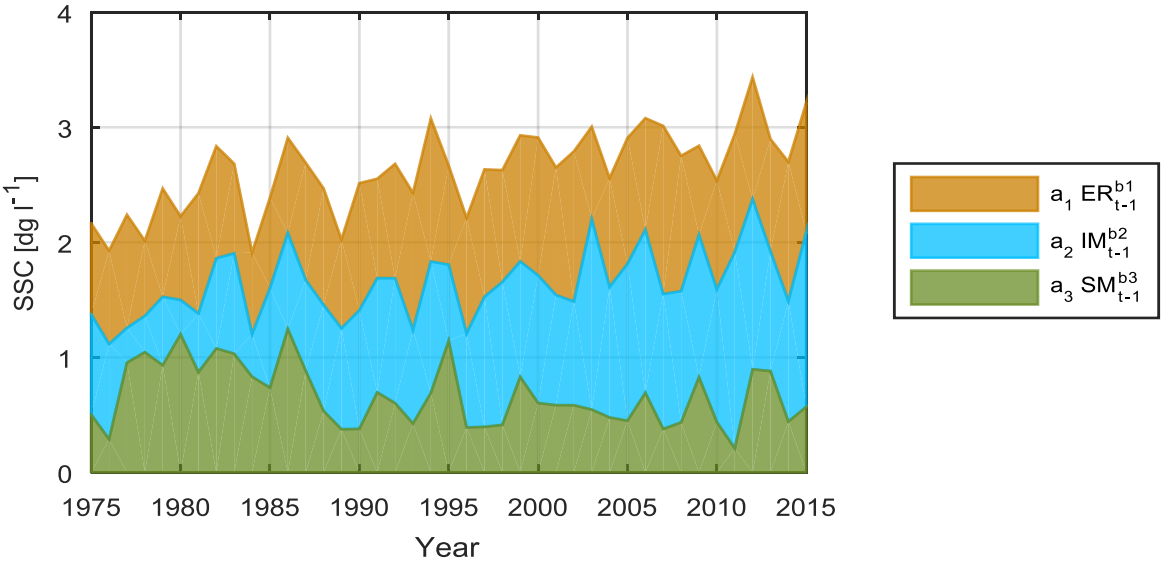

Figure 3.9: Mean annual contribution to SSC of ER_{t-1}, IM_{t-1} and SM_{t-1} simulated with the HMRC.

3.6 Conclusions

In this paper, we analyse how hydroclimatic factors influence suspended sediment concentration (SSC) in Alpine catchments by differentiating among the potential contributions of erosional and transport processes typical of Alpine environments, driven by (1) erosive rainfall (ER) defined as liquid precipitation over snow free surfaces, (2) icemelt (IM), and (3) snowmelt (SM). For regulated catchments, we include the potential effect of hydropower by considering the contribution to SSC of fluxes released from reservoirs due to hydropower operations (HP). We obtained the hydroclimatic variables ER, SM, IM by using a conceptual spatially distributed model of snow accumulation, snow and ice melt driven by precipitation and temperature at a daily resolution and we computed HP via a unique virtual reservoir which was operated on the basis of a target volume function, which is aimed at reproducing the cumulated effect of the historical operations of the several hydropower facilities. We then used the Iterative Input Selection (IIS) algorithm to select the variables that play a significant role in predicting SSC and to quantify their relative importance and predictive power in simulating observed changes in SSC in the Rhône Basin over a period of 40 years. We tested our approach on the upper Rhône basin in Switzerland. Our main findings can be summarized as follows. (1) The three hydroclimatic processes ER, IM, and SM are significant predictors of mean daily SSC at the outlet of the upper Rhône basin, explaining respectively 75%, 12% and 4 % of the total observed variance; hydropower releases HP do not play a significant role in defining the variance of SSC most likely because fluxes released from reservoirs are poor in sediment due to sediment trapping. The characteristic time lag of 1 day for the ER, IM and SM fluxes, representing the time necessary to produce sufficient runoff and to entrain and transport sediment from a given location in the catchment to the outlet, are in agreement with typical concentration times of the catchment; conversely for HP the time lag is lower than one day.

(2) Although ER is responsible for the greatest fraction of the variability of SSC at a daily basis, coefficients of the HMRC indicate that IM generates the greatest contribution to SSC per unit of water volume and contributes the most in terms of mean annual sediment yield. This is in agreement with the high suspended sediment concentration that characterizes icemelt fluxes and with finding of previous studies that indicate the increase in icemelt as most plausible explanation of changes in suspended sediment dynamics in the catchment (Costa et al., 2014).

(3) The HMRC is capable of reproducing the pattern of SSC even though it does not include discharge as an input variable. Although the HMRC and traditional discharge based RC perform similarly in simulating observed SSC over the calibration period, the

HMRC performs better than the traditional RC in validation at the daily scale, and in capturing seasonality, especially in summer when SSC are highest. This is particularly relevant because more than 66% of the total suspended sediment load reaching the outlet of the upper Rhône basin in the observation period is transported by SSC values larger than the 90^{th} percentile.

(4) With the HMRC approach we are able to reproduce changes in SSC in the past 40 years that have occurred in the catchment due to a temperature change, and we can demonstrate that the shift in SSC is most likely due to the increase in icemelt fluxes.

In summary, our approach provides an insight on how hydroclimatic variables control SSC dynamics in Alpine catchments, and the results suggest that a more process and data informed approach in predicting suspended sediment concentrations, which accounts for sediment sources and transport processes driven by erosive rainfall, snowmelt and icemelt, instead of only discharge, allows to analyze climate-induced changes in sediment dynamics. Although these results are specific for the upper Rhône basin only, the approach is general and may be employed in other Alpine catchments with pluvio-glacio-nival hydrological regimes where sufficient data are available.

Author contribution A. Costa, D. Anghileri and P. Molnar designed the methodology. A. Costa and D. Anghileri developed the code and carried out simulations and computations. All co-authors contributed to the manuscript. The authors declare that they have no conflict of interest.

Acknowledgments We thank the Federal Office of the Environment (FOEN) for providing discharge, suspended sediment concentration and turbidity data. We also thank Alessandro Grasso (FOEN) for the explanation on the SSC and turbidity measurement procedures. This research was supported by the Swiss National Science Foundation Sinergia grant 147689 (SEDFATE). Daniela Anghileri was supported by the Swiss Competence Centre on Energy - Supply of Energy (SCCER-SoE).

3.7 Supplementary Material

Table 3.2: List of the main 13 hydropower reservoirs included in this study and their capacity.

Name	Capacity $[10^6 m^3]$
Griessee	18
Mattmark	100
Moiry	77
Grande Dixence	400
Mauvoisin	211.5
Les Toules	20
Emosson	205
Salanfe	40
Tseuzier	50
Cleuson	20
Gibidum	9.2
Illsee	6.6
Arnensee	10.3

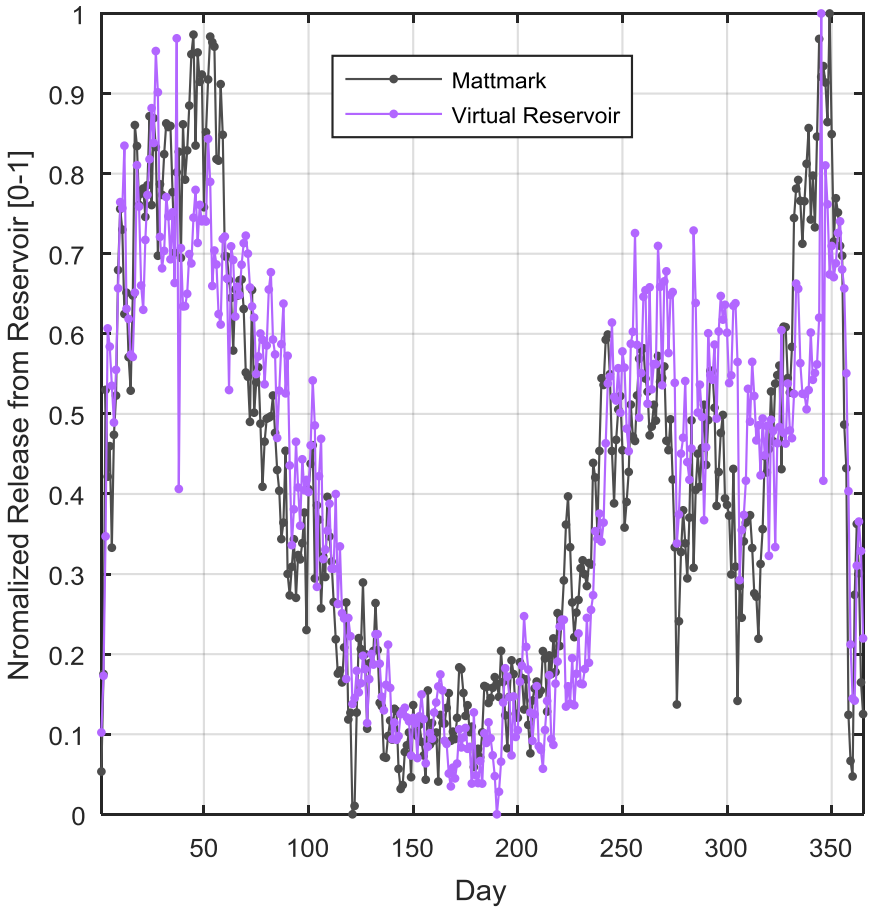

Figure 3.10: Mean daily normalized water release from the hydropower reservoir Mattmark (average of observations over the period January 1994 - December 2015) and from the virtual reservoir (average of simulations over the period January 1975 - December 2015).

Chapter 4

Flow Regulation in Alpine Rivers: a Network-Based Model to Investigate the Impacts on Bedload and Grain Size Distribution*

** Costa A, Molnar P, Schmitt RJP and Burlando P (submitted) Flow Regulation in Alpine Rivers: a Network-Based Model to Investigate the Impacts on Bedload and Grain Size Distribution. Water Resources Research*

Figure 4.1: View of the upper Rhône River at Pfynwald (by F. Textor).

Abstract

Hydrology in alpine catchments is often subject to flow regulation by hydropower on top of climate-induced changes in runoff generation. The changes in streamflow affect sediment transporting capacity throughout the river network. Sediment dynamics are also impacted by a reduction in sediment supply due to sediment trapping in reservoirs. The cumulative impacts of these changes on the spatio-temporal dynamics of bedload are generally poorly understood. We present a model-based evaluation of these effects on a river network scale for a large Alpine catchment, the upper Rhône Basin. The river network is conceptualized as a series of connected river links. The model simulates 1-D flow, bedload, channel bed grain size distribution (GSD), and erosion and deposition. Discharge in the river network is simulated by a physically-based hydrological model including hydropower infrastructure. We apply the model to quantify the impacts of hydropower operation on bedload and the GSD, by comparing pre and post-dam scenarios. Results indicate that hydropower operation has substantially reduced bedload, especially in summer and for coarser grains. After hydropower, deposition is higher and erosion is lower, with insignificant changes in their spatial distribution. Likewise, river bed GSDs do not show systematic changes, with local effects visible at longer time scales only. Results show that the hierarchical structure of the river network controls the impacts of perturbations by structuring their effects, which are either enhanced or dampened in the downstream direction. The approach may be useful for analyzing river network scale impacts of perturbations on bedload in other Alpine catchments.

4.1 Introduction

Dams and hydropower infrastructures are known to affect the geomorphology and ecology of fluvial systems on reach and network scales (e.g. Gabbud and Lane, 2016; Graf, 2006; Williams Wolman, 1984). Reservoirs and flow regulation associated with their operation disrupt the natural streamflow and sediment regime by creating discontinuities between upstream and downstream reaches (e.g. Andrews, 1986; Bakker et al., 2018; Csiki and Rhoads, 2014; Curtis, et al., 2010; Petts and Gurnell, 2005; Schmidt and Wilcock, 2008; Surian and Rinaldi, 2003; Williams Wolman, 1984). At the global scale, sediment trapping behind reservoirs substantially decreases sediment load reaching coastal areas, increasing the risk of coastal erosion (Syvitski et al., 2005). Erosion and sediment transport are particularly relevant processes in mountainous regions. Steep slopes, the presence of coarse grains, the strong coupling to hillslopes, and specific stream morphologies (e.g. Montgomery Buffington, 1997), make predictions of bedload and their changes complex und uncertain (e.g. Rickenmann, 2001). Sediment transport in steep streams also represents a

natural hazard during extreme events when large amounts of sediment may be mobilized (e.g. Hilker et al., 2009; Rickenmann Koschni, 2010; Turowski et al., 2009). Hydropower effects are most strong in Alpine regions where dams and reservoirs of all sizes are located on many streams, and snowmelt and ice melt-fed rivers represent a crucial resource for hydroelectric energy production. In common hydropower schemes, runoff from headwater catchments is collected and stored in reservoirs during the melting season, in spring and summer, and released in winter for energy production. As a result, the hydrological regime of downstream reaches is less variable, the sediment transporting capacity of the flow is affected, and ultimately sediment transport is impacted.

Sediment trapping behind dams generally leads to downstream erosion, because sediment supply is reduced, which often results in channel narrowing and vegetation encroachment, (Andrews, 1986; Petts and Gurnell, 2005; Schmidt and Wilcock, 2008; Williams Wolman, 1984). Previous studies have shown that flow regulation generally leads to degradation just downstream of dams, followed by a gradual aggradation further downstream (Curtis et al., 2010; Williams Woman, 1984; Petts Gurnell, 2005). Based on observations of over 20 regulated alluvial rivers in western USA, Williams and Woman (1984) suggested that hydropower results in sediment coarsening downstream of reservoirs, followed by a phase of stabilization and subsequent fining (Williams and Woman, 1984). However, the effects of hydropower on bedload and river bed grain size distribution are not easily predictable because of the non-linearity and threshold nature of sediment transport (e.g. Rickenmann, 2001; Shields, 1936), because sediment transport is closely linked to sediment supply (e.g. Montgomery and Buffington, 1997; Saletti et al., 2015) and because of the high spatial variability in channel morphology.

Furthermore, previous studies have demonstrated that to analyze the impacts of local perturbations of sediment transport along rivers it is necessary to apply an approach which accounts for the entire river network (e.g. Benda and Dunne, 1997; Czuba and Foufoula-Georgiou, 2014; Czuba and Foufoula-Georgiou, 2015; Ferguson et al., 2015; Schmitt et al., 2016). These studies have demonstrated the effects of perturbations, such as instantaneous sediment inputs, changes in sediment transport capacity, reduced sediment supply, propagate along the river network and are either emphasized or dampened in the downstream direction (e.g. Benda and Dunne, 1997; Williams and Wolman, 1984). Moreover, spatially and temporally separated perturbations can aggregate along the river network and amplify the impacts in the downstream direction (e.g. Czuba and Foufoula-Georgiou, 2014). Especially in catchments characterized by high elevation gradients, river morphology changes rapidly and alterations in riverbed conditions may have strong effects on hydraulics and sediment transport. In addition, spatial variability of sediment sources

may result in different responses of the fluvial system to the same hydrological conditions (Schmitt et al., 2018a).

In the literature, there are different modelling approaches to analyze human impacts on sediment transport at the river network scale. For example, by representing sediment transport from each source as a suite of individual cascading processes, Schmitt et al. (2016) developed a modelling framework to evaluate sediment connectivity at the river network scale. This modelling framework provides information on patterns of sediment connectivity and dis-connectivity, i.e. locations of bottlenecks. Ferguson et al. (2015) implemented a river network model for bedload transport to investigate the impacts of mining activities along the main stem of the Fraser River in Canada. Their simulations showed the interaction of changes in flow and sediment supply on grain size distributions, and demonstrated that mining resulted in rapid bed fining, which ultimately led to a major increase in bed load transport in the mining area and significant sediment export to downstream reaches (Ferguson et al., 2015). However, none of these frameworks was developed explicitly for the cumulative, network-scale effects of dam sediment trapping and changed hydrographs on sediment connectivity and bedload transport. In this paper we develop a network modelling approach to study the effects of hydropower reservoirs and flow regulation on bedload transport in a large Alpine catchment, the upper Rhône Basin in southern Switzerland, which has been intensively regulated by hydropower since the 1960s. Many large hydropower facilities are operating in the catchment. Water from upstream channels is either directly impounded in reservoirs or extracted at water intakes and diverted to reservoirs through a complex network of tunnels and pumping stations (Bakker et al., 2018). While the large storage reservoirs in the basin likely trap all coarse sediment, reducing the sediment supplied to downstream river reaches, at water intakes sediment is still transferred downstream through periodic flushing. Equally important is streamflow regulation below intakes and dams, which dramatically changes the flow throughout the entire Rhône Basin (e.g., Fatichi et al., 2015) and hence potentially the transport capacity. The impacts of these basin scale modifications on sediment supply and transport are potentially further compounded with natural climatic variability and climate change which is likely to have major impact on a partially glacierized basin.

In this paper, we hence explore the compounding human impacts on bedload, bed grain size distributions and erosion and deposition patterns at the river network scale. The main objectives are (1) to quantify the effects of hydropower on bedload rates, (2) to estimate erosion and deposition with and without hydropower and identify possible changes in their spatial patterns, (3) to evaluate how alterations in sediment transport due to hydropower reflect on the river bed grain size distribution at the river network scale, (4) to explore how perturbations of sediment supply and sediment transport capacity caused by up-

stream hydropower operation propagate along the river network and how the hierarchical structure of the river network filters these perturbations, (5) to explore the sensitivity of bedload transport to hydrological change (e.g. warmer temperatures), and (6) to disentangle the compounding effect of flow regulation and sediment storage in reservoirs. To this end, we develop a river network bedload model in which the river network is conceptualized as a series of connected links. The model simulates 1-D flow, bedload transport, channel bed grain size distribution, and erosion and deposition, given discharge and geometric characteristics of the channels. We apply the model to the upper Rhône Basin under different scenarios representing the conditions before and after the construction of the hydropower system. Discharge values are simulated with the spatially-distributed, physically-based hydrological model Topkapi-ETH for both scenarios, assuming climatic conditions of the period 1997-2008 (Fatichi et al, 2015). The model is also used to evaluate long-term changes (100-year simulation), and to explore the sensitivity of streamflow and bedload response to warmer temperatures under climate change scenarios. The aim is to provide a framework for quantifying concurrent change in hydrology and sediment transport across the river network of a regulated catchment that can be applied in other Alpine systems with similar conditions.

4.2 Study Area and Data

The upper Rhône River drains an area of almost 5338 km2 from the Rhône Glacier to Lake Geneva (Figure 1). More than 10% of the catchment surface is covered by glaciers (Figure 1), including the Aletsch Glacier, which is the largest glacier in the European Alps. The basin covers a wide elevation range (370 to 4634 m a.s.l). Bedrock is composed of three main litho-tectonic units with different erodibilities (Figure 1): the Penninic domain with oceanic metasedimentary and ophiolitic rocks, the External Massifs constituted of variscan crystalline rocks, and the Helevetic Nappes characterized by calcareous metasedimentary rocks of the European continental margin (Stutenbecker et al., 2016). The main stem of the upper Rhône River is roughly 170 km long. Several important tributary catchments contribute discharge to the main valley (Stutenbecker et al., 2017). The longitudinal profiles of these tributaries range from almost undisturbed concave to s-shaped (concaveâconvex), to almost completely convex profiles reflecting glacial inheritance (Stutenbecker et al., 2017). Channel gradients vary also widely, from 0.04% along the downstream reaches on the main river to 15% in headwater channels.

Anthropogenic activities have strongly influenced the hydrological and sediment regime of the catchment during the last century. Two major projects of channelization were im-

plemented along the main course of the river for flood protection purposes in late 19^{th} and early 20^{th} centuries, significantly reducing the length of the active channel (Weber et al., 2007). Gravel mining operations are today carried out along the main channel and some tributaries also to reduce flood risk. Since 1960s several large dams have been built in the catchment reaching a storage capacity of roughly 20% of the total annual volume of water discharged into the Lake Geneva (Loizeau and Dominik, 2000). A complex network of water intakes, tunnels, and pumping stations extract water from channels and transfer it to the reservoirs (Bakker et al., 2018). Water diversions and flow regulation associated with hydropower operations have led to significant alteration of the flow regime of the catchment (Fatichi et al., 2015). However, the effects of hydropower vary greatly along the river network, from almost no flow downstream of dams and intakes, to seasonally regulated discharge downstream of hydropower stations where summer flow is reduced and winter flow is increased, to reaches with natural runoff production and practically no effects on the flow regime. The sediment regime is also affected by hydropower. For suspended sediment transport, previous studies show that flow regulation may play a secondary role compared to climatic forcing (Costa et al., 2018b). An increase in suspended sediment concentration at the outlet of the upper Rhône Basin was observed in the mid-1980s when hydropower was already in full operation for a period of more than 10 years. This increase in suspended sediment transport, which occurred simultaneously with a jump in basin mean air temperature, has been linked to the enhanced ice melt and glacier retreat observed in those years (Costa et al., 2018a). For bedload transport, instead, sediment transport might have been reduced because of flow regulation reducing peak flows and hence transport capacity. Moreover, sediment trapping behind reservoirs might have reduced the availability of sediment, and operations of water intakes might have altereed bedload dynamics by delaying sediment transfer downstream (Bakker et al., 2018).

For the present work we used the datasets listed in Table 1. Sediment transport in the river network is driven by discharge which is simulated with the spatially distributed, physically based watershed model Topkapi-ETH (Fatichi et al., 2015) for the period 1992-2008. This model uses precipitation, air temperature and cloud cover as climatological input. River network topology and channel reach geometry are derived from a high resolution (10 Ã 10 m) digital elevation model (DEM) and aerial photographs. The location and volume of reservoirs and the intake network and typical hydropower operation rules were taken from the Swiss Federal Office for the Environment and from the archive of the Swiss Committee on Dams. Areas of the catchment affected by hydropower are depicted in Figure 1 in light blue. We measured the grain size distribution GSD of the river bed at 10 locations: 7 along tributaries and 3 along the main river. Sediment size was sampled by three different

methods: by linear sampling as described in Fehr (1987), by the Wolman grid method (Wolman, 1954), and with BASEGRAIN, which is a semi-automated digital pebble count method available in Matlab (Detert and Weitbrecht, 2013).

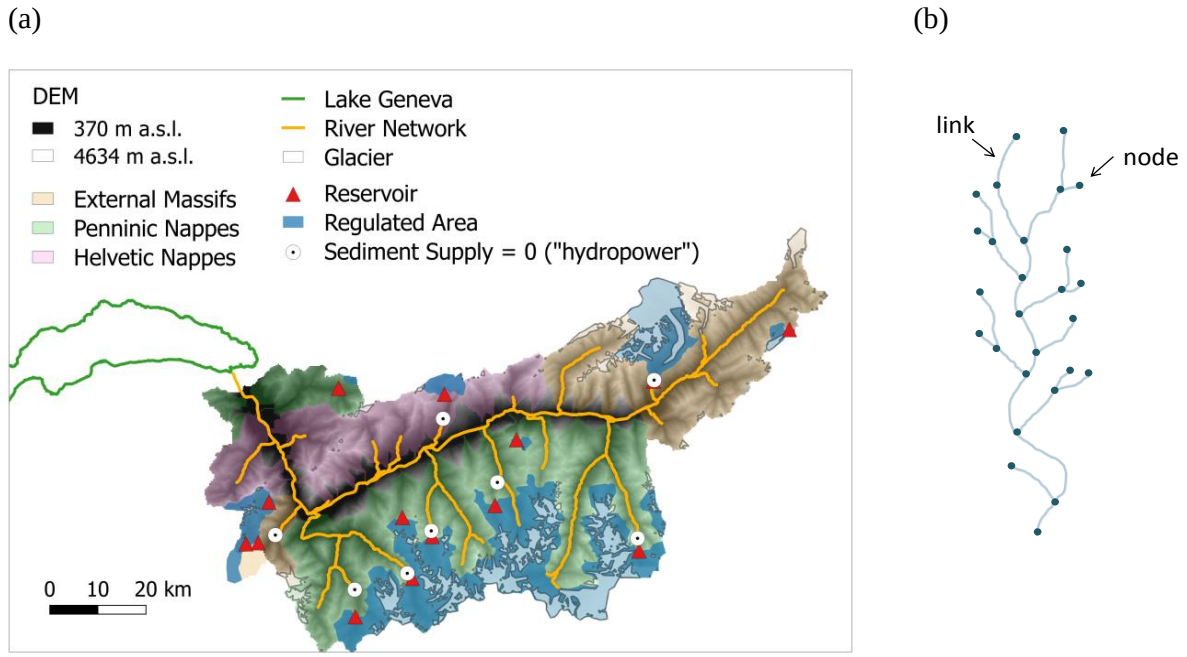

Figure 4.2: (*a*) Map of the upper Rhône Basin representing topography (DEM), main lithological units, glaciers (white area), river network, major reservoirs (red triangle), areas regulated by hydropower (blue shaded area), links downstream of main reservoirs, where sediment input is set equal to zero in the "hydropower" scenario. (*b*) Scheme of the river network with links and nodes.

Table 4.1: List of major data products and sources used in this study.

Data	**Source**
Gridded Daily Precipitation (2x2 km) - RhiresD	Swiss Federal Office of Meteorology and Climatology (MeteoSwiss)
Hourly Precipitation at 9 stations	”
Hourly temperature at 16 stations	”
Short wave incoming solar radiation at 12 stations	”
Digital Elevation Model (DEM) 250 x 250 m resolution	ETH Geodata Portal
Global Land Cover Product (GlobCover)	ESA
Glacier Cover	GLIMS Glacier Database
Soil Map	Agroscope
Map of agricultural areas	Swiss Federal Office for the Environment (FOEN)
River diversion information - “Restwasserkarte”	”
Reservoir information	Swiss Committee on Dams
Digital Elevation Model (DEM) 10 x 10 m resolution	Swiss Federal office of Topography (Swisstopo)
Grain Size Distribution at 10 locations	ETH-IfU

4.3 Methods

The river network model simulates 1-D flow, bedload transport rates, channel bed volume and grain size distribution along streams in the network, given discharge and geometric characteristics of the channel links. We apply the model with different scenarios representing pre- and post-dam conditions. We compare the results of the simulations to assess the impacts of hydropower on bedload and river bed grain size distribution at the network scale.

4.3.1 River Network Model

The river network is conceptualized as a series of river reaches, which we call links, joined by nodes (Fig. 4.2b). We first extract the river network on the basis of the 10 x 10 m digital elevation model (DEM) in QGIS using a threshold area for channel initialization of 5 km2 . We choose this threshold to obtain a satisfactory level of detail in reproducing the mapped river network. The resulting Strahler orders of the streams are from 1 to 3 (Horton, 1945; Strahler, 1952). We divide the river network of the Upper Rhône Basin into 82 links, roughly 10 km long (Fig. 4.2a). We use the DEM to derive the average slope and the length of each link. We estimate the average channel width on the basis of multiple measurements (roughly 20 per link) derived from satellite images (Google Earth Pro). These geometric characteristics of the river network are assumed constant throughout the simulations.

At the link scale, the balance between transport capacity and sediment supply determines bedload transport and quantifies erosion and deposition for multiple grain size classes. Volumetric bedload transport rates Q_{b_i} of each grain size class i are computed as the minimum between transport capacity Q_{tc_i} and sediment supply Q_{ss_i} (Q_{b_i}= min [Q_{tc_i},Q_{ss_i}]). If sediment transported from an upstream link (Q_{IN_i}) is larger than the transport capacity, deposition occurs. Otherwise sediment is eroded from the channel bed if available,

$$\frac{dz}{dt} = Q_{IN_i} - Q_{b_i} \tag{4.1}$$

where z is channel bed elevation. The transport capacity (Q_{tc_i}) is computed with a revised version of the Wilcock and Crowe (2003) method, accounting for increased flow resistance in steep streams. Sediment supply (Q_{ss_i}) is the sum of sediment entering the link from upstream links (Q_{IN_i}) and sediment available in the channel bed. Likewise, the GSD of the sediment potentially transported is obtained by combining the GSDs of the sediment

input from upstream links and of the sediment available to be eroded from the channel bed in the link. We do not account for sediment supplied by hillslopes along the links, but we allow for in-channel bed and bank erosion.We do also not account for sediment removal due to gravel mining activities and river works, because no data on local extractions in each link are available to our knowledge. In each time step, sediment is routed along the river network and the grain size distribution of the channel bed is updated according to erosion/deposition of each grain class. The time step of analysis is 1 day.

We consider that the channel bed is divided into two layers, an active layer and a substrate layer. Following the approach of Ferguson et al. (2015), we assume that gravel is deposited in the active layer, while 50% of the deposited sand enters the substrate layer. Sediment is eroded from the substrate layer only if the active layer is completely depleted. We set the initial depth of the active layer equal to 3 d_m where d_m is the mean grain size (Ferguson et al., 2015).

In the network model we consider 15 grain size fractions ranging from fine sand (0.0125 cm) to large boulders (150 cm): four classes of sand, five classes of gravel, cobbles, and five classes of boulders. Settling velocity w_s is computed with the equation of Ferguson and Church (2004), and the ratio $w_s/\mathrm{u}^* < 0.3$ (Dade and Friend, 1998), where u* is shear velocity, is used to calculate the grain size transported as bedload. We exclude fractions finer than fine sand because in two third of the links grains finer than 0.125 mm are always transported in suspension.

Under the assumption of a prismatic rectangular cross section and normal flow conditions, we compute the water depth in each link with an iterative procedure. We use the flow resistance equation proposed by Ferguson (2007),

$$\sqrt{\frac{8}{f}} = \frac{a_1 a_2 (h/d_{84})}{a_1^2 + a_2^2 (h/d_{84})^{5/8}} \tag{4.2}$$

where f is the dimensionless Darcy-Weisbach friction factor, h is the flow depth, d_{84} is the grain size for which 84% of the sediment is finer, and a_1 and a_2 are dimensionless empirical constants. In applications in which more detailed information about cross sections is available, it can be included in the modelling procedure. Based on a large field dataset, Rickenmann and Recking (2011) evaluated the performance of several resistance equations in predicting flow velocity for gravel-bed rivers. They show that the variable-power equation of Ferguson (2007) with a_1=6.5 and a_2=2.5 presents the best performance (Rickenmann and Recking, 2011). Moreover, it is applicable for gravel-bed rivers both with shallow and deep flows (Ferguson et al., 2007) and it can be used to predict flow velocity over a wide range of discharges.

We estimate transport capacity with the Wilcock and Crowe surface-based transport model for multiple grain sizes (Wilcock and Crowe, 2003). The model is for transport of mixed sand and gravel. It was developed using flume measurements of flow, sediment transport and bed surface grain size, covering a wide range of flow conditions and grain sizes (Wilcock et al., 2001). The model is built on concepts of previous surface-based transport models (Parker, 1990; Proffitt and Sutherland, 1983), but it includes a nonlinear effect of sand content on gravel transport rate (Wilcock and Crowe, 2003).

Traditional bedload transport equations often overestimate bedload transport in steep streams because flow resistance due to macro-roughness is not accounted for (e.g. Lamb et al., 2008; Nitsche et al., 2011; Rickenmann, 2012; Yager et al., 2007). Channel morphology (e.g. plane-bed, step-pool, cascade), larger structural bed stability, the presence of immobile boulders, bedrock constrictions and large woody debris contribute to increase flow resistance (Schneider et al., 2015). Besides drag resistance due to channel banks and bed morphology, Lamb et al. (2008) include variable friction angles, grain emergence, flow aeration, changes in local flow velocity and turbulent fluctuations as the main factors increasing grain stability in steeper streams. To account for flow energy dissipation due to macro-roughness, we use a modified version of the Wilcock and Crowe model proposed by Schneider et al. (2015) in combination with the effective shear stress computed as in Rickenmann and Recking (2011) for first and second order links.

The effective shear stress $\tau^{'}$ is the shear stress available for transport after energy dissipation due to macro-roughness. $\tau^{'}$ is computed using a reduced energy slope S_{red} in place of the channel slope (Rickenmann and Recking, 2011)

$$\tau^{'} = \rho \, g \, S_{red} \, h \tag{4.3}$$

where ρ is water density (kg m^{-3}) and g is gravitational acceleration (m s^{-2}). The reduction of the energy slope is based on the concept of partitioning total flow resistance, f (Equation (4.2)), into base level resistance f_0 and macro-roughness resistance, which is defined as all additional resistance due to large roughness elements and small relative flow depths (Nitsche et al. 2011; Rickenmann and Recking, 2011).

$$S_{red} = S(\frac{f_0}{f})^{e/2} \tag{4.4}$$

where we use the exponent e equal to 1.5 according to Meyer-Peter and Müller (1948), Chiari and Rickenmann (2011) and Nitsche et al. (2011). Base level resistance f_0 is com-

puted from the Manning-Strickler equation for small-scale roughness using a_1=6.5 (Ferguson, 2007; Rickenmann and Recking, 2011; Schneider et al., 2015).

$$\sqrt{\frac{8}{f_0}} = a_1(\frac{h}{d_{84}})^{0.167} \tag{4.5}$$

The similarity collapse function of the Wilcock and Crowe model relates the ratio between bed shear stress and reference shear stress to the dimensionless fractional bedload transport rate W_i^* (Wilcock and Crowe, 2003),

$$W_i^* = \frac{R\, g\, q_{tc_i}}{u^{*3}} \tag{4.6}$$

where R=ρ_s / $\rho - 1$, ρ_s is sediment density (kg m^{-3}), u*=(τ / ρ)$^{0.5}$ is shear velocity and q_{tc_i} is volumetric transport rate per unit width of grain size i (m^3 s^{-1} m^{-1}). The modified version proposed by Schneider et al. (2015) that we use in this work refers explicitly to the effective shear stress τ' rather than the total shear stress and is expressed in terms of dimensionless shear stress $\tau_i^{*'}$

$$\tau_i^{*'} = \frac{\tau'}{R\, \rho\, g\, d_i} \tag{4.7}$$

where d_i (m) is the diameter of the grain size i. Schneider et al. (2015) estimated the similarity collapse function following the reference approach of Parker et al. (1982) on a large field dataset of fractional bedload transport rates covering a wide range of flow discharges, channel slopes and grain sizes:

$$\begin{cases} W_i^* = 0.002(\tau_i^{*'}/\tau_{ri}^{*'})^{6.82} & \tau_i^{*'}/\tau_{ri}^{*'} < 1.33 \\ W_i^* = 14(1 - \frac{0.894}{(\tau_i^{*'}/\tau_{ri}^{*'})^{0.5}})^{4.5} & \tau_i^{*'}/\tau_{ri}^{*'} \geq 1.33 \end{cases} \tag{4.8}$$

In the revised equation, the power law exponent for $\tau_i^{*'}/\tau_{ri}^{*'} < 1.33$ is equal to 6.82, the dimensionless reference shear stress $\tau_{ri}^{*'}$ is computed as described in Appendix A with a constant dimensionless reference shear stress for median grain size $\tau_{rd_{50}}^{*'}$ equal to 0.03.

4.3.2 Hydrological Input Scenarios

We simulate discharge at the upstream node of each link with the spatially distributed, physically based hydrological model Topkapi-ETH (Fatichi et al., 2015). The model is an

enhanced version of the Topkapi (Topographic Kinematic Approximation and Integration) rainfall-runoff model developed by Ciarapica and Todini (2002) and Liu and Todini (2002). The original model has been further developed for mountainous regions (Ragettli and Pellicciotti, 2012; Ragettli et al., 2013a, b).

The hydrological model is based on a cell-grid representation of the topography where cells are connected according to the maximum gradient. The routing of subsurface, overland and channel flow is based on a kinematic wave approximation (Liu and Todini, 2005), by which the original differential equations are converted into non-linear reservoir equations analytically solved at each grid cell. The subsurface is divided into three layers: the first two layers, representing shallow and deep soil are conceptualized as non-linear reservoirs, while the third layer is modelled as a linear reservoir to simulate groundwater flow. Runoff can be generated by infiltration and saturation excess runoff. The model estimates potential evapotranspiration with Priestley-Taylor equation (Priestley and Taylor, 1972), with a correction factor accounting for landuse and seasonal changes in leaf area index. Precipitation is divided in liquid and solid form with a temperature threshold. Snow and ice melt are estimated with the enhanced temperature index approach (Pellicciotti et al., 2005), incorporating incoming radiation and albedo, which is computed after Brock et al. (2000). Melt from glaciers is modelled by a temperature index method and transferred to runoff by means of a linear reservoir representing subglacial flow routing.

Topkapi-ETH allows the implementation and modelling of anthropogenic infrastructures such as water abstractions, water diversions, reservoirs, conduits to hydropower plants, and hydropower operations. Water diversions are modelled by assigning a diversion capacity between intake and return points and assuming an average transfer time of one hour, which represents the delay corresponding to average flow velocities along typical diversion channels. Reservoirs are represented using technical information (maximum and minimum regulation level, spillway, turbine and outlet capacity, volume-level curves) and are operated on the basis of target level functions.

Based on detailed information provided by the Swiss Federal Office of the Environment, Fatichi et al. (2015) implemented in the model Topkapi-ETH the hydropower scheme of the Upper Rhône Basin by including a total number of 115 conduits/diversions and the 14 main reservoirs. Diversion capacities were available from technical documentation, and target level functions for hydropower operations were obtained either from observations or by adopting normalized reference curves. The model was successfully calibrated and validated on the basis of discharge data collected at 15 gauging stations in the Upper Rhône Basin for the period 1990-2008, and snow cover maps retrieved from the Moderate Resolution Imaging Spectroradiometer (MODIS) for the period 2000-2008. Fatichi et

al. (2015) ran the calibrated Topkapi-ETH model in "natural" conditions, i.e. removing anthropogenic infrastructures, but with climatic forcing of the period 1990-2008 because high resolution meteorological data were not available for the pre-dam period. They compared simulated streamflow time series with observations available for the period before hydropower at six gauging stations within the catchment. Results confirm that the model can reproduce satisfactorily both the "hydropower" and the "natural" flow regime. For a detailed description of the model, its calibration and results of the simulations see Fatichi et al. (2015).

In this work we simulate streamflow with Topkapi-ETH for the 17-year period 1992-2008 both for the "natural" and the "hydropower" hydrological scenario, with climatic forcing of the period 1990-2008. We record hourly discharge data at each node of the river network, and we compute mean daily values which we use as input in the river network bedload transport model.

4.3.3 Initialization of Grain Size Distribution and Upstream Sediment Supply

The river network model requires an initialization of the GSD in each link. We implement here a procedure to assign initial GSD to each link which is based on a combination of coarse grain mobility during floods and available observations of GSDs in the river. We consider that the ratios between d_{90} and other characteristic grain sizes such as d_{10}, d_{16}, d_{30}, d_{50}, d_{65}, and d_{84} (where d_x represents the grain size for which x% of the sediment is finer) derived from observations are similar for the entire river network. We hypothesize that mean annual maximum discharge is responsible for mobilizing the coarse grains (d_{90}). Under the assumption of a prismatic rectangular cross section and normal flow conditions, we use a numerical iterative procedure to compute d_{90} by using the resistance equation of Ferguson (2007) (Equation 4.2), the d_{90}/d_{84} ratio, and slope-dependent values for the dimensionless critical shear stress τ^*_{cr} after Lamb et al. (2008) for every link,

$$\tau^*_{cr} = \frac{\tau_{cr}}{R\,\rho\,g\,d_{90}} \tag{4.9}$$

where τ_{cr} is the critical value of shear stress for incipient motion condition of d_{90}, which is related to flow through Equation (4.3) where slope energy is equal to channel bed slope S (instead of S_{red}). We account for the energy dissipation due to macro-roughness in steep streams to avoid overestimation of diameters of coarse grains. Besides reducing the applied shear stress as we did for transport capacity, another commonly used approach is

to increase the critical shear stress required for mobilizing sediments. By fitting a large set of experimental and field data from incipient motion studies, Lamb et al. (2008) proposed a relation between channel bed slope S and critical shear stress τ^*_{cr}

$$\tau^*_{cr} = 0.15S^{0.25} \tag{4.10}$$

which we solve for d_{90}. The numerical procedure is described in more details in Appendix B. We then compute the characteristic grain sizes listed above based on the d_{90}/d_x ratios (x = 10, 16, 30, 50, 65 and 84), and we compute the cumulative volume fraction for all the 15 sediment size fractions included in this study by linear interpolation.

A second important boundary condition is the upstream sediment supply to the links located at the most upstream end of the river network (order 1 streams). We assume that sediment supply to these links is equal to the transport capacity corresponding to the median discharge conditions. We tested different quantiles of discharge and selected the one leading to more stable quasi-equilibrium conditions, where we defined quasi-equilibrium as when the long-term change in channel bed elevation is smaller than 0.5 cm year^{-1} throughout the entire river network.

4.3.4 Initial Conditions and Scenario Analysis

After initialization of the GSD and defining the sediment supply for the most upstream links, we run the river network bedload model by using the mean daily streamflow regime obtained at each link by averaging the daily streamflow time series simulated with Topkapi-ETH in the "natural" scenario. We run the model for 75 years by repeating this mean daily regime and we check if the system reaches quasi-equilibrium conditions, i.e. if links are subject to erosion/deposition lower than 0.5 cm year^{-1}. Only few links out of 82 experienced deposition larger than 0.5 cm year^{-1} during the last ten years of simulation.

We use this quasi-equilibrium condition as the initial condition to run the river network bedload model for the 17-year period 1992-2008 with the same daily climatic input under different scenarios representing pre and post-dam conditions. The scenario with hydropower ("hydropower") represents the current conditions in the catchment where flow is regulated by hydropower operations and sediment is stored behind reservoirs. The scenario without hydropower ("natural") represents the catchment before the construction of reservoirs and reflects the natural flow regime. In addition, we analyze long-term effects by simulating both scenarios for 100 years by repeating the hydrological input of 1992-2008.

We also evaluate the relative effects of flow regulation and storage of sediment behind dams by developing a scenario in which only flow regulation is considered but sediment is not stored in the reservoirs ("hydropower â no sediment storage"). We finally explore the sensitivity of bedload transport to changes in air temperature by running the hydrological and river network model for the natural and the hydropower scenarios with discharge obtained assuming a spatially and temporally constant increase in air temperature of 1 and 2 °C. We analyze the results of the simulations by focusing on three main variables: bedload transport rates, volume of erosion/deposition, and channel bed GSD.

4.4 Results

4.4.1 Bedload Transport Rates

Water diversions and flow regulation due to reservoir operation in the Rhône Basin lead to a substantial alteration of the flow regime. In the "hydropower" scenario, the river network is subject to an average 36% reduction in discharge at the annual scale, compared to the "natural" flow regime (Table 2). The relative reduction in discharge is greater for second order links, where it reaches on average -51%, than for first and second order links in which mean values are around -39% and -12% respectively (Figs. 4.3a, 4.3b, 4.3c). Operations of reservoirs result in an overall decrease of discharge almost equal to -43% (Table 4.2) in summer (Figs. 4.4a, 4.4b) when water is diverted and stored in the reservoirs, and a relative increase in winter (Figs. 4.4c, 4.4d) when water is released for energy production. In winter, while on average the river network is subject to an increase of 45% of discharge in the "hydropower" scenario (Table 4.2), second order links are still subject to reduced flow conditions (on average -12%; Table 4.2).

Alterations of the flow regime are linked to changes in sediment transport capacity and bedload transport. Accordingly, the catchment is subject to an overall reduction of bedload transport rates with respect to the "natural" conditions (Figs. 4.3d, 4.3e, 4.3f, 4.4e and 4.4f, Table 4.2). As a result, the southern part of the catchment, where the major hydropower reservoirs are operating, experiences a substantial reduction in bedload (Figs. 4.4e and 4.4f). While some first order links are not or only slightly affected by "hydropower" (Fig. 4.3d), effects are observable in all second and third order links (Figs. 4.3e and 4.3f). For second order links, the relative reduction in bedload rate is substantially greater than for first and third order links (Table 2; Fig. 4.3d, 4.3e and 4.3f): median values of changes are respectively equal to -91% for second order links, and -47% and -39% for first and third order links. Few first order links are characterized by greater annual

bedload transport in the "hydropower" scenario than in the "natural" one (Fig. 4.3d), which is associated with an increase in discharge (Fig. 4.3a) due to inputs from water diversion. As shown in Fig. 4.3 and in Table 4.2, the relative reduction in bedload is considerably greater than the reduction in annual discharge, especially for second and third order links. This is because of a combination of non-linearity in the sediment transport capacity relations as well as the interplay of GSD adjustment with sediment supply and transport.

The reduction in bedload transport in the "hydropower" scenario is greater for coarser than for finer grains. In relative terms, transport of gravel and coarser grains decreases more than the transport of sand (Fig. 4.5 and Table 4.2). This is more evident in second order links, which are characterized by a median relative increase of around 12% for sand and a median relative decrease greater than 80% for coarser grains. According to seasonal changes in discharge and transport capacity (Figs. 4.3a, 4.3b, and 4.3c), the decrease of bedload transport due to hydropower is greater during summer months than in winter (Fig. 4.5, Table 4.2). At the river network scale, summer bedload decreases by more than 76%, while median changes in winter bedload are around 0%. Only third order links experience an increase in bedload due to higher flows in the winter months (Fig. 4.5). Going downstream from first to third order links, the seasonal variability becomes stronger (Fig. 4.5).

Simulations indicate that sediment yield transported at the outlet of the catchment as bedload has significantly decreased in the "hydropower" scenario with respect to "natural" conditions (Table 4.2, Fig. 4.6). The reduction occurs largely in summer (June-August) (Table 4.2, Fig. 4.6), while in winter bedload is higher in the "hydropower" than in "natural" scenario, following a higher sediment transporting capacity (Table 4.2). Actually bedload rates at the outlet of the Rhône Basin are greater in "hydropower" than in "natural" conditions for more than 200 days per year, according to our model due to flow regulation. However, the increase in winter bedload is not sufficient to counterbalance the large reduction in summer, and the volume of bedload reaching Lake Geneva in the "hydropower" scenario is estimated to be less than half of the "natural" scenario (Table 4.2). In relative terms, the drop in bedload sediment transport is evenly distributed among the different grain size classes with values of the reduction around -70% for sand, gravel and coarser grains (Table 4.2, Fig. 4.6). The model indicates that gravel contributes most of the total bedload sediment yield at the catchment outlet.

Table 4.2: Changes in discharge and bedload between "hydropower" and "natural" scenarios, expressed as relative to the "natural" conditions, and median annual changes in channel bed thickness for the "natural" and "hydropower" scenarios. Values are listed for first, second, and third order links, as median values for the entire river network and at the outlet of the upper Rhône River.

17-year (1992 - 2008)	**1^{st} Strahler Order**	**2^{nd} Strahler Order**	**3^{rd} Strahler Order**	**River Network**	**Outlet**
Changes in Discharge (Q) [%]					
mean relative δQ_{annual}	-39%	-51%	-12%	-36%	1%
mean relative δQ_{summer}	-47%	-52%	-26%	-43%	-25%
mean relative δQ_{winter}	59%	-12%	75%	45%	118%
Changes in Bedload (Q_b) [%]					
median relative $\delta Q_{bannual}$	-47%	-91%	-39%	-48%	-71%
median relative $\delta Q_{bsummer}$	-78%	-91%	-63%	-76%	-81%
median relative $\delta Q_{bwinter}$	-34%	-93%	370%	0%	480%
median relative δQ_{bsand}	0%	12%	-33%	-17%	-68%
median relative $\delta Q_{bgravel}$	-43%	-84%	-38%	-45%	-71%
median relative $\delta Q_{bcobble}$	-50%	-89%	-48%	-52%	-73%
median relative $\delta Q_{bboulder}$	-63%	-94%	-56%	-66%	-74%
Changes in Channel Bed Thickness (h_b) [cm year^{-1}]					
"natural"	-0.93	-0.43	0.08	-0.48	-0.02
"hydropower"	-0.32	0.17	0.05	-0.04	0.03

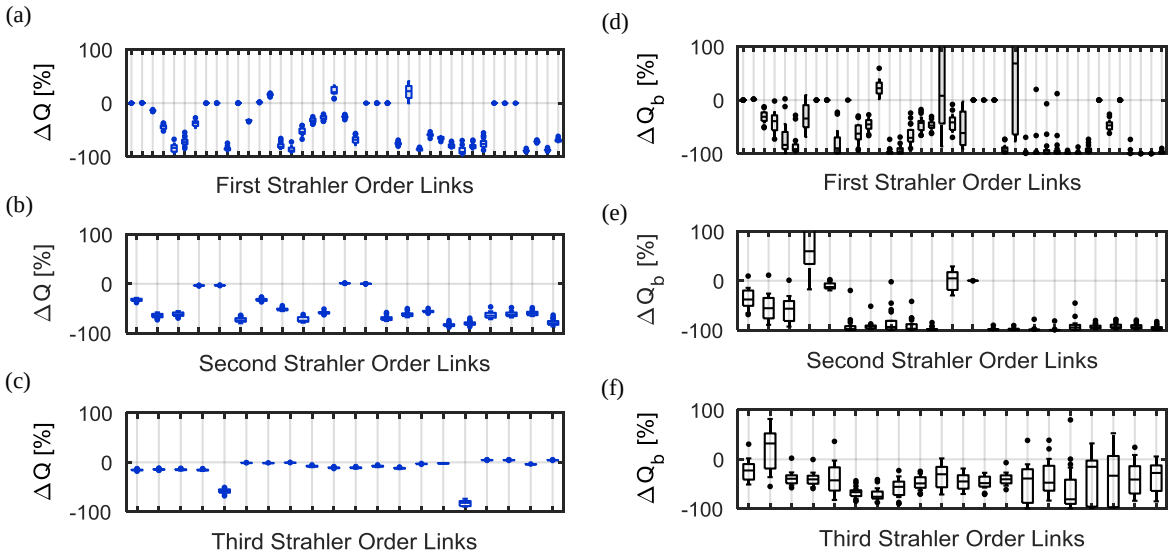

Figure 4.3: Box plots of change in (a, b, c) annual discharge and (d, e, f) annual bedload between "hydropower" and "natural" scenarios, expressed as differences relative to the "natural" scenario, for (top; a and d) first, (middle; b and e) second, and (bottom; c and d) third Strahler order streams. In the x-axis are the links, in the y-axis the interannual variability of annual discharge (right) and annual bedload (left).

4.4.2 Erosion and Deposition

To analyze erosion and deposition rates and spatial patterns throughout the river network, we consider changes in channel bed sediment volume expressed as changes in channel bed thickness (active layer + substrate layer) neglecting porosity. Simulations show that most of the first order links experience erosion after flow regulation (Figs. 4.7, 4.8). Going from first to second and third order channels, the number of links characterized more frequently by deposition increases. Median values of changes in channel bed thickness are generally higher in the "hydropower" scenario than in the "natural" ones, suggesting that, at the river network scale, hydropower reduces erosion and/or increase deposition (Figs. 4.7, 4.8). Median annual values of changes in river bed thickness in "natural" and "hydropower" scenarios are respectively equal to -0.93 cm year^{-1} and -0.32 cm year^{-1} for first order links, and -0.43 cm year^{-1} and +0.17 cm year^{-1} for second order links. Differences between the two scenarios are less evident for third order links, where median values of river bed volume change are positive (deposition) and close to zero in both "natural" and "hydropower" conditions (Figs. 4.7c, 4.8) However, despite differences in the magnitude of changes in channel bed volume, the spatial patterns of erosion and deposition do not change significantly between the two scenarios, as shown in Fig. 4.8.

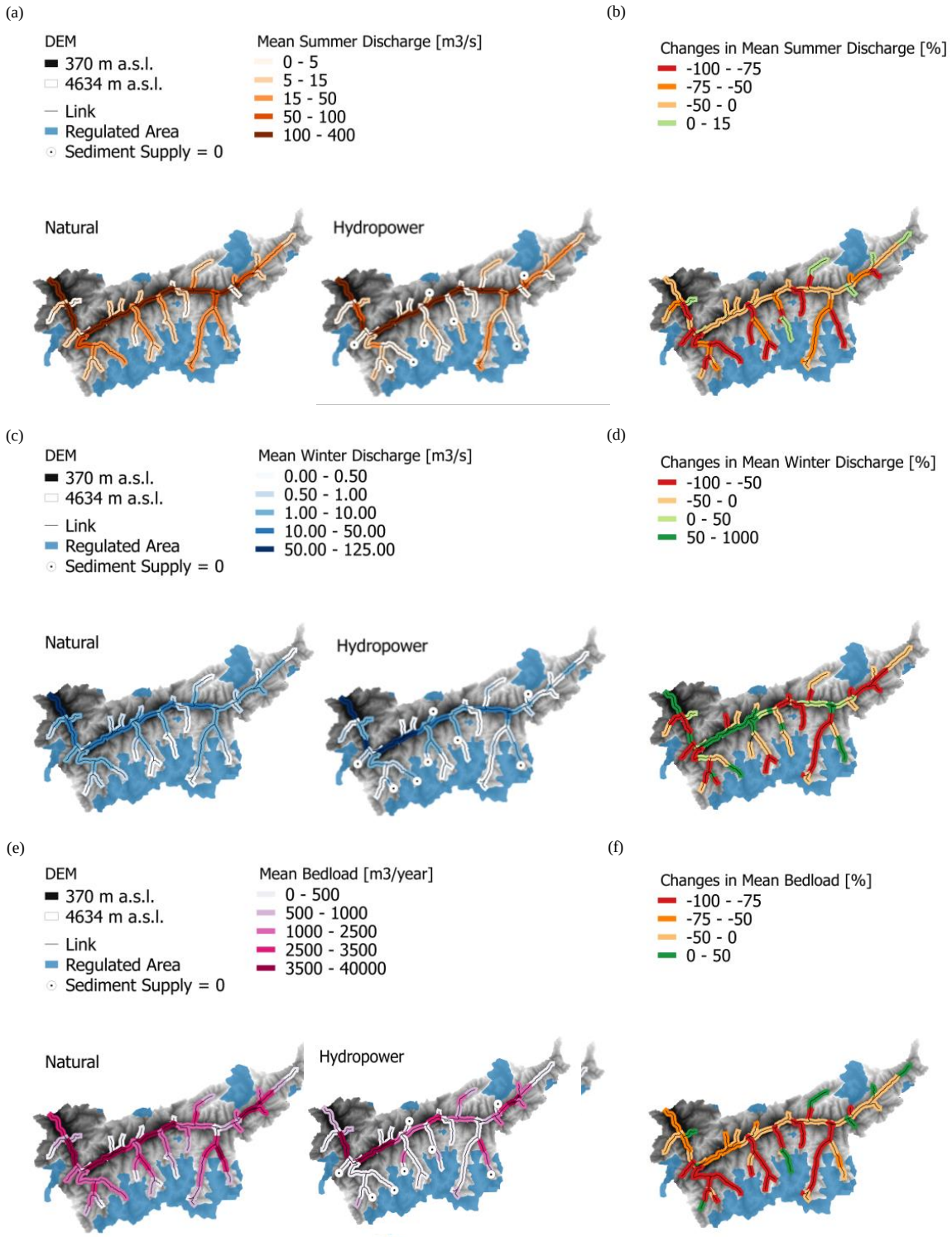

Figure 4.4: Maps of (a) mean summer (June-August) discharge, (b) change in mean summer discharge, (c) mean winter (January-March) discharge, (d) change in mean winter discharge, (e) mean bedload, change in mean bedload (f) . Changes between "hydropower" and "natural" scenarios are expressed as relative to the "natural" scenario.

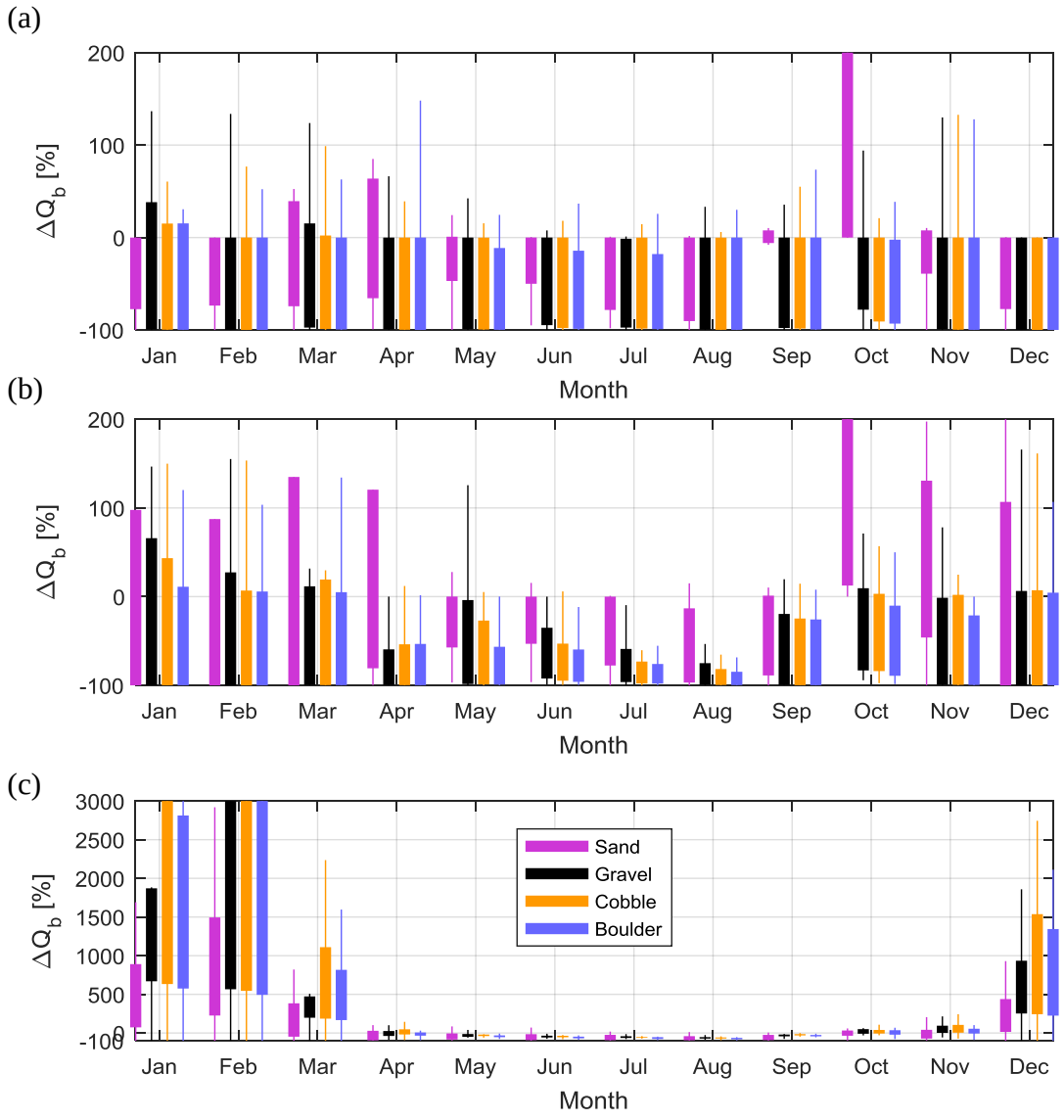

Figure 4.5: Box plots of change in total monthly bedload of sand, gravel, cobble and boulder, between "hydropower" and "natural" scenarios, expressed as differences relative to the "natural" scenario, for first (a), second (b), and third (c) Strahler order links.

Almost all links which for most of the time are subject to erosion (deposition) in "natural" conditions, experience erosion (deposition) also in the "hydropower" scenario.

4.4.3 Grain Size Distribution

The impact of flow regulation on the grain size distribution is smaller than on bedload transport, as can be seen by changes in the mean values of characteristic diameters (d_{10},

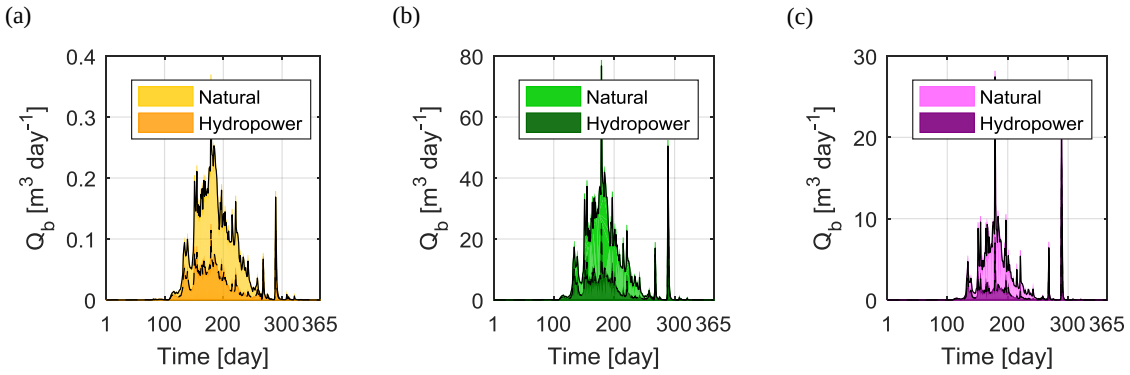

Figure 4.6: Mean daily bedload transport of sand (a), gravel (b) and cobbles (c) at the outlet of the catchment for the "natural" and the "hydropower" scenarios.

d_{16}, d_{30}, d_{50}, d_{65}, and d_{84}) over the last five years of the 17-year simulation (Figs. 4.9a, 4.9b, and 4.9c) and of the 100-year simulation (Figs. 4.9d, 4.9e, and 4.9f). The channel bed GSD after 17 years of simulation (1992-2008) does not show systematic changes between "natural" and "hydropower" scenarios (Figs. 4.9a, 4.9b, 4.9c). Besides few isolated links which show a reduction in channel bed GSD, only the finer fractions, d_{10} and d_{16}, are reduced in the first and second order links. However, differences between the two scenarios are more evident after 100 years of simulation, especially for first and second order channels (Figs. 4.9d, 4.9e). At longer time scales, hydropower regulation leads to a reduction of the grain size locally, in agreement with the reduced sediment transport capacity and reduced bedload rates. However, this reduction affects only few links below hydropower systems. Overall, the results suggest that GSDs of the river network are not likely to show regulations effects at short (17-year) or at longer (100-year) time scales.

Similarly, differences in the spatial distribution of GSDs for the "natural" and "hydropower" scenarios, with respect to the initial conditions, are also quite small (Fig. 4.10). While in the "hydropower" scenario both d_{50} and d_{90} after 100 years of simulations are almost identical to the initial conditions (Fig. 4.10), some links are characterized by coarser grains in the "natural" scenario.

4.4.4 Sensitivity to Air Temperature and Effect of Sediment Trapping

The mean monthly bedload transport at the outlet of the upper Rhône basin for the 17-year simulation, under "natural" (Fig. 4.11a) and "hydropower" (Fig. 4.11b) scenarios was examined under current climatic conditions (1992-2008) and with a constant increase in mean air temperature equal to 1 and 2°C. In "natural" conditions, the increase in air

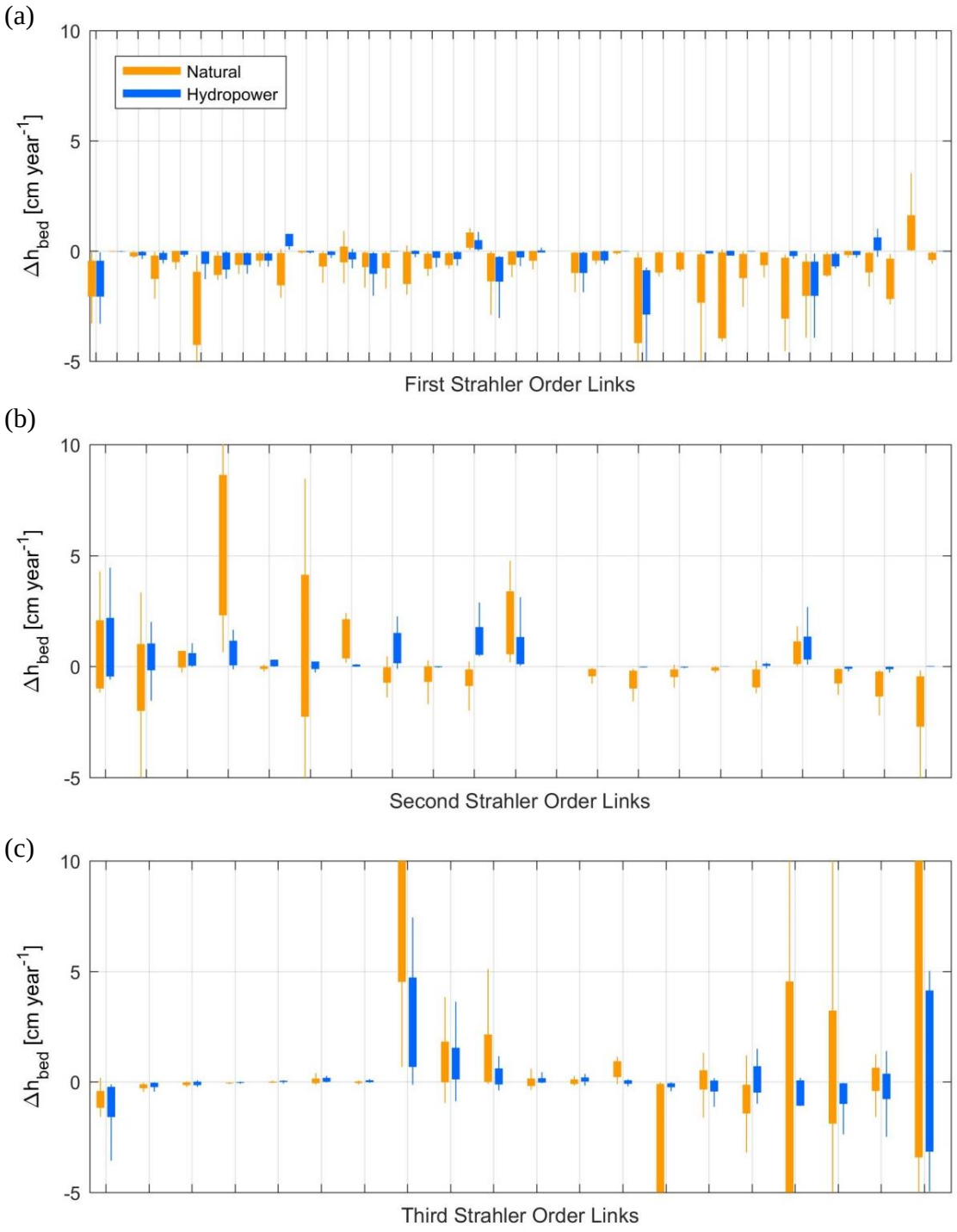

Figure 4.7: Box plot of mean annual change in channel bed elevation (sum of active layer and substrate layer with porosity equal to zero) in "natural" and "hydropower" scenarios for links of (a) first, (b) second, and (c) third Strahler order.

temperature leads to greater bedload in spring (May) and smaller bedload in June and July (Fig. 4.11a). This is due to the earlier snow melting driven by warmer temperature which implies first an increase of discharge (sediment transport capacity) in spring, and

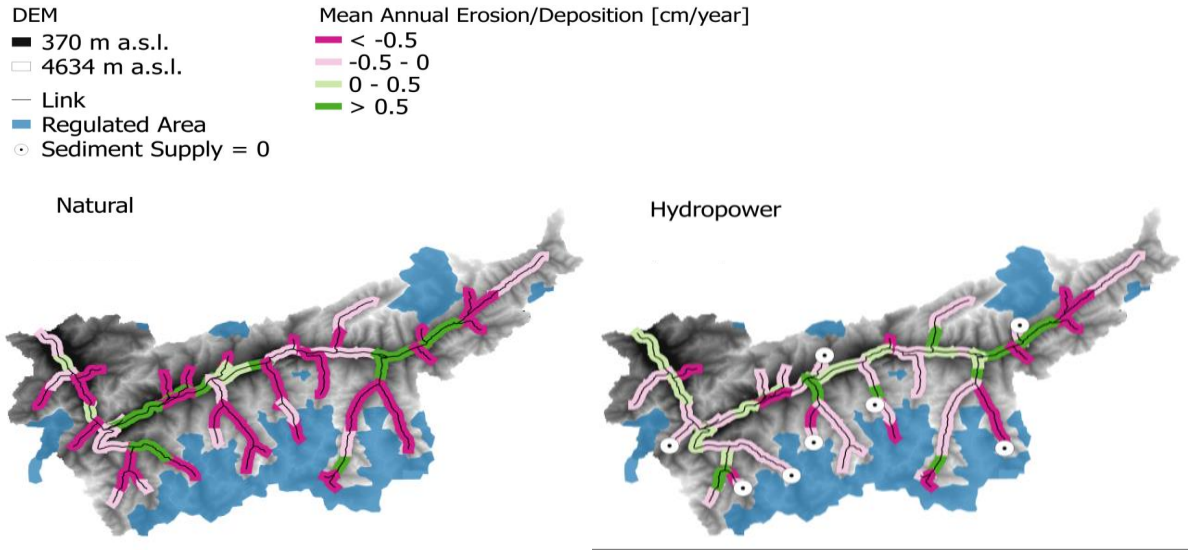

Figure 4.8: Maps of mean annual erosion/deposition expressed as change in channel bed thickness (porosity equal to zero) for "natural" and "hydropower" scenarios.

consequently a reduction of discharge (sediment transport capacity) in summer due to the limited residual snow pack. Warmer temperatures also enhance ice melt both by higher melt rates and by reduced snow cover and reduced albedo. As a consequence, sediment transport capacity and bedload in August, September and October are greater for the scenarios with increased air temperature than for the "natural" scenario (Fig. 4.11a). The effect of warmer temperature on the seasonal pattern of bedload is similar in the "hydropower" scenario (Fig. 4.11b). However, reservoir operations adjust the impacts of earlier snow melting leading to greater bedload in June for warmer scenarios, and to a smaller reduction of bedload simulated in July (Fig. 4.11b). At the annual scale, higher air temperature results in greater bedload for both scenarios. However, the relative increase in bedload is much greater in the "hydropower" than in the "natural" scenario. In the "natural" scenario, bedload increases by 15% and by 30% for respectively 1°C and 2°C increases in air temperature. Conversely, in the "hydropower" scenario, the rise in bedload is equal to almost 40% and 80%.

Results are quite similar at the basin scale. Mean annual bedload rates show that under warmer climatic conditions bedload increases in all three stream orders (Fig. 4.12), and especially in third order links which experience a greater rise in sediment transport (Fig. 4.12c). The increase associated with higher temperatures does not recover the decrease due to hydropower, suggesting that the signal of sediment blocking in reservoirs and lower

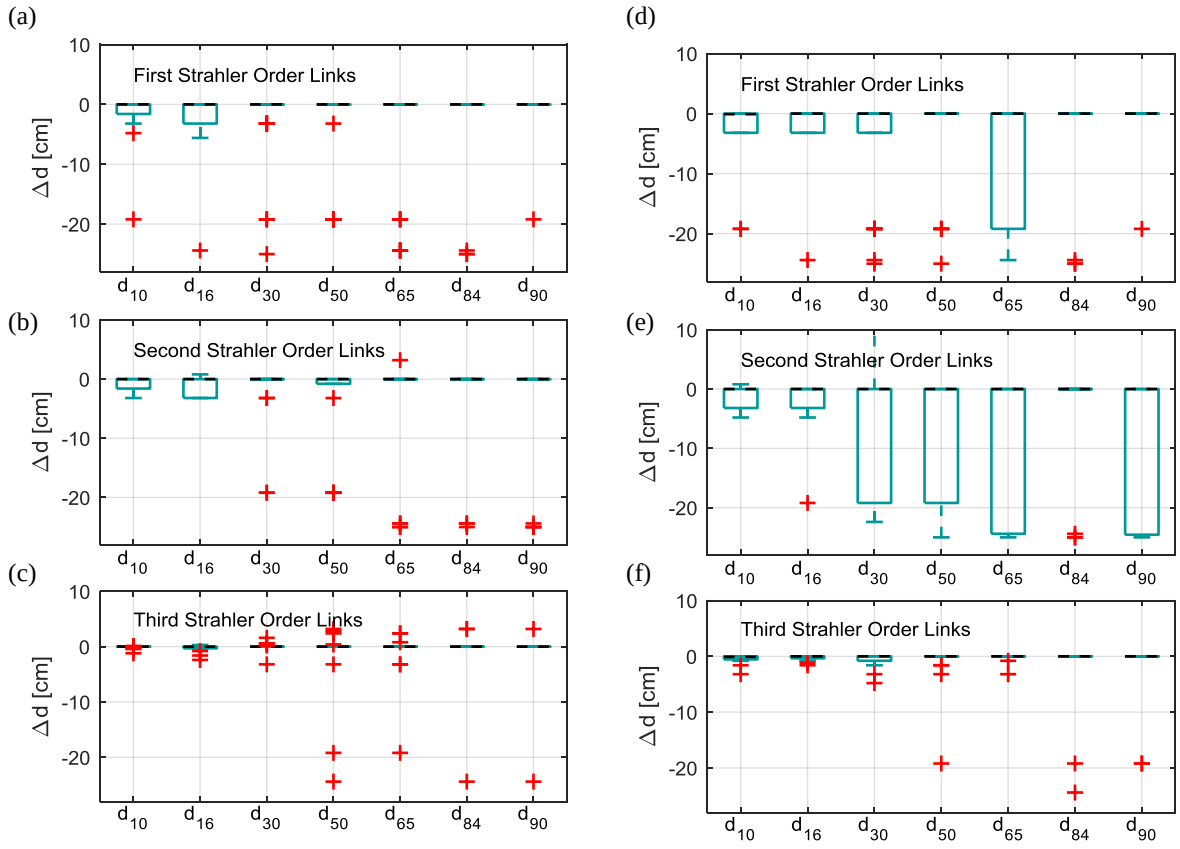

Figure 4.9: Box plot of changes in characteristic grain sizes for first, second and third order links between the "hydropower" and the "natural" scenario obtained (a, b, c) after 17 years and (d, e, f) after 100 years of simulation.

transport capacity may persist under climate change. To this end we also show bedload rates for the scenario with flow regulation only, i.e. without setting to zero the sediment input to links located downstream of reservoirs for comparison in Fig. 4.12. The results suggest that sediment trapping in reservoirs indeed has a local effect on bedload transport rates downstream of dams only.

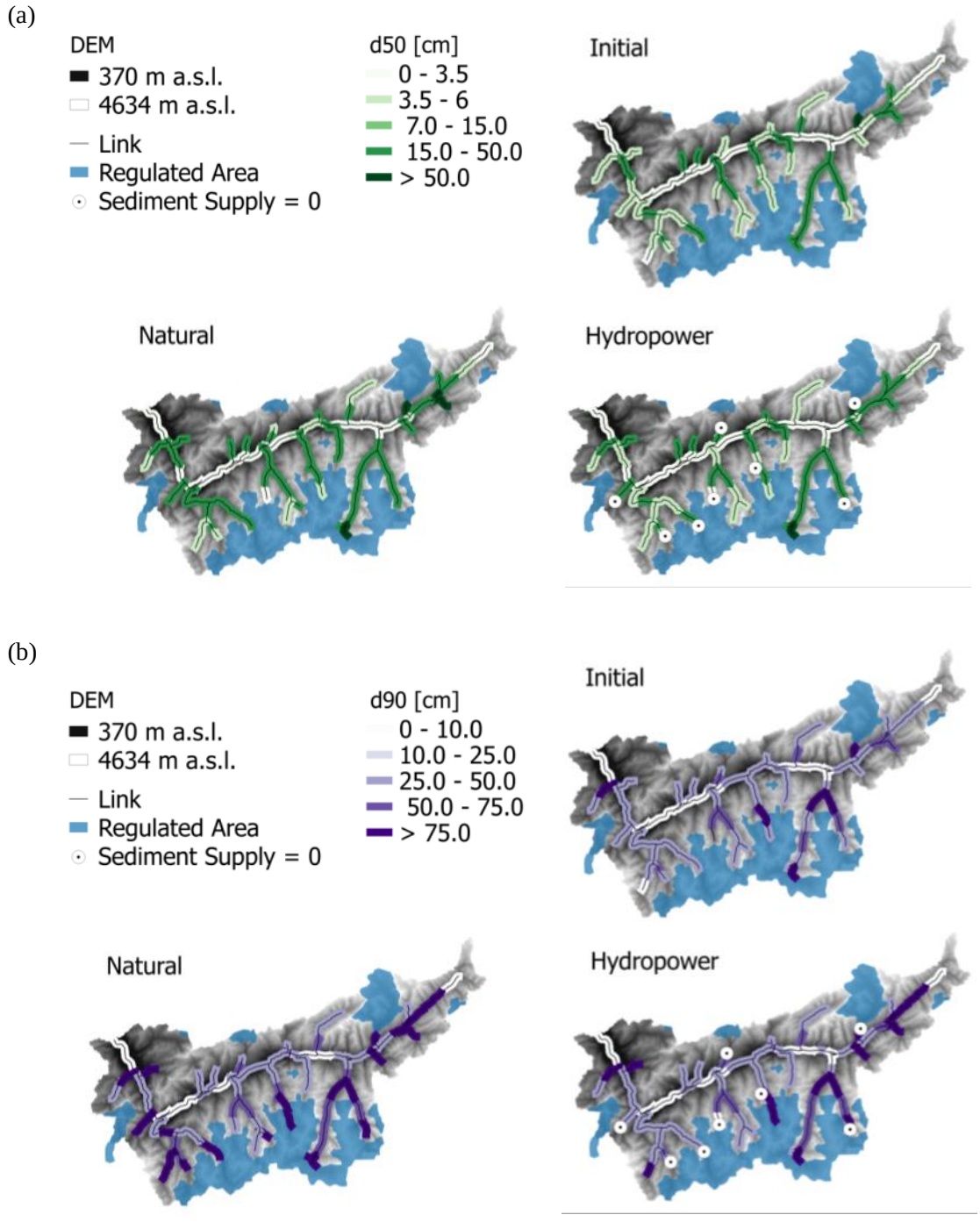

Figure 4.10: Maps of (a) d_{50} and (b) d_{90} at the initial conditions and after 100 years of simulation under "natural" and "hydropower" scenarios.

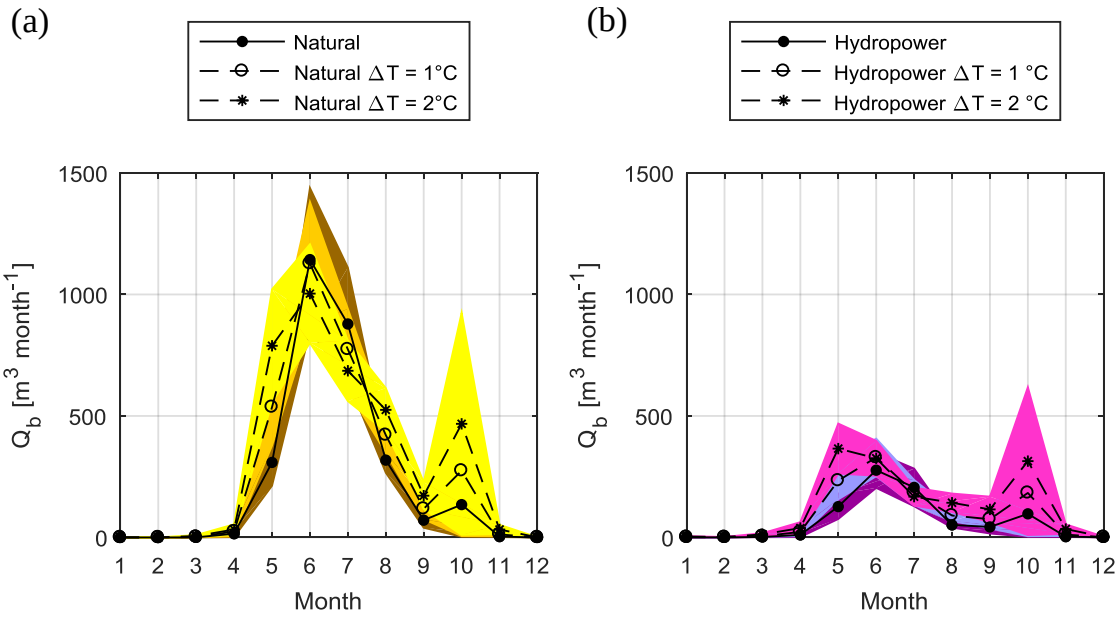

Figure 4.11: Mean monthly bedload transport at the outlet of the catchment for (*a*) "natural" and (*b*) "hydropower" scenarios, under current climatic conditions (1992-2008) and with a constant increase in air temperature equal to 1°C and 2°C. Colored bands represent the range of variability expressed as Â± standard error.

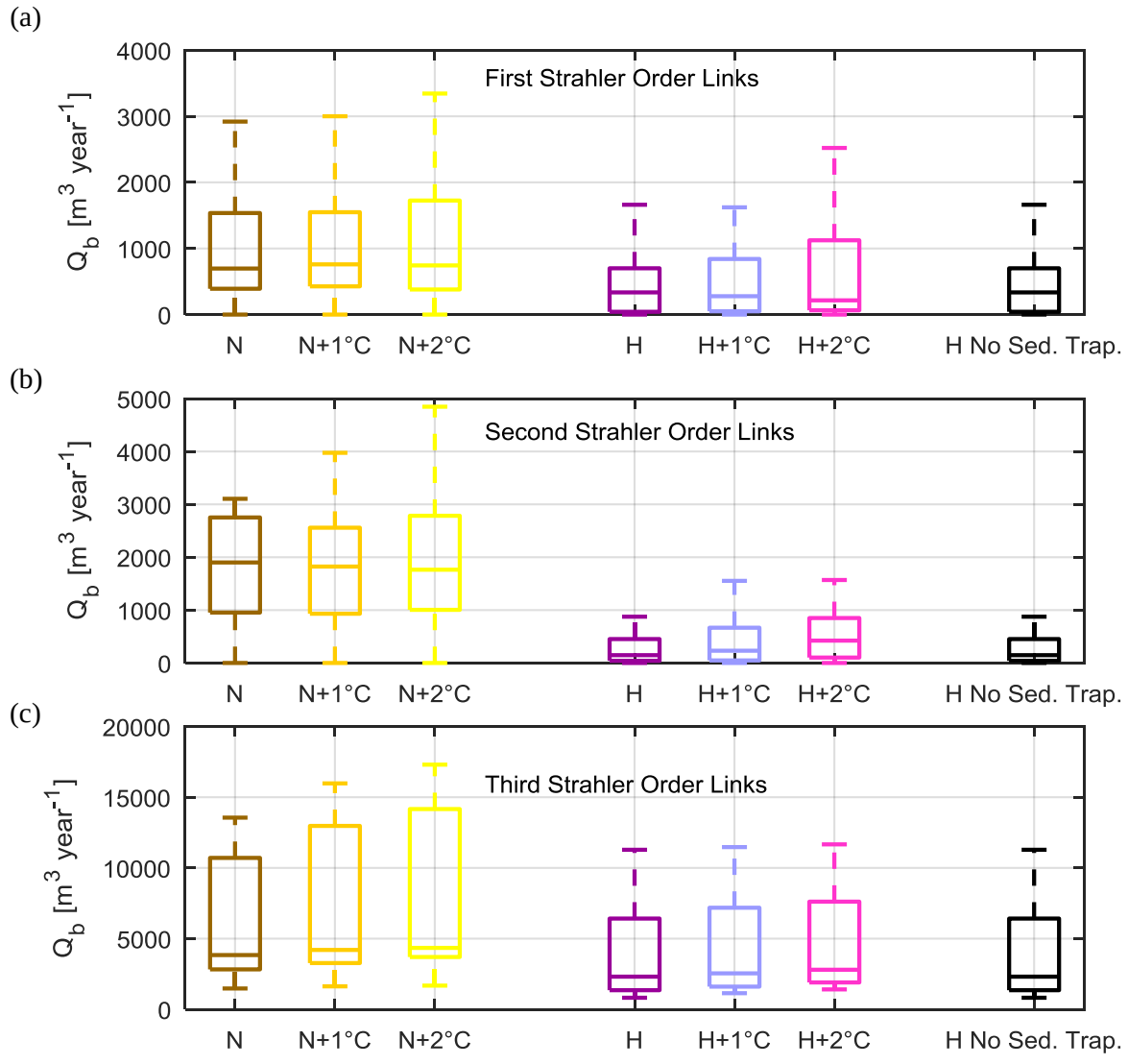

Figure 4.12: Box plot of mean annual bedload transport for links of first (*a*), second (*b*), and third (*c*) Strahler order, for "natural" scenario (N), "natural" scenario with a constant increase in air temperature of 1°C (N+1°C), and 2°C (N+2°C), "hydropower" scenario (H), "hydropower" scenario with a constant increase in air temperature of 1°C (H+1°C), and 2°C (H+2°C), and "hydropower" scenario with only flow regulation and no sediment trapping behind reservoirs (H No Sed. Trap.).

4.5 Discussion

4.5.1 Effects of Flow Regulation at the River Network Scale

Model results indicate that while not all first order links are subject to a decrease in bedload due to hydropower, all second and third order links are affected (Figs. 4.3d, 4.3e and 4.3f, Table 4.2). This shows how the effects of perturbations imposed in headwater streams propagate along the river network to gradually involve the entire system and to accumulate in downstream reaches. This result confirms that dam impacts on network sediment transport (Schmitt et al., 2018b) and to explore the effects of local disturbances, it is necessary to analyze the whole river network system instead of considering isolated parts, in line with findings of previous studies of network connectivity (e.g. Benda and Dunne, 1997; Czuba and Foufoula-Georgiou, 2014; Czuba and Foufoula-Georgiou, 2015; Schmitt et al., 2016).

Based on field measurements and model simulation, Benda and Dunne (1997) showed how the effects of punctuated sediment supply to channels result in sediment storage along the river network that is non-uniform in space and unsteady in time. They demonstrated how the probability of occurrence of channel aggradation is a function of the drainage area: first the probability increases with drainage area because more sediment sources are integrated until it decreases because of channels widening and sediment fining (Benda and Dunne, 1997). Similarly, our model simulations show that both reductions in bedload rates (Figs. 4.3d, 4.3e, and 4.3f, Table 4.2) and long term changes in channel bed GSD (Fig. 4.9, Table 4.2) are greater for second than for first and third order links. Effects of hydropower are mostly limited and localized at headwater channels, increase for second order streams because the river network integrates upstream perturbations and streamflow is generally higher, and decrease in higher order channels where the contribution of upstream undisturbed and disturbed links is combined. Conversely, changes in the seasonal pattern of transport (Fig. 4.5, Table 4.2) and alterations associated with a warmer climate (Fig. 4.21) are emphasized in third order channels, because they integrate the changing flow regime of the upstream basin. Similarly, third order links are almost exclusively characterized by an increase in bedload during winter months (Fig. 4.5, Table 4.2). In summary, our results show how the hierarchical structure of the river network controls the impacts of perturbations by integrating and structuring their effects, and as a result either emphasizing or dampening their consequences (Benda and Dunne, 1997; Benda et al., 2004; Czuba and Foufoula-Georgiou, 2014; Czuba and Foufoula-Georgiou, 2015; Schmitt et al., 2016, 2018a, 2018b). The non-linear and threshold nature of bedload transport emerges in several aspects of our model simulations. Going from “natural” to

"hydropower" scenarios, the reduction in transport is smaller for sand than for coarser grains (Table 2, Fig. 4.5). This is associated with the non-linearity of the transport equation (4.8) and with the fact that coarser grains are characterized by larger reference shear stress than finer grains, and thus, it is more likely that, for the same decrease in effective shear stress, the ratio $\tau_i^{*'}/\tau_{ri}^{*'}$ becomes lower than the threshold value of 1.33. For the same reason, changes in transport rates are much greater than changes in discharge, as shown in Fig. 4.3. Conversely, although first order links are subject to an increase in winter discharge in the "hydropower" scenario, there is not a clear increase in winter bedload in these links because the increase in effective shear stress is not sufficient to exceed the threshold of motion. The effects of the non-linearity and the power law nature of the bedload transport equation is also observable at the outlet of the catchment. Although total annual discharge flowing into Lake Geneva stays almost the same (δQ = -1%) before and after the construction and activation of the hydropower system, the total annual bedload is substantially decreased (δQ_b = -70%).

Our model shows how hydropower has an immediate effect on bedload transport rates in the upper Rhône Basin. Bedload drops substantially at the river network scale in the "hydropower" scenario (Figs. 4.3b, 4.4e, and 4.4f). Channel bed erosion is also smaller in "hydropower" than in "natural" conditions (Fig. 4.7), but the patterns of erosion and deposition are similar between the two scenarios (Fig. 4.8). Similarly, changes in the GSD of the channel bed are more gradual and only after 100 years of simulation it is possible to observe a small reduction in grain sizes. This demonstrates how the impacts of flow regulation emerge at different temporal scales. However, the limited effects that we observe on the river bed GSDs could also be connected with the procedure of initialization. We initialize the GSD of the active and the substrate layer based on discharge and observations collected in a limited number of locations in post-dams conditions because pre-dam measurements are not available.

4.5.2 Anthropogenic Activities and Sediment Fluxes in the upper Rhône Basin

By dating sediment cores collected in the northern part of the upper Rhône River delta, Loizeau et al. (1997) identified a significant reduction in sedimentation rates after 1960s, when the main hydropower reservoirs started operating. They estimated a reduction of sediment input of roughly 50%, and they suggested the decrease of sediment input from the Rhône River due to hydropower operation as the most probable explanation (Loizeau et al., 1997). It has been argued that the decrease in sediment load entering Lake Geneva in 1960s could have also been driven by a reduction in ice melt fluxes associated with

glacier advance due to colder temperatures in this period as well (Costa et al., 2018a), and not only by hydropower infrastructures. We are aware that the analysis of Loizeau et al. (1997) refers mainly to fine grains, transported in suspension, while our model provides estimations of bedload, which is estimated to represent only 9-10% of the total sediment load in this catchment (Hinderer et al., 2013; Schlunegger and Hinderer, 2003). Nonetheless, our simulations clearly demonstrate that flow regulation associated with hydropower operation may lead to a substantial reduction of bedload reaching the outlet of the upper Rhône River delta (Fig. 4.6), at least for sediment transported as bedload.

The impacts of flow regulation are strongest in the southern part of the catchment, in the Penninic region (Figs. 4.2, 4.4e and 4.4f), where the largest reservoirs and the main hydropower systems are located. The reduction of bedload along the tributaries of the Penninic region is among the largest in the catchment (Figs. 4.4e and 4.4f). This supports the finding of a sediment fingerprinting study in this catchment (Stutenbecker et al., 2017). Stutenbecker et al. (2017) showed that, despite presenting some of the highest denudation rates in the basin, the Penninic region is substantially underrepresented in the sediment budget of the upper Rhône River. They argue that human activities, such as sediment trapping behind reservoirs and sediment mining, could explain most of the mismatch between the erosion rates and the sediment composition of the main Rhône River (Stutenbecker et al., 2017). Our simulations suggest that, in addition to sediment storage behind reservoirs and sediment removal through mining, flow regulation itself may have led to a 50% reduction of bedload input from the tributaries located in the southern part of the catchment (Penninic Nappes).

Model simulations indicate that flow regulation may have a strong impact on bedload transport, exceeding that of sediment trapping behind dams (Fig. 4.12). The hydropower system of the upper Rhône catchment differs from other regulated Alpine basins because a significant fraction of the drainage area is affected by water diversions which redistribute discharge (Fatichi et al., 2015). While only roughly 8% of the basin flows directly into reservoirs, almost 17% of the drainage area is diverted to reservoirs by intakes. In the latter area, water is extracted from headwater channels and diverted to reservoirs and hydropower plants, and, thus the sediment transporting capacity is significantly reduced. Instead, the sediment that is first trapped in water intakes, is then regularly flushed back to the river network with a frequency that depends on the season (Bakker et al., 2018). Therefore, this area is characterized more by reduced transporting capacity than by reduced sediment supply. This would be in line with our model results which indicate that in this catchment flow regulation has larger impacts on bedload than sediment storage in hydropower reservoirs. For the expansion of smaller diversion-type hydropower schemes, for example in the Himalayas (Schwanghart et al., 2016), this result indicates that flow

regulation because of water diversion schemes can have a substantial impact on network sediment transport, even though little sediment is trapped.

Previous studies have estimated that roughly 25% of total sediment load reaching the outlet of the catchment is semi-permanently stored behind the main six reservoirs operating in the basin (Beyer-Portner, 1998; Hinderer et al., 2013; Stutenbecker et al., 2017). Although this value refers to total sediment, and not only to coarser grains transported as bedload, it is expected that storage of sediment behind reservoirs also has an impact on bedload. Our approach cannot directly reproduce the effects of sediment trapping because there is no supply limitation, other than the limitation imposed by the sediment input into first order links. In this application, sediment supply entering the first order streams located most upstream, is estimated as function of mean discharge conditions, and we do not account for flushing operations of water intakes, which have been shown to have substantial local impacts on bedload dynamics (Bakker et al., 2018). The structure of this modelling approach allows to implement specific sediment supply conditions, which could partially represent the flushing of sediment from water intakes.

Model simulations show that bedload is sensitive to increases in air temperature, through changes in runoff related to alteration of snow and ice melt. Even a constant increase in air temperature of 1°C and 2°C which are within the expected range of changes expected in this basin in the future, lead to a substantial increase in bedload. However, the rise in bedload rates due to a warmer climate is smaller than the reduction due to hydropower. These comparisons between anthropogenic and climatic influences on bedload transport are critical and require to be further studied. Our analysis provides a first order assessment based solely on spatially and temporally constant increases in air temperature. Secondly, our simulations do not take into account possible changes in the quantity and the GSD of sediment supply associated with a warmer climate (e.g. greater fine sediment supply from glacierized areas). Third, the model does not account for changes in the operational rules of the reservoirs and of the water abstraction facilities, which would most likely be implemented in order to adapt to climate-driven changes in the flow regime. We plan to deal with these three main criticisms in the future to adapt the model for comparative assessment between climatic and anthropogenic impacts.

4.6 Conclusions

We present a model for estimating bedload transport at the river network scale. We conceptualize the river network as a series of connected links. The model computes 1-D flow depth, bedload transport rates, erosion and deposition, given discharge and the

geometric characteristics of the links. Channel bed volume and the GSD of the river bed are updated at each time step (1 day).

We apply the river network model to estimate the cumulative impacts of hydropower via changing hydrographs and sediment supply on bedload transport and the GSD of a large Alpine catchment located in the Swiss Alps: the upper Rhône Basin. Several large dams and a complex network of water intakes, water diversions, and pumping stations have been built along the tributaries of the catchment since 1960s. The main effects of these are altered discharge (sediment transport capacity), which on average increases in the winter and decreases in the summer, and a reduced sediment supply due to sediment trapping in reservoirs behind dams. We estimate the impacts of these perturbations by running the model under conditions before hydropower ("natural" scenario) and after ("hydropower" scenario), by assuming the climatic conditions of the 17-year period 1992-2008. We also evaluate the long-term effects by running the model for 100 years, and by excluding any limitation on sediment supply downstream of reservoirs to separate the impacts of flow regulation and sediment storage behind dams.

Model results indicate that bedload rates are substantially reduced in the "hydropower" scenario, compared to the "natural" conditions (-48% at the river network scale, -70% at the outlet). Changes in bedload are (1) site-dependent, (2) grain size-dependent and (3) characterized by a clear seasonal pattern. (1) While not all the first order links are affected by hydropower, all second and third order links are influenced. This shows how effects of local perturbations propagate along the river network and involve the entire system. Reductions in bedload rates are greater for second than for first and third order links. The effect is emphasized in second order links, because they integrate the impacts of first order links. Conversely, in third order links, the impacts of hydropower are smoothed because both disturbed and undisturbed upstream links are aggregated. (2) The transport of sand is reduced less than the transport of coarser grains, in agreement with the non-linear and the threshold nature of the bedload equation. (3) Bedload reduction occurs mainly in summer (-76% at the river network scale), according to the substantial decrease of discharge due to the filling of the reservoirs. In winter, water releases from reservoirs for hydropower energy production, lead to greater sediment transport capacity. Although the rise in discharge is not sufficient to increase bedload transport for first order links, the drop in bedload is significantly smaller than in the summer. Some second and all third order links experience higher transport in winter, showing a much more evident seasonal pattern than upstream channels. As a result, at the river network scale, winter bedload does not change between the two scenarios. Higher order streams are characterized by higher (lower) deposition (erosion). Under the "hydropower" scenario, links are characterized by less (more) erosion (deposition) than under "natural" conditions. How-

ever, despite differences in the magnitude, the spatial patterns of erosion and deposition do not change between the two scenarios. Likewise, the channel bed GSDs are similar in the "hydropower" and the "natural" conditions. Only after 100 years of simulation, some links experience a reduction in GSDs but median values of characteristic diameters stay the same.

Our results suggest that sediment trapping behind reservoirs may have a lower impact on bedload at the river network scale compared to flow regulation. This could be related to the specific characteristics of the hydropower system of the upper Rhône catchment, which is heavily based on water diversions, characterized by reduced transport capacity without limitations on sediment supply. As a result, we do not observe major incision. The model shows that bedload is sensitive to rise in air temperature. The seasonal pattern changes: temperature-driven earlier snow melt and increased ice melt due also to reduced snow cover and reduced albedo, result in higher bedload in May and during the period August-October both for "natural" and "hydropower" scenarios. Warmer climate leads to increase in total annual bedload for both scenarios. Although the relative increase is greater in "hydropower" scenario, it is not sufficient to recover the reduction associated to flow regulation. The approach in principle allows the quantification of impacts of hydropower on bedload in any other mountainous catchment regulated for hydroelectric energy production purposes (or any other water use). Because the model is developed for modelling at the scale of the entire river network, it provides a useful tool to quantify the effects of alteration in sediment supply and in sediment transport capacity at locations distant from the sources of changes. This allows the identification of vulnerabilities which would not be possible to detect with reach-scale modelling. In addition, thanks to a fairly low computational demand, this modelling framework can be used to evaluate long term changes in bedload, river bed grain size distribution and erosion/deposition of Alpine river networks including stochastic climate inputs and parameter uncertainties.

Appendix A: Dimensionless Reference Shear Stress We compute the dimensionless reference shear stress $\tau_{ri}^{*'}$ following the procedure of Wilcock and Crowe (2003) starting from a constant dimensionless reference shear stress for median grain size $\tau_{rd50}^{*'}$ equal to 0.03 as suggested by Schneider et al. (2015).

$$\tau_{rd50}^{*'} = \frac{\tau_{rd50}^{'}}{R\,\rho\,g\,d_{50}} \tag{4.11}$$

$$b = \frac{0.67}{1 + exp(1.5 - \frac{d_i}{d_{50}})} \tag{4.12}$$

$$\frac{\tau_{ri}^{'}}{\tau_{rd50}^{'}} = (\frac{d_i}{d_{50}})^b (4.13)$$

$$\tau_i^{*'} = \frac{\tau^{'}}{R\,\rho\,g\,d_i} \tag{4.14}$$

Appendix B: Numerical Procedure to Initialize d_90 The numerical iterative procedure applied to compute d_{90}consists of: [1] assigning an initial value to flow depth h, [2] computing τ_{cr} from Equation (4.3) with channel bed slope S instead of S_{red}, [3] calculating d_{90} from Equation (4.10), and [4] d_{84} from d_{90}/d_{84}ratio, [5] computing discharge by using the resistance equation of Ferguson (2007). Flow depth is updated and the procedure is repeated until the difference between estimated discharge and measured discharge is smaller than a given tolerance (0.01 $m^3\ s^{-1}$).

Acknowledgments We are thankful to Simone Fatichi for providing the input data and the set-up for running the hydrological model Topkapi-ETH, used to simulate discharge along the river network. We thank Florian Textor for collecting the grain size distribution data in the catchment. We acknowledge the members of the Sedfate Project, Laura Stutenbecker, Maarten Bakker, Tiago A. Silva, Stephanie Girardclos, Stuart N. Lane, Jean-Luc Loizeau and Fritz Schlunegger for the fruitful discussions. This research was supported by the Swiss National Science Foundation Sinergia grant 147689. The authors declare that they have no conflict of interest. Data on grain size distribution used in this paper are available under request to the authors.

Chapter 5

Conclusions

Figure 5.1: View of the Sionne, tributary of the upper Rhône catchment (by F. Textor).

5.1 Concluding remarks

This thesis analyzes the controls of hydroclimate and hydropower operation on the sediment dynamics of a large Alpine catchment. The focus of the analysis is the upper Rhône basin, a 5338 km^2 catchment located in southwestern Switzerland. Roughly 10% of the catchment is covered by glaciers and its hydrology is characterized by a pluvioâglacioânival regime typical of mountainous regions. These features make the basin particularly sensitive to changes in climatic conditions. In fact, warmer temperatures and changes in precipitation intensity, observed in the Alpine region, are expected to influence the hydrological regime of the catchment by altering snow cover, snowmelt and ice melt, ultimately affecting streamflow, sediment transport, and erosion. The catchment has also been highly impacted by anthropogenic activities during the last century. Mainly, several large dams have been built in the catchment for hydroelectric energy production. The storage capacity of the reservoirs is about 20% of the mean annual flow into Lake Geneva. Water abstraction, water impoundment and flow regulation have substantially altered the hydrological regime of the basin and it is expected that these changes will also have significantly impacted sediment fluxes through sediment trapping and changed sediment transporting capacity. In this sense, the catchment represents a unique opportunity to examine and quantify the effects of climate and hydropower on sediment dynamics in Alpine catchments.

Both suspended sediment transport and bedload are investigated. The first step of the analysis focuses on suspended sediment and explores the link between climate and suspended sediment fluxes (Chapter 2). *The assumption is that erosive rainfall, defined as liquid precipitation over snow-free surfaces, ice melt, snowmelt and snow cover dynamics are the main drivers of suspended sediment fluxes in Alpine regions, and due to the diversity of the erosional processes and the variety of sediment sources involved, these hydroclimatic variables contribute to suspended sediment dynamics in a complementary way.* Data analysis revealed that a statistically significant step-like increase in suspended sediment concentration occurred at the outlet of the basin in mid-1980s simultaneously with an increase in basin-wide mean air temperature. The casual link is investigated by statistical analysis of changes both in sediment transport capacity, i.e. discharge, and in sediment supply associated with spatio-temporal changes in the hydroclimatic activationâdeactivation of sediment sources. For this purpose, starting from gridded datasets of daily precipitation and mean, minimum, and maximum air temperature, we modelled erosive rainfall, ice melt, snowmelt and snow cover, by using spatially distributed degree-day models calibrated on the basis of satellite-derived snow cover maps and discharge at highly glacierized tributary catchments. Results of the analysis indicate the ice melt

played a dominant role in the suspended sediment concentration rise observed in mid 1980s, through (1) increased flow derived from sediment-rich subglacial and proglacial areas, (2) a larger relative contribution of sediment-rich ice melt compared to snowmelt and precipitation, and (3) increased sediment supply in proglacial areas. The reduced extent and duration of snow cover may also have contributed to the increase in suspended sediment concentration through enhanced rainfall.

Driven by the outcomes of this analysis, the control of hydroclimatic forcing on suspended sediment dynamics was explored further by examining the predictive performance of individual hydroclimatic factors. In this second step (Chapter 3), *we accounted for hydropower by delivering sediment produced in areas draining directly or indirectly to reservoirs, and by estimating hydropower releases by a conceptual approach with a unique virtual reservoir regulated on the basis of a targetâvolume function.* An objective automatic input variable selection algorithm was applied on erosive rainfall, ice melt, snowmelt and hydropower releases, to identify the variables with highest power of predicting suspended sediment concentration, their fraction of explained variance and characteristic time lags. In addition, a hydroclimatic multivariate rating curve (HMRC) accounting for the contributions of the most relevant hydroclimatic input variables was developed and calibrated with a gradientâbased nonlinear optimization method. The HMRC was first compared with a traditional rating curve based on discharge, and second, used to quantify the contribution of hydroclimatic variables to suspended sediment concentration. Results indicate that all the three hydroclimatic processes erosive rainfall, ice melt and snowmelt are significant predictors of mean daily suspended sediment concentration at the outlet of the upper Rhône basin. Erosive rainfall explains the largest fraction of the variability in suspended sediment concentration because intense rainfall events generate peaks of suspended sediment transport. Hydropower releases do not play a significant role in determining the variance of suspended sediment concentration, because fluxes released from reservoirs are scarce of sediment. Ice melt generates the greatest contribution to suspended sediment concentration per unit of water volume and contributes the most in terms of mean annual sediment yield.

The third step of this thesis focuses on coarse grain transport at the river network scale. *To this end a new river network bedload model has been developed to investigate the impacts of hydropower on sediment transport rates, channel bed grain size distribution and erosion/deposition patterns* (Chapter 4). The river network is conceptualized as a series of connected river links and nodes. Given discharge and geometric characteristics of the links, the model simulates 1-D flow depth and bedload transport rates by balancing sediment transport capacity, computed with an adjusted Wilcock and Crowe equation, and sediment supply given by the sediment input from upstream links and sediment available

in the channel bed to be eroded. The model is run with a daily time step, under the conditions before the construction of dams ("natural") and after ("hydropower"). Discharge is modelled with the spatially distributed and physically-based hydrological model Topkapi-ETH. Model simulations indicate that hydropower has substantially reduced bedload rates, especially in summer and for coarser grains. Results show that, after hydropower, the river network experience less erosion and more deposition, however, spatial patterns of erosion and deposition are almost identical to pre-dam conditions. Similarly, river bed grain size distribution does not show systematic changes after hydropower, only local effects are visible at longer time. Simulations demonstrate that the river network structures the impacts of perturbations in transport capacity and sediment supply, and the effects result either enhanced or dampened in the downstream direction. With warmer temperatures, the model reproduces larger bedload rates, which, however, do not exceed the reduction due to hydropower. Detailed conclusions of the individual analyses are described in the previous Chapters. Here more general conclusions are drawn based on those results and their importance is presented.

Impacts of climate on suspended sediment and of hydropower on bedload

Results of the analysis suggest that *climate has a significant and measurable influence on suspended sediment fluxes in the catchment.* Outputs of the input variable selection algorithm indicate that erosive rainfall, ice melt and snowmelt are all relevant predictors of suspended sediment concentration, while hydropower releases do not play a significant role (Chapter 3). The analysis presented in Chapter 2 also showed that the increase in mean air temperature observed in the catchment in mid 1980s resulted in a statistically significant increase in suspended sediment concentration at the outlet. The increase in suspended sediment concentration in July-August can only be explained by concurrent increases in ice-melt in those months. Therefore it is most likely the signal of enhanced fine sediment supply by glacial erosion that ice-melt mobilizes that is observed at the catchment outlet , demonstrating that *climate has a major impact on suspended sediment dynamics*, even in a heavily regulated catchment such as the Rhône Basin.

Conversely, *hydropower substantially impacts the transport of coarser grains.* River network model simulations show that after the construction of the dams, the river network is transporting less sediment, it is affected by lower erosion than before, although after 17 years of simulation, the spatial patterns of erosion and deposition are similar between the two scenarios. Likewise, reductions in channel bed grain size distribution are only localized and are visible only after 100 years of simulation. However, the river network bedload model indicates that *flow regulation induced by hydropower, mainly reduced summer discharge and increased winter discharge, has resulted in significantly lower bedload transport rates, especially in summer and for coarser grains* (Chapter 4). In addition, the

analysis on the sensitivity of bedload to warmer climate showed how discrete, spatially and temporally constant increases in temperature would result in greater bedload at the annual scale (because of higher streamflow) and changes in the seasonal pattern would increase bedload in May, August and September (Chapter 4). However, the rise in bedload rates associated with warmer temperature is not sufficient to counterbalance the reduction driven by hydropower, confirming that in the upper Rhône basin, *impacts of hydropower on bedload may prevail over impacts of changing climatic conditions*, although this point needs further investigation with more detailed climate change scenarios for the region.

Glaciers as crucial sediment sources

This thesis emphasizes the *crucial role of glaciers as sediment sources*. The input variable selection algorithm indicates that while all three hydroclimatic variables, erosive rainfall, ice melt and snowmelt contribute to suspended sediment concentration, erosive rainfall explains the largest fraction of its variability, because intense rainfall events are responsible for entraining large amount of sediment and producing peaks in suspended sediment concentration. Conversely, the parameters of the HMRC indicate that *ice melt water coming from glaciers generates the highest suspended sediment concentration per unit runoff and represents the greatest contribution to total suspended sediment yield* (Chapter 3). This is in agreement with the analysis presented in Chapter 2, in which it is demonstrated that the *increase in suspended sediment concentration observed at the outlet of the basin is most likely due to enhanced ice melt and glacier retreat occurred in the Alpine region in mid 1980s*. Increased melt water derived from sediment-rich subglacial and proglacial areas, larger relative contribution of ice melt compared to snowmelt and increased sediment supply in proglacial areas, due to glacier recession, result to be the major drivers of suspended sediment concentration rise (Chapter 2). The increase in suspended sediment export from the upper Rhône catchment after mid 1980s has been also detected by colleagues sampling sediment in the Lake Geneva cores (Silva et al., in preparation). Silva collected several sediment cores in the Rhône Delta and estimated sediment accumulation rates based on ^{1}37Cs chronology. Peaks of ^{1}37Cs can be used to detect the years of 1954, 1964 and 1986, which mark respectively periods of nuclear tests and the catastrophe of Chernobyl. Preliminary results on seven sediment cores, show that *mass accumulation rats are high for the period 1953 to 1964, decrease from 1964 to 1986, and increase again during the period 1986 to 2014*.

As discussed by Stutenbecker et al. (2017), glaciers represent a major source of sediment in the Alpine region, and the high contribution of sediment derived from glacierized areas, which is commonly low in ^{1}0Be, would also explain the low ^{1}0Be concentration measured at the basin outlet and consequent high denudation rates. Preliminary results of the grain size analysis on sediment cores collected at Lake Geneva, indicate that, while the decrease

in mass accumulation rates occurred between 1964 and 1986 is uniform for all grain sizes, the increase observed after mid 1980s is mainly associated with increases in very fine grain sizes such as silt and clay (Silva et al., in preparation). Because glacially derived sediment is notoriously very fine, these results further suggest the role played by glaciers in the rise of suspended sediment yield entering Lake Geneva.

Climatic signal propagates even through highly human-impacted Alpine catchments

By linking the increase in suspended sediment concentration to the enhanced glacier retreat and increased ice melt (Chapter 2), this thesis demonstrates how *even catchments significantly regulated by hydropower and by other human activities are highly sensitive to changes in climate*. Even if the upper Rhône basin is highly regulated, and a complex network of water intakes and tunnels completely disrupt the natural regime of the catchment, the effects of warmer temperature are observed at the outlet through the increase in suspended sediment concentration. Likewise, results of the river network bedload model indicate that climate also impacts bedload transport, although the effects are smaller than those generated by flow regulation which affects the sediment transporting capacity of flow for coarse grains (Chapter 4). It has to be mentioned that enhanced fine sediment supply by glacial erosion is contingent on active glacier retreat generating this sediment supply. It is not likely to continue when small and mid-size glaciers reach their equilibrium point (Huss and Hock, 2018).

By analyzing the uppermost reaches of the Borgne, Bakker et al. (2018) demonstrate that despite substantial flow abstraction, significant sediment transfer takes place downstream of water intakes. In fact, the increase in glacial sediment export that Bakker et al. (2018) found in the late 1980s to early 1990s in the Borgne, correspond to the suspended sediment concentration rise that was found at the outlet of the Rhône, tens of kilometers downstream. This confirms how the *signal of warmer temperature propagates through hydropower infrastructures and travel along the river network potentially reaching the outlet* (Bakker et al., 2018).

Sediment sources at the basin scale

The research presented in this thesis proposes that, *to explore the causes of changes in sediment dynamics, it is necessary to adopt an approach that includes information on sediment sources and their hydroclimatic conditioning* (Chapter 2). For example, adopting traditional methods such as rating curves based on discharge only, would not have allowed understanding the casual link between suspended sediment concentration and ice melt. Considering that different sediment sources, both in terms of spatial distribution (e.g. lithology, degree of connectivity) and in terms of processes of erosion and transport (e.g glacier erosion, hillslope erosion), are activated by different hydroclimatic forcing al-

lowed us to develop an understanding of possible causes of change. Likewise, by using the HMRC, which includes the individual contributions of erosive rainfall, ice melt, snowmelt and hydropower releases, it was possible to reproduce the rise in suspended sediment concentration observed in the basin in the 1980s, although the simulated changes are more gradual than those observed.

Regarding sediment sources, Stutenbecker et al. (2017) investigated the sediment budget of the upper Rhône basin in our project. The spatial distribution of denudation rates in the catchment, was estimated based on concentrations of terrestrial nuclide 10Be in quartz isolated from fluvial sediment of selected tributaries. Through petrography, heavy mineral concentrations, and bulk geochemistry, three main sediment sources were fingerprinted and their contributions to the sediment at the outlet of the basin were estimated by compositional mixing modelling. Results indicate that the Penninic nappes, located in the southern part of the basin, are characterized by the highest denudation rates. However, sediment fingerprinting and compositional mixing model suggest that this lithological unit, covering more than 50% of the catchment surface, represents only 23% of the sediment along the main upper Rhône River. The discrepancy between erosion rates and sediment yield may be explained by the fact that the tributaries located in this lithological unit are severely affected by human activities. Stutenbecker et al. (2017) discuss that mining activities and hydropower are potentially responsible for 50% reduction of the total sediment load generated in the Penninic nappes, explaining why this part of the upper Rhône is under-represented in the sediment budget. In agreement with results presented in this thesis, this study highlights *how the spatial variability of sediment sources plays a crucial role on the composition of sediment yield and its vulnerability to potential drivers of change* (Stutenbecker et al., 2017).

The river network is a system that structures the effects of localized perturbation

Simulations of the river network bedload model in this thesis indicate that the effect of hydropower are site- and grain size-dependent and vary significantly with the season. On one hand, the non-linearity and threshold nature of bedload transport equations, make prediction on the effects of altered flow conditions difficult to assess. For example, simulations show that the increase in winter discharge does not reflect in higher bedload transport. Likewise, given the same reduction in summer discharge, the transport of gravel reduces much more that the transport of sand. On the other hand, this thesis demonstrates that localized perturbations may propagate along the river network and involve the entire system. As an example, while only some first order links are affected by hydropower, all third order links are influenced. Moreover, the river network structures the perturbations in such a way that individual effects are either enhanced or dampened in the downstream direction. All these considerations indicate that *to analyze the impacts*

of localized perturbations it is necessary to account for the entire river network system. It should be recognized that heavily regulated reaches downstream of dams gradually recover natural flow dynamics downstream through the river network. However, a river network perspective is required to predict this recovery, and its impact on river morphological development and ecosystem (habitat) quality.

5.2 Outlook

This research raised some interesting questions which should be addressed in the future. Some of the main research directions are summarized in the following.

Impacts of sediment storage and water intakes on fine sediment fractions

While this thesis demonstrates the impacts of climate on suspended sediment fluxes, the effect of sediment trapping behind dams needs further investigation. Especially for finer fractions, such as fine sand, silt and clay, it is not clear how much sediment is stored in the reservoirs and how much is released through the power stations and spillways and reaches the catchment outlet. A quantification of the reservoir trapping efficiency for finer grain sizes, and the analysis of how it varies seasonally can be conducted by measuring turbidity at the outlet and in the reservoir. Other measurement options are satellite-derived turbidity estimates of the water surface for large lakes and bathymetric measurements of the lake bed. Likewise, the effects of water intakes on fine sediment transfer need to be further explored. How much fine sediment is delivered to the reservoirs and how much is instead transferred to downstream river reaches through flushing at intakes remains an open question. By addressing these questions, it would be possible to explore if the cause of the reduction in lake sedimentation rates observed by Loizeau et al. (1997) in the 1960s in Lake Geneva, is related to hydropower or to colder climatic conditions. More generally, estimating the storage of fine sediment behind dams, would allow a better quantification of the counteracting effects of warmer temperatures (augmented supply) and hydropower on suspended sediment load of Alpine regulated catchments.

Channel bed sediment supply and sediment input from hillslopes

For coarse grains (sand, gravels and coarser), results of the river network bedload model indicate that flow regulation has a dominating impact on bedload transport in the upper Rhône River, compared to sediment trapping behind reservoirs. This could be partially related to the water intakes, which affect a large fraction of the catchment by significantly reducing sediment transport capacity and yet preserving high sediment supply. However, the small impact associated to sediment storage in the reservoirs showed by the model results, could also be associated to how sediment supply is described in the model. In

the present version of the model, sediment supply is limited by the sediment input from upstream links and sediment available on the river bed. It is envisaged to improve this aspect by better estimating the actual sediment supply characterizing the river network. The expectation is that a better representation of the sediment supply limitation, would allow a more realistic quantification of the relative effects of flow regulation and sediment trapping on bedload transport at the basin scale. This consideration is also based on observations of gravel transport in the Borgne, which showed that the supply of sediment is much lower than previously thought, and that even with water withdrawals at this intake, sediment supply was only approaching transport capacity after regulation. Therefore supply limitation for coarse material may be an important factor at low order streams in periglacial areas (Lane et al., 2017, Bakker et al., 2018) In addition, regarding sediment supply, an important component that is planned to be implemented in the bedload model is related to the contribution of sediment from hillslopes. It would be particularly interesting to quantify how the river network system would respond to localized input of sediment, mimicking the contribution from events such as debris flow or landslides. The relatively low computational requirements of the river network bedload model would allow investigating this aspect in a statistical framework, including stochastic forcing of climate and mass events producing sediment (e.g. sediment cascade approach of Bennett et al., 2016), possibly revealing interesting aspects related to spatial and temporal scales of geomorphic changes associated with punctual inputs of sediment.

Channel bed GSD: initialization and equilibrium

Results presented in this thesis indicate that basin-scale channel bed GSD is less sensitive to alterations of discharge than bedload transport rates. However, as discussed in glaciers represent a major source of sediment in the Alpine region, this could be partially related to the initialization of GSD which was based on an equilibrium concept across the network. It would be particularly useful to verify this concept by wide-spread measurement of the spatial distribution of GSDs across many links in the river network. This would allow to quantify the effects of the GSD initialization on model results and to identify an initialization procedure specific for the scenario before hydropower, accounting not only for altered flow conditions but including information on sediment supply. During this PhD, in the context of a Master Thesis, a first attempt of mapping GSDs in the catchment was started. Digital images of the channel bed were obtained with a low-cost drone at seven river reaches along the main upper Rhône River and along tributaries. The image processing method developed by Carbonneau et al. (2004), was used in combination with field measurements to obtain spatial maps of river bed GSD. A predictive relationship between measured ground truth data and metrics of the local semivariance (sill and lag values) in image brightness is first established, and second applied to map the values of

d64. A more intensive data collection following this method is foreseen in the catchment to better explore how GSD adjusts to changes in hydrological conditions.

Climate change and sediment dynamics in the Alps

A comprehensive understanding of how climate change will impact suspended sediment transport and bedload transport in Alpine environments in general remains an open issue. Although the effects of climate change on hydrology are widely investigated at the global and regional scales, impacts on erosion and sediment transport remain poorly understood. Some of the main open research questions are highlighted in the following. The role of climatic extremes (extraordinary events) on the overall sediment budget is not yet clear. Likewise, the effect of climate change on short and long-term sediment-related processes needs further investigation. How and if the discrepancy between long-term denudation rates and present-day sediment loads is associated to the recurrence of large-magnitude sediment-transport events needs to be explored (Covault et al., 2013). Another crucial aspect to investigate is the partitioning of the uncertainty, as it has already been done for climate (Fatichi et al., 2016). The uncertainties associated to natural climate variability and climate change predictions, the uncertainty associated to the stochasticity in sediment production and transport, and the uncertainty associated to hydropower operation should be objectively compared. And last, if the anthropogenic impacts on sediment transport are even comparable to the natural variability in erosion rates is not yet understood.

Chapter 6

References

Aas, E. and Bogen, J.: Colors of Glacier Water, *Water Resources Research*, **24(4)**, 561–565, 1988.

Allouche, O., Tsoar, A., Kadmon, R.: Assessing the accuracy of species distribution models: prevalence, kappa and the true skill statistic (TSS), *J. Appl. Ecol.*, **43**, 1223–1232, 2006.

Andrews, E.D.: Downstream effects of Flaming Gorge Reservoir on the Green River, Colorado and Utah. *Geological Society of America Bulletin* **97 (8)**, 1012–1023, 1986.

Anselmetti, F.S., Bühler, R., Finger, D., Girardclos, S., Lancini, A., Rellstab, C., Sturm, M.: Effects of Alpine hydropower dams on particle transport and lacustrine sedimentation, *Aquatic Science*, **69**, 179–198, 2007.

Arnell, N., Döll, P., Kabat, P., Jimènez, B., Miller, K., Oki, T., Sen, Z., Shiklomanov, I.: *IPCC, Impact, Adaptation and Vulnerability.* Fourth Assessment Report, Working Group II Report, Section 3.4.5., 2007.

Asselman, N. E. M.: Suspended sediment dynamics in a large drainage basin: the River Rhine, *Hydrological Processes*, **13**, 1437–1450, 1999.

Asselman, N. E. M.: Fitting and interpretation of sediment rating curves, *Journal of Hydrology*, **234**, 228–248, 2000.

Auer, A. H.: The rain versus snow threshold temperatures, *Weatherwise*, **27**, 67–67, doi:10.1080/00431672.1974.9931684, 1974.

Bakker, M., Costa, A., Silva, T. A., Stutenbecker, L., Girardclos, S., Loizeau, J.-L., Molnar, P., Schlunegger, F., and Lane, S.: Combined flow abstraction and climate change impacts on an aggrading Alpine river. *Water Resources Research*, **54**, https:// doi.org/10.1002/2017WR021
2018.

Ballantyne, C.K.: A general model of paraglacial landscape response, *The Holocene*, **12**, 371–6, 2002.

Bavay, M., Lehning, M., Jonas, T., Löwe, H.: Simulations of future snow cover and discharge in Alpine headwater catchments, *Hydrological Processes*, **23**, 95–108, 2009.

Begueria, S.: Validation and Evaluation of Predictive Models in Hazard Assessment and Risk Management, *Natural Hazards*, **37**, 315–329, doi 10.1007/s11069–005–5182–6, 2006.

Benda, L., and Dunne, T.: Stochastic forcing of sediment routing and storage in channel networks. *Water Resources Research*, **33**, 2865–2880, doi:10.1029/97WR02387, 1997.

Benda, L., Andras, K., Miller, D., and Bigelow, P., Confluence effects in rivers: Interactions of basin scale, network geometry, and disturbance regimes, *Water Resources Research*, **40**, W05402, doi:10.1029/2003WR002583, 2004.

Beniston, M.: Variations of snow depth and duration in the Swiss Alps over the last 50 years: Links to changes in large–scale climatic forcings, *Climatic Change*, **36**, 281–300, 1997.

Beniston, M. and Rebetez, M.: Regional behavior of minimum temperatures in Switzerland for the period 1979–1993, *Theoretical and Applied Climatology*, **53**, 231–243, 1996.

Beniston, M., Rebetez, M., Giorgi, F., Marinucci, R.: An analysis of regional climate change in Switzerland, *Theoretical and Applied Climatology*, **49**, 135–159, 1994.

Bennett, G., Molnar, P., Eisenbeiss, H., and McArdell, B. W.: Erosional power in the Swiss Alps: characterization of slope failure in the Illgraben, *Earth Surface Processes and Landforms*, **37**, 1627–1640, doi:10.1002/esp.3263, 2012.

Bertoldi, W., Siviglia, A., Tettamanti, S., Toffolon, M., Vetsch, D.F., Francalanci, S.: Modeling vegetation controls on fluvial morphological trajectories, *Geophysical Research Letters*, doi: 10.1002/2014GL061666, 2014.

Beyer-Portner, N.: *Erosion des bassins versant alpins suisses par ruissellement de surface.* PhD thesis. Ecole Polytechnique Federal, Lausanne, Switzerland, 1998.

Boscarello, L., Ravazzani, G., Rabuffetti, D., Mancini, M.: Integrating glaciers raster–based modelling in large catchments hydrological balance: the Rhône case study, *Hydrological Processes*, **28**, 496–508, doi: 10.1002/hyp.9588, 2014.

Boulton, G.S.: *Processes and patterns of glacial erosion*, (In Coates, ed.), Glacial Geomorphology, New York State University, 41–87, 1974.

Braatne, J. H., Rood, S. B., Goater, L. A., Blair, C. L.: Analyzing the impacts of dams on riparian ecosystems: a review of research strategies and their relevance to the Snake River through Hells Canyon. *Environ Manage.*, **41**, 267–281, 2008

Bracken, L. J., Turnbull, L., Wainwright, J., Bogaart, P.: Sediment connectivity: a framework for understanding sediment transfer at multiple scales, *Earth Surface Processes and Landforms*, **40**, 177–188, 2015.

Braun, J. and Sambridge M.: Modelling landscape evolution on geological timescales: a new method based on irregular spatialdiscretization, *Basin Research*, **9**, 27–52, 1997.

Braun, L. N., Aellen, M., Funk, M., Hock, R., Rohrer, M. B., Steinegger, U., Kappenberger, G.: Müller–Lemans, H.: Measurement and simulation of high alpine water balance components in the Linth– Limmern head watershed (north–eastern Switzerland), *Zeitschrift für Gletscherkunde und Glazialgeologie*, **30**, 161–185, 1994.

Brown, L. C. and Foster, G. R.: Storm erosivity using idealized intensity distributions, *Transactions of the Asae*, **30**, 379–386, 1987.

Brönnimann, S., Appenzeller, C., Croci–Maspoli, M., Fuhrer, J., Grosjean, M., Hohmann,R., Ingold, K., Knutti, R., Liniger, M. A., Raible, C. C., Röthlisberger,R., Schär,C., Scherrer, S. C., Strassmann, K., Thalmann. P.: *Climate change in Switzerland: a review of physical, institutional, and political aspects*, WIREs Clim Change 2014, doi: 10.1002/wcc.280, 2014.

Brune G. M.: Trap Efficiency of Reservoirs. *Eos Transactions, American Geophysical Union.* **34(3)**, pp. 407-418. ISSN 0096-3941, 1953.

Caine, N.: The rainfall intensity–duration control of shallow landslides and debris flows, *Geogr. Ann. A.* **62**:23–27, 1980.

Camp T. R.: *Sedimentation and the design of settling tanks.* In: Transactions of the American Society of Civil Engineers. **111**, Paper No. 2285, pp. 895-936. ISSN 0066-0604, 1946.

Campbell, F. B., and Bauder, H. A.: A rating curve method for determining silt discharge of streams, *Am. Geophys. Union Trans.*, part 2, 603–607, 1940.

Carbonneau, P. E., Lane, S. N., and Bergeron, N. E.: Catchment-scale mapping of surface grain size in gravel bed rivers using airborne digital imagery. *Water Resources Research*, **40(7)**, 2004.

Cavalli, M., Trevisani, S., Comiti, F., Marchi, L.: Geomorphometric assessment of spatial sediment connectivity in small Alpine catchments, *Geomorphology*, doi: 10.1016/j.geomorph.2012.05.007, 2013.

Chen, C.-N.: Design of sediment retention basins. *In: National symposium on urban hydrology and sediment control. University of Kentucky*, 28-31 July 1975. Lexington - Kentucky: Office of Research and Engineering Services. pp. 285-298, 1975.

Chiari, M., Friedl, K., and Rickenmann, D.: A one dimensional bedload transport model for steep slopes, *Journal of Hydraulic Research*, **48(2)** 152–160, doi:10.1080/00221681003704087, 2010.

Chiari, M., and Rickenmann, D.: Back-calculation of bedload transport in steep channels with a numerical model. *Earth Surface Processes and Landforms*, **36(6)**, 805–815, doi:10.1002/esp.2108, 2011.

Ciarapica, L., and Todini, E.: TOPKAPI: a model for the representation of the rainfall–runoff process at different scales. *Hydrological Processes*, **16**, 207–229, doi: 10.1002/hyp.342, 2002.

Collins, W. D., Rasch, P. J., Boville, B. A., Hack, J. J., McCaa, J. R., Williamson, D. L., Kiehl, J. T., Briegleb, B.: Description of the NCAR community atmosphere model (CAM3), *Tech. Rep. NCAR/TN– 464+STR*, **226**, 2004.

Corbari, C., Ravazzani, G., Martinelli, J., Mancini, M.: Elevation based correction of snow coverage retrieved from satellite images to improve model calibration, *Hydrology and Earth System Sciences*, **13**, 639–649, 2009.

Costa, A., Molnar, P., Stutenbecker, L., Bakker, M., Silva, T. A., Schlunegger, F., Lane, S. N., Loizeau, J.-L., and Girardclos, S.: Temperature signal in suspended sediment export from an Alpine catchment, *Hydrology and Earth System Sciences*, **22**, 509-528, https://doi.org/10.5194/hess-22-509-2018, 2018a.

Costa, A., Anghileri, D., and Molnar, P.: Hydroclimatic control on suspended sediment dynamics of a regulated Alpine catchment: a conceptual approach. *Hydrology and Earth System Sciences Discussion*, https://doi.org/10.5194/hess-2018-5, in review, 2018b.

Coulthard, T.J., Kirkby, M.J., Macklin, M.G.: Modelling geomorphic response to environmental change in an upland catchment. *Hydrological Processes*, **14**, 2031-2045, 2000.

Covault, J. A., Craddock, W. H., Romans, W., Fildani, A., and Gosai M.: Spatial and Temporal Variations in Landscape Evolution: Historic and Longer-Term Sediment Flux through Global Catchments, *Journal of Geology*, **121**, 35-56, 2013.

Crawford, C. G.: Estimation of suspended–sediment rating curves and mean suspended–sediment loads, *Journal of Hydrology*, **129**, 331–348, 1991.

Csiki, S. J. C., and Rhoads, B. L.: Influence of four run-of-river dams on channel morphology and sediment characteristics in Illinois, USA. *Geomorphology*, **206**(Supplement C), 215–229. https://doi.org/10.1016/j.geomorph.2013.10.009, 2014.

Czuba, J. A., and Foufoula-Georgiou, E.: A network-based framework for identifying potential synchronizations and amplifications of sediment delivery in river basins, *Water Resources Research*, **50**, 3826–3851, doi:10.1002/ 2013WR014227, 2014.

Czuba, J. A., and Foufoula-Georgiou, E.: Dynamic connectivity in a fluvial network for identifying hotspots of geomorphic change. *Water Resources Research*, **51**, 1401–1421, doi:10.1002/2014WR016139, 2015.

Dade, W. B., and Friend, P. F: Grain size, sediment-transport regime, and channel slope in alluvial rivers. *Journal of Geology*, **106**, 661–675, 1998.

Dadson, S. J., Hovius, N., Chen, H., Dade, W. B., Lin, J.-C., Hsu, M.-L., Lin, C.-W., Horng, M.-J., Chen, T.-C., Milliman, J. D., Stark, C. P.: Earthquake-triggered increase in sediment delivery from an active mountain belt, *Geology*, **32**, 733–736, 2004.

Darby S. E., Hackney, C. R., Leyland, J., Kummu, M., Lauri, H., Parsons, D. R., Best, J. L., Nicholas, A. P., Aalto, R.: Fluvial sediment supply to a mega-delta reduced by shifting tropical-cyclone activity, *Nature*, **539(7628)**:276–279, doi:10.1038/nature19809, 2016.

Dedieu, J.–P., Boos, A., Kiage, W., Pellegrini, M.: Snow cover retrieval over Rhône and Po river basins from MODIS optical satellite data (2000–2009), *Geophysical Research Abstracts*, **12**, 5532, EGU General Assembly, 2010.

De Girolamo, A.M., Pappagallo, G., Lo Porto, A.: Temporal variability of suspended sediment transport and rating curves in a Mediterranean river basin: The Celone (SE Italy), *Catena* **128**, 135–143, doi: 10.1016/j.catena.2014.09.020, 2015.

Delunel, R., van der Beek, P., Bourlès, D., Carcaillet J., Schlunegger, F.: Transient sediment supply in a high–altitude Alpine environment evidenced through a 10Be budget of the Etages catchment (French Western Alps). *Earth Surface Processes and Landforms*, **39**, 890–899, doi:10.1002/esp.3494, 2014.

Detert, M. and Weitbrecht, V.: User guide to gravelometric image analysis by BASEGRAIN, *Advances in Science and Research*, 1789–1795, 2013.

De Vente, J., Poesen, J., Bazzoffi, P., Van Rompaey, A., Verstraeten, G.: Predicting catchment sediment yield in Mediterranean environments: the importance of sediment sources and connectivity in Italian drainage basins, *Earth Surface Processes and Landforms*, **31**, 1017–1034, 2006.

Dhakal, A. S., Sidle, R. C.: Distributed simulations of landslides for different rainfall conditions, *Hydrological Processes*, **18**, 757–776, 2004.

Duan, N: Smearing estimate: a nonparametric retransformation method, *J. Am. Stat. Ass.*, **78**, 605–610, 1983.

England, P. and Molnar, P.: Surface uplift, uplift of rocks, and exhumation of rocks, *Geology*, **18**, 1173–1177, 1990.

Fatichi, S., V. Y. Ivanov, A. Paschalis, N. Peleg, P. Molnar, S. Rimkus, J. Kim, P. Burlando, and E. Caporali: Uncertainty partition challenges the predictability of vital details of climate change, *Earth's Future*, **4**, 240–251, doi:10.1002/2015EF000336, 2016.

Fatichi, S., Rimkus, S., Burlando, P., Bordoy, R., Molnar, P.: High–resolution distributed analysis of climate and anthropogenic changes on the hydrology of an Alpine catchment, *Journal of Hydrology*, **525**, 362–382, 2015.

Fehr, R.: Einfache Bestimmung der Korngrössenverteilung von Geschiebematerial mit Hilfe der Linienzahlanalyse. *Schweizer Ingenieur und Architekt*, **105(38)**, 1987.

Ferguson, R. I.: River loads underestimated by rating curves, *Water Resources Research*, **22**, 74–76, 1986.

Ferguson, R.: Flow resistance equations for gravel- and boulder-bed streams, *Water Resources Research*, **43**, W05427, doi:10.1029/2006WR005422, 2007.

Ferguson, R. I., and Church, M.: A simple universal equation for grain settling velocity, *Journal of Sedimentary Research*, **74**, 933–937, 2004.

Ferguson, R. I., Church, M., Rennie, C. D., and Venditti, J. G.: Reconstructing a sediment pulse: Modeling the effect of placer mining on Fraser River, Canada, *Journal of Geophysical Research: Earth Surface*, **120**, 1436–1454. doi:10.1002/2015JF003491, 2015.

Finger, D., Schmid, M., Wüest, A.: Effects of upstream hydropower operation on riverine particle transport and turbidity in downstream lakes, *Water Resources Research*, **42**, 8, 2006.

Finsinger, W. et al.: Holocene vegetation and land-use changes in response to climatic changes in the forelands of the southwestern Alps, Italy, *Journal of Quaternary Science*, **21**, 243–58, 2006.

FOEN: *Auswirkungen der Klimaänderung auf Wasserressourcen und Gewässer*. Synthesebericht zum Projekt "Klimaänderung und Hydrologie in der Schweiz" (CCHydro). Bundesamt für Umwelt, Bern. Umwelt–Wissen, **Nr. 1217**, 76, 2012.

Fischer, M., Huss, M., Hoelzle, M.: Surface elevation and mass changes of all Swiss glaciers 1980–2010, *The Cryosphere*, **9**, 525–540, doi:10.5194/tc-9-525- 2015, 2015.

Foster, G.C., Dearing, R.A., Jones, R.T., Crook, D.S., Siddle, D.J., Harvey, A.M., James, P.A., Appleby, P.G., Thompson, R., Nicholson, J., Loizeau, J.-L.: Meteorological and land use controls on past and present hydro-geomorphic processes in the pre-alpine environment: an integrated lake-catchment study at the Petit Lac d'Annecy, France, *Hydrological Processes*, **17**, 3287–3305, 2003.

Francipane, A., Ivanov, V.Y., Noto, L.V., Istanbulluoglu, E., Arnone, E. and Bras, R.: tRIBS-Erosion: A parisomonious physically-based model for studying catchment hydrogeomorphic response. *Catena*, **92**, 216–231, 2012.

Frei, C.: Interpolation of temperature in a mountainous region using nonlinear profiles and non-Euclidean distances, *International Journal of Climatology*, **34**, 1585–1605, 2014.

Frei, C., R. Schöll, S. Fukutome, J. Schmidli and P.L. Vidale: Future change of precipitation extremes in Europe: An intercomparison of scenarios from regional climate models, *Journal of Geophysical Research*, **111**, D06105, doi:10.1029/2005JD005965, 2006.

Gabbud, C. and Lane, S.N.: Ecosystem impacts of Alpine water intakes for hydropower: the challenge of sediment management. *WIREs Water*, **3(1)**, 41–61. doi:10.1002/wat2.1124, 2016.

Galelli, S. and Castelletti, A.: Tree-based iterative input variable selection for hydrological modeling, *Water Resources Research*, **49**, 4295–4310, doi:10.1002/wrcr.20339, 2013.

Geurts, P., Ernst, D., Wehenkel, L.: Extremely randomized trees, *Mach. Learn.*, **63(1)**, 3–42, 2006.

Gardner, A. S., Moholdt, G., Cogley, J. G., Wouters, B., Arendt, A. A.,Wahr, J.: A reconciled estimate of glacier contributions to sea level rise: 2003 to 2009, *Science*, **340**, 852–857, doi:10.1126/science.1234532, 2013.

Giguet-Covex, C. et al.: Changes in erosion patterns during the Holocene in a currently treeless subalpine catchment inferred from lake sediment geochemistry (Lake Anterne, 2063 m a.s.l., NW French Alps): The role of climate and human activities, *The Holocene*, **21**, 651–65, 2011.

Gippel, C. J.: Potential of turbidity monitoring for measuring the transport of suspended solids in streams, *Hydrological Processes*, **9**, 83–97, 1995.

Graf, W. L.: Downstream hydrologic and geomorphic effects of large dams on American rivers. *Geomorphology*, **79**(3–4, Sp. Iss. SI):336–60, doi:10.1016/j.geomorph.2006.06.022, 2006.

Grasso, A., Bérod, D., Hodel, H.: Messung und Analyse der Verteilung von Schwebstoffkonzentrationen im Querprofil von Fliessgewässern, *"Wasser Energie Luft"* – **104**, Jahrgang 2012, Heft 1, CH–5401 Baden, 2012.

Grønsten, H.A., Lundekvam, H.: Prediction of surface runoff and soil loss in southeastern Norway using the WEPP Hillslope model, *Soil and Tillage Research*, **85**, 186–199, 2006.

Gurnell. A., Hannah, D., Lawler, D.: Suspended sediment yield from glacier basins, Erosion and Sediment Yield: Global and Regional Perspectives (Proceedings of the Exeter Symposium, July 1996), *IAHS Publ.* **no. 236**, 1996.

Guzzetti, F., Peruccacci, S., Rossi, M., Stark, C. P.: The rainfall intensity–duration control of shallow landslides and debris flows: an update, *Landslides*, **5**, 3–17, 2008.

Haeberli, W. and Holzhauser, H.: Alpine glacier mass changes during the past two millennia, *PAGES News*, **11**, 1, 13–15, 2003.

Haeberli, W., Hoelzle, M., Paul, F., Zemp, M.: Integrated monitoring of mountain glaciers as key indicators of global climate change: the European Alps, *Annals of Glaciology*, **46(1)**, 150–160, 2007.

Habersack, H. and Nachtnebel, H. P.: *Development of sediment transport and river engineering methods.* In: Proc. Internat. Symp. East-West, North-South Encounter on State-of-the-Art in River Engineering Methods and Design Philosophies (Si. Petersburg, Russia), 1994.

Heckmann, T. and Schwanghart, W.: Geomorphic coupling and sediment connectivity in an alpine catchment â Exploring sediment cascades using graph theory, *Geomorphology*, **182**, 89–103, 2013.

Herman, F., Beyssac, O., Brughelli, M., Lane, S.N., Leprince, S., Adatte, T., Lin, J.Y.Y. and Avouac, J.P.: Erosion by an Alpine glacier, *Science*, **350**, 193–5, 2015.

Hilker, N., Badoux, A. and Hegg C.: The Swiss flood and landslide damage database 1972–2007, *Natural Hazards Earth Syst. Sci.*, **9**, 913–925, 2009.

Hinderer, M., Kastowski, M., Kamelger, A., Bartolini, C., Schlunegger, F.: River loads and modern denudation of the Alps – A review, Earth–Science Reviews, 118, 11–44, 2013.

Hock, R.: Temperature index melt modelling in mountain areas, *Journal of Hydrology*, **282**, 104–115, 2003.

Holliday, C. P. Rasmussen, T. C, Miller, W. P., Establishing the relationship between turbidity and total suspended sediment concentration, Georgia Water Resources Conference, Athens, GA: *Georgia Water Science Center Publications*, 2003.

Hornung, J., Pflanz, D., Hechler, A., Beer, A., Hinderer, M., Maisch, M. and Bieg, U.: 3-D architecture, depositional patterns and climate triggered sediment fluxes of an alpine alluvial fan (Samedan, Switzerland), *Geomorphology*, **115**, 202–14, 2010.

Horton, R. E.: Erosional development of streams and their drainage basins: hydro-physical approach to quantitative morphology. *Geological Society of America Bulletin*, **56 (3)**, 275–370, http://dx.doi.org/10.1130/0016-7606(1945)56[275:EDOSAT]2.0.CO;2, 1945.

Horowitz, A. J.: An evaluation of sediment rating curves for estimating suspended sediment concentrations for subsequent flux calculations, *Hydrological Processes*, **17**, 3387–3409, 2003.

Horowitz, A. J.:A quarter century of declining suspended sediment fluxes in the Mississippi River and the effect of the 1993 flood., *Hydrological Processes*, **24**, 13–34, 2010.

Huang, M. Y.–F., Montgomery, D. R.: Altered regional sediment transport regime after a large typhoon, southern, Taiwan. *Geology*, **41**, 1223–1226, 2013.

Huggel, C., Clague, J. J. and Korup, O.: Is climate change responsible for changing landslide activity in high mountains? E*arth Surface Processes and Landforms*, **37**, 77–91, 2012.

Huss, M. and Farinotti, D.: Distributed ice thickness and volume of all glaciers around the globe, Journal of Geophysical Research, 117: F04010, doi: 10.1029/2012JF002523, 2012.

Huss, M. and Hock, R.: A new model for global glacier change and sea–level rise, *Front. Earth Sci.*, **3**:54, doi: 10.3389/feart.2015.00054, 2015.

Huss, M. and Hock, R.: Global-scale hydrological response to future glacier mass loss, *Nature Climate Change*, **8**, 135–140, https://doi.org/10.1038/s41558-017-0049-x, 2018.

Huss, M., Farinotti, D., Bauder, A., Funk, M.: Modelling runoff from highly glacierized alpine drainage basins in a changing climate, *Hydrological Processes*, **22**, 3888–3902, 2008.

Jouvet, G., Huss, M., Funk, M., Blatter, H.: Modelling the retreat of Grosser Aletschgletscher, Switzerland, in a changing climate, *Journal of Glaciology*, **57(206)**, 1033–1045, 2011.

Kondolf, G. M. et al.: Sustainable sediment management in reservoirs and regulated rivers: Experiences from five continents, *Earth's Future*, **2**, 256–280, doi:10.1002/2013EF000184, 2014.

Konz, N., Prasuhn, V., Alewell, C.: On the measurement of alpine soil erosion, *Catena*, **91**, 63–71, 2012.

Korup, O., McSaveney, M. J., Davies, T. R. H., Sediment generation and delivery from large historic landslides in the Southern Alps, New Zealand, *Geomorphology*, **61**, 189–207, 2004.

Korup, O. and Schlunegger, F.: Rock-type control on erosion induced uplift, eastern Swiss Alps, *Earth Planet. Sc. Lett.*, **278**, 278–285, 2009.

Kremer, K., Corella, J.P., Hilbe, M., Marillier, F., Dupuy, D., Zenhäusern, G., Girardclos, S.: Changes in distal sedimentation regime of the Rhone delta system controlled by subaquatic channels (Lake Geneva, Switzerland/France). *Mar. Geol.*, **370**, 125–135. doi:10.1016/j.margeo.2015.10.013, 2015.

Lacour, C., Joannis, C., Chebbo, G.: Assessment of annual pollutant loads in combined sewers from continuous turbidity measurements: sensitivity to calibration data, *Water Resources Research*, **43 (8)**, 2179–2190, 2009.

Laflen, J.M., Lane, L.J., and Foster, G.R.: WEPP - a new generation of erosion prediction technology, *Journal of Soil and Water Conservation*, **46**, 34–38, 1991.

Lal, R.: Soil degradation by erosion, *Land Degradation and Development*, **12**, 519–539, 2001.

Lamb, M. P., Dietrich, W. E., and Venditti, J. G.: Is the critical Shields stress for incipient sediment motion dependent on channel-bed slope? *Journal of Geophysical Research*, **113**, F02008, doi:10.1029/2007JF000831, 2008.

Lane, S.N., Bakker, M., Gabbud, C., Micheletti, N., Saugy, J. N: Sediment export, transient landscape response and catchment–scale connectivity following rapid climate warming and Alpine glacier recession, *Geomorphology*, http://dx.doi.org/10.1016/j.geomorph.2016.02.015, 2016.

Lawler, D. M. and Dolan, M.: Temporal variability of suspended sediment flux from a subarctic glacial river, southern Iceland, Erosion and Sediment Transport Monitoring Programmes in River Basins (Proceedings of the Oslo Symposium, August 1992), *IAHS Publ.* **no. 210**, 1992.

Laternser, M. and Schneebeli, M.: Long–term Snow Climate Trends of the Swiss Alps (1931–99), *International Journal of Climatology*, **23**, 733–750, 2003.

Lenzi, M. A., Mao, L., Comiti, F.: Interannual variation of suspended sediment load and sediment yield in an alpine catchment, *Hydrological Science Journal*, **48:6**, 899–915, doi: 10.1623/hysj.48.6.899.51425, 2003.

Lenzi, M.A. and Marchi, L.: Suspended sediment load during floods in a small stream of the Dolomites (northeastern Italy). *Catena*, **39**, 267–282, 2000.

Leonarduzzi, E., Molnar, P., and McArdell, B.W.: Predictive performance of rainfall thresholds for shallow landslides in Switzerland from gridded daily data, *Water Resources Research*, **53**, doi:10.1002/2017WR021044, 2017.

Lewis, J.: Turbidity-controlled suspended sediment sampling for runoff-event load estimation, *Water Resources Research*, **32 (7)**, 2299–2310, 1996.

Liu, Z., and Todini, E.: Towards a comprehensive physically-based rainfall–runoff model, *Hydrology and Earth System Sciences*, **6 (5)**, 859–881, 2002.

Liu, Z., and Todini, E.: Assessing the TOPKAPI non-linear reservoir cascade approximation by means of a characteristic lines solution. *Hydrological Processes*, **19 (10)**, 1983–2006, http://dx.doi.org/10.1002/hyp.5662, 2005.

Loizeau, J.–L. and Dominik J., Luzzi, T., Vernet J.–P.: Sediment Core Correlation and Mapping of Sediment Accumulation Rates in Lake Geneva (Switzerland, France) Using Volume Magnetic Susceptibility, *Journal of Great Lakes and Reservoirs*, **23(4)**, 391–402, 1997.

Loizeau, J.–L. and Dominik J., Evolution of the Upper Rhône River discharge and suspended sediment load during the last 80 years and some implications for Lake Geneva, *Aquatic Science*, **62**, 54–67, 1015–1621/00/010054–14, 2000.

Magilligan, F.J., Nislow, K.H.: Changes in hydrologic regime by dams. *Geomorphology*, **71 (1–2)**, 61–78, 2005.

Mao, L. and Carrillo, R.: Temporal dynamics of suspended sediment transport in a glacierized Andean basin, *Geomorphology*. doi:10.1016/j.geomorph.2016.02.003, 2016.

Marty, C.: Regime shift of snow days in Switzerland, *Geophysical Research Letters*, **35**, L12501, doi: 10.1029/2008GL033998, 2008.

Mason, S. J. and Graham, N. E.: Conditional Probabilities, Relative Operating Characteristics, and Relative Operating Levels, *Weather Forecast.*, **14(5)**, 713–725, 1999.

Merritt, W.S., Letcher, R.A., Jakeman A.J.: A review of erosion and sediment transport models, *Environmental Modelling and Software*, **18**, 761–799, 2003.

Meyer-Peter, E., and Mueller, R.: *Formulas for bedload transport*, Proceedings of the 2nd Meeting of the International Association for Hydraulic Structures Research, 39–64, Int. Assoc. for Hydraul. Struct. Res., Stockholm, 1948.

Métadier, M., Bertrand-Krajewski, J.-L., The use of long-term on-line turbidity measurements for the calculation of urban stormwater pollutant concentrations, loads, pollutographs and intra–event fluxes, *Water Resources Research*, **46**, 6836–6856, 2012.

Meteoswiss, Federal Office of Meteorology and Climatology: *Documentation of MeteoSwiss Grid–Data Products Daily Precipitation (final analysis): RhiresD*, http://www.meteoswiss.admin.ch, 2013.

Meteoswiss, Federal Office of Meteorology and Climatology: *Documentation of MeteoSwiss Grid–Data Products Daily Mean, Minimum and Maximum Temperature: TabsD, TminD, TmaxD*, http://www.meteoswiss.admin.ch, 2013.

Meusburger K., Alewell C.: *Soil Erosion in the Alps. Experience gained from case studies (2006–2013)*. Federal Office for the Environment, Bern. Environmental studies **no. 1408**: 116 pp, 2014.

Meusburger, K., Steel, A., Panagos, P., Montanarella, L., Alewell, C.: Spatial and temporal variability of rainfall erosivity factor for Switzerland, *Hydrology and Earth System Sciences*, **16**, 167–177, 2012.

Micheletti, N., Lambiel, C., Lane, S.N.: Investigating decadal–scale geomorphic dynamics in an alpine mountain setting, *Journal of Geophysical Research Earth Surf.*, **120**, 2155–2175, doi:10.1002/2015JF003656, 2015.

Micheletti, N. and Lane, S. N.: Water yield and sediment export in small, partially glacierized Alpine watersheds in a warming climate, *Water Resources Research*, **52(6)**, 4924–4943, doi: 10.1002/2016WR018774, 2016.

Milliman, J.D., Meade, R.H.: World-wide delivery of river sediment to the oceans. *Journal of Geology*, **91 (1)**, 1–21, 1983.

Molnar, P.: Late Cenozoic increase in accumulation rates of terrestrial sediment: How might climate change have affected erosion rates? *Annual Review of Earth and Planetary Sciences*, **32**, 67–89, 2004.

Montgomery, D. R.: Valley formation by fluvial and glacial erosion, *Geology*, **30**, 1047–1050, 2002.

Nash, J. E. and Sutcliffe, J. V.: River Flow Forecasting Through Conceptual Models Part 1 – A Discussion of Principles, *Journal of Hydrology*, **10**, 282–290, 1970.

Newman, M. C.: Regression analysis of log–transformed data: statistical bias and its correction, *Environmental Toxicology and Chemistry*, **20 12**, 1129–1133, 1993.

Nitsche, M., Rickenmann, D., Turowski, J. M., Badoux, A., and Kirchner, J. W.: Evaluation of bedload transport predictions using flow resistance equations to account for macro-roughness in steep mountain streams, *Water Resources Research*, **47**, W08513, doi:10.1029/2011WR010645, 2011.

Oerlemans, J. and Reichert, B.K.: Relating glacier mass balance to meteorological data using a Seasonal Sensitivity Characteristic (SSC). *Journal of Glaciology*, **46(152)**, 1–6, 2000.

Oliver, J.-M., Carrel, G., Lamouroux, N., Dole-Oliver, M.-J., Malard, F., Bravard, J.-P., Amoros, C.: *The Rhône River Basin*, In: Rivers of Europe, Chpt. 7, pp 247–295, Academic Press, London, 2009.

Ollesch, G., Kistner, I., Meissner, R., Lindenschmidt, K.-E.: Modelling of snowmelt erosion and sediment yield in a small low-mountain catchment in Germany, Catena, 68, 161 – 176, 2006.

Palazòn, L., Navas, A.: Land use sediment production response under different climatic conditions in an alpine–prealpine catchment, *Catena*, **137**, 244–255, 2016.

Paul, F., Kääb, A., Maisch, M., Kellenberger, T., Haeberli, W.: Rapid disintegration of Alpine glaciers observed with satellite data, *Geophysical Research Letters*, **31 (L21)**, L21402, (10.1029/2004GL020816.), 2004.

Paul, F., Machguth, H., Kääb, A.: On the impact of glacier albedo under conditions of extreme glacier melt: the summer of 2003 in the Alps, *EARSeL eProceedings* 4(2), 139–149, 2005.

Paul, F., Kääb, A. and Haeberli, W.: Recent glacier changes in the Alps observed from satellite: Consequences for future monitoring strategies, *Global and Planetary Change*, **56(1/2)**, 111–122, 2007.

Parker, G.: Surface-based bedload transport relation for gravel rivers. *Journal of Hydraulic Research*, **28(4)**, 417–436, doi:10.1080/00221689009499058, 1990.

Parker, G., Klingeman, P. C., and Mclean, D. G., Bedload and size distribution in paved gravel-bed streams, *Journal of the Hydraulic Division American Society of Civil Engineers*, **108(4)**, 544–571, 1982.

Pavanelli, D. and Pagliarani, A.: Monitoring water flow, turbidity and suspended sediment load, from an Apennine catchment basin, Italy, *Biosystems Engineering*, **83(4)**, 463–468, 2002.

Pellicciotti, F., Brock, B., Strasser, U., Burlando, P., Funk, M., Corripio, J.: An enhanced temperature–index melt model including the shortwave radiation balance: development and testing for Haut Glacier dâArolla, Switzerland, *Journal of Glaciology*, **51(175)**, 573–587, 2005.

Pettitt, A. N.: A Non–parametric Approach to the Change-point Problem, *Appl. Statist.*, **28(2)**, 126–135, 1979.

Petts, G. E., and Gurnell, A. M.: Dams and geomorphology: Research progress and future directions. *Geomorphology*, **71(1)**, 27–47. https://doi.org/10.1016/j.geomorph.2004.02.015, 2005.

Priestley, C., and Taylor, R.: On the assessment of surface heat flux and evaporation using large-scale parameters, *Monthly Weather Review*, **100(2)**, 81– 92, http://dx.doi.org/10.1175/1520-0493(1972)100<0081:OTAOSH>2.3.CO;2, 1972.

Proffitt, G. T., and Sutherland, A. J.: Transport of non-uniform sediments. *Journal of Hydraulic Research*, **21(1)**, 33–43. doi:10.1080/00221688309499448, 1983.

Quinton, W. L. and Carey, S. K.: Towards an energy–based runoff generation theory for tundra landscapes, *Hydrological Processes*, **22**, 4649–4653, 2008.

Ragettli, S., and Pellicciotti, F.: Calibration of a physically based, spatially distributed hydrological model in a glacierized basin: on the use of knowledge from glaciometeorological processes to constrain model parameters, *Water Resources Research*, **48** (W03509), http://dx.doi.org/10.1029/2011wr010559, 2012.

Ragettli, S., Cortés, G., McPhee, J., and Pellicciotti, F.: An evaluation of approaches for modeling hydrological processes in high-elevation, glacierized Andean watersheds. *Hydrological Processes*, **28(23)**, 5674–5695, http://dx.doi.org/10.1002/hyp.10055, 2013a.

Ragettli, S., Pellicciotti, F., Bordoy, R., and Immerzeel, W.W.: Sources of uncertainty in modeling the glaciohydrological response of a Karakoram watershed to climate change. *Water Resources Research*, **49**, 6048–6066, 2013b.

Raymond Pralong, M., Turowski, J. M., Rickenmann, D., and Zappa, M.: Climate change impacts on bedload transport in alpine drainage basins with hydropower exploitation. *Earth Surface Processes and Landforms*, **40(12)**, 1587–1599, https://doi.org/10.1002/esp.3737, 2015.

Renard, K. G., Foster, G. R., and Weesies, G. A.: *Predicting soil erosion by water; a guide to conservation planning with the revised universal soil loss equation (RUSLE)*, Agriculture Handbook **No. 703**, USDA-ARS, 404 pp., 1997.

Rebetez, M. and Reinhard, M.: Monthly air temperature trends in Switzerland 1901–2000 and 1975–2004, *Theoretical and Applied Climatology*, **91**, 27, doi 10.1007/s00704–007–0296–2, 2008.

Richards J. F.: *Land trandformation.* In: The Earth as Transformed by Human Action: Global and Regional Changes in Biosphere Over the past 3000 Years, Turner B. L., Clark W.C., Kate R. W., Richards J. F., Mathews J. T., Mayer W. B. (eds). Cambridge University Press: New York; 163–178, 1991.

Rickenmann, D.: Comparison of bed load transport in torrent and gravel bed streams, *Water Resources Research*, **37**, 3295–3305, doi:10.1029/2001WR000319, 2001.

Rickenmann, D., and Recking, A.: Evaluation of flow resistance in gravel-bed rivers through a large field data set, *Water Resources Research*, **47**, W07538, doi:10.1029/2010WR009793, 2011.

Rickenmann, D., Chiari, M., and Friedl, K.: *SETRAC – A sediment routing model for steep torrent channels*. River Flow 2006. 1, 843–852, edited by: Ferreira, R., Leal, E. A. J., and Cardoso, A., Taylor and Francis, London, 2006.

Sadeghi, S.H.R., Mizuyama, T., Miyata, S., Gomi, T., Kosugi, K., Fukushima, T., Mizugaki, S., Onda, Y.: Development, evaluation and interpretation of sediment rating curves for a Japanese small mountainous reforested watershed, *Geoderma*, **144**, 198–211, 2008.

Saletti, M., P. Molnar, A. Zimmermann, M. A. Hassan, and M. Church: Temporal variabil ity and memory in sediment transport in an experimental step-pool channel, *Water Resources Research*, **51**, 9325–9337, doi:10.1002/2015WR016929, 2015.

Santiago, S., Thomas, R. L., McCarthy, L., Loizeau, J. L., Larbaigt, G., Corvi, C., Rossel, D., Tarradellas, J., Vernet, J. P.: Particle Size Characteristics of Suspended and Bed Sediments in The Rhône River, *Hydrological Processes*, **6**, 227–240, 1992.

Schaefli, B., Hingray, B., Niggli, M., Musy, A.: A conceptual glaciohydrological model for high mountainous catchments. *Hydrology and Earth System Sciences*, **9**, 95–109, 2005.

Scherrer, S.C., Appenzeller, C.: Swiss Alpine snow pack variability: major patterns and links to local climate and large–scale flow. *Climate Research*, **32(3)**, 187–199, 2006.

Scherrer, S.C., Appenzeller C., Laternser, M.: Trends in Swiss Alpine snow days: the role of local– and large–scale climate variability, *Geophysical Research Letters*, **31**, L13215, doi: 10.1029/2004GL020255, 2004.

Schlunegger, F., and Hinderer, M.: Crustal uplift in the Alps: why the drainage pattern matters, *Terra Nova*, **13**, 425–432, 2001.

Schlunegger, F., and Hinderer, M.: Pleistocene/Holocene climate change, reestablishment of fluvial drainage network and increase in relief in the Swiss Alps. *Terra Nova*, **15**, 88–95. 10.1046/j.1365-3121.2003.00469.x, 2003.

Schmidt, J. C., and P. R. Wilcock: Metrics for assessing the downstream effects of dams, *Water Resources Research*, **44**, W04404, doi:10.1029/2006WR005092, 2008.

Schmidt, S., Alewell, C., Panagos, P., Meusburger, K.: Seasonal Dynamics of Rainfall Erosivity in Switzerland, *Hydrology and Earth System Sciences Discuss.*, doi:10.5194/hess–2016–208, 2016.

Schmitt, R. J. P., Bizzi, S., and Castelletti, A.: Tracking multiple sediment cascades at the river network scale identifies controls and emerging patterns of sediment connectivity, *Water Resource Research*, **52**, 3941–3965, doi:10.1002/ 2015WR018097, 2016.

Schmitt, R.J.P., Bizzi, S., Castelletti, A.F., and Kondolf, G.M.: Stochastic Modeling of Sediment Connectivity for Reconstructing Sand Fluxes and Origins in the Unmonitored

Se Kong, Se San, and Sre Pok Tributaries of the Mekong River. *Journal of Geophysical Research: Earth Surface.*, https://doi.org/10.1002/2016JF004105, 2018a.

Schmitt, R.J.P., Bizzi, S., Castelletti, A., and Kondolf, G.M.: Improved trade-offs of hydropower and sand connectivity by strategic dam planning in the Mekong, *Nature Sustainability*, **1**, 96–104, https://doi.org/10.1038/s41893-018-0022-3, 2018b.

Schneider, J.M., Rickenmann, D., Turowski, J. M., Bunte, K., and Kirchner, J. W.: Applicability of bed load transport models for mixed size sediments in steep streams considering macro-roughness, *Water Resources Research*, **51**, 5260–5283, doi:10.1002/2014WR016417, 2015.

Schoorl, J.M., Sonneveld M.P.W., Veldkamp A.: Three-dimensional landscape process modelling: the effect of DEM resolution, Earth Surface Processes and Landforms 25: 1025–1034, 2000.

Schwanghart, W., Worni, R., Huggel, C., Stoffel, M., Korup, O.: Uncertainty in the Himalayan energy–water nexus: estimating regional exposure to glacial lake outburst floods, *Environmental Research Letters*, **11**, 074005, https://doi.org/10.1088/1748-9326/11/7/074005, 2016.

Serquet, G., Christoph, M., Dulex, J. P., Rebetez, M.: Seasonal trends and temperature dependence of the snowfall/precipitation–day ratio in Switzerland, *Geophysical Research Letters*, **38**, L07703, doi:10.1029/2011GL046976, 2011.

Silva, T.A., Girardclos, S., Stutenbecker, L., Bakker, M., Costa, A., Schlunegger, F., Lane, S.N., Molnar, P., Loizeau, J.-L, Submitted. The sediment budget and dynamics of a delta-canyon-lobe system over the Anthropocene timescale: the Rhone River Delta, Lake Geneva (Switzerland/France). Under review in *Sedimentology.*

Smith, R.E., Goodrich, D.C., and Quinton, J.N.: Dynamic, distributed simulation of watershed erosion- the Kineros2 and Eurosem models, *Journal of Soil Water Conservation*, **50**, 517–520, 1995.

Strahler, A. N.: Hypsometric (area-altitude) analysis of erosional topology. *Geological Society of America Bulletin*, **63 (11)**, 1117–1142, doi:10.1130/0016- 7606(1952)63[1117:HAAOET]2.0.CO;2, 1952.

Stutenbecker L.: *Spatial and temporal variability of sediment sources in the upper Rhône basin, Switzerland.* Doctoral dissertation **no. 5.09**, University of Bern, 2017.

Stutenbecker, L., Costa, A., Schlunegger, F.: Lithological control on the landscape form of the upper Rhône Basin, Central Swiss Alps, *Earth Surface Dynamics*, **4**, 253–272, 2016.

Stutenbecker, L., Delunel, R., Schlunegger, F., Silva, T.A., Å egviÄ, B., Girardclos S., Bakker M., Costa A., Lane S.N., Loizeau J.-L., Molnar P., Akar N., Christl M.: Reduced sediment supply in a fast eroding landscape? A multi-proxy sediment budget of the upper Rhne basin, Central Alps, *Sedimentary Geology*, https://doi.org/10.1016/j.sedgeo.2017.12.013, 2017.

Surian, N., and Rinaldi, M.: Morphological response to river engineering and management in alluvial channels in Italy. *Geomorphology*, **50(4)**, 307–26, doi:10.1016/S0169-555X(02)00219-2, 2003.

Swift, D.A., Nienow, P.W. and Hoey, T.B.: Basal sediment evacuation by subglacial meltwater: suspended sediment transport from Haut Glacier d'Arolla, Switzerland, *Earth Surface Processes and Landforms*, **30(7)**, 867–883, 2005.

Syvitski, J.P.M., Vörösmarty, C.J., Kettner, A.J., Green, P.: Impact of Humans on the Flux of Terrestrial Sediment to the Global Coastal Ocean, *Science*, **308**, 2005.

Syvitski, J. P. M., Morehead, M. D., Bahr, D. B., Mulder, T.: Estimating fluvial sediment transport: the rating parameters, *Water Resources Research*, **36**, 2747–2760, 2000.

Tealdi, S., Camporeale, C., and Ridolfi, L.: Long-term morphological river response to hydrological changes, *Advances in Water Resources*, **34(2011)**, 1643–1655, 2011.

Tockner, K., and Stanford J. A.: Riverine flood plains: present state and future trends, *Environmental conservation*, **29(3)**, 308–330, 2002.

Tucker, G. E., and Slingerland, R.: Erosional dynamics, flexural isostasy, and long-lived escarpments: a numerical modelling study, *Journal of Geophysical Research*, **99**, 229–12, 1994.

Tucker, G.E., et al.: An object-oriented framework for hydrologic and geomorphic modeling using triangulated irregular networks, *Computers and Geosciences*, **27**, 959–973, 2001.

Turowski, J. M., Yager, E. M., Badoux, A., Rickenmann, D. and Molnar, P.: The impact of exceptional events on erosion, bedload transport and channel stability in a step-pool channel, *Earth Surface Processes and Landforms*, **34**, 1661–1673, doi:10.1002/esp.1855, 2009.

Valla, P. G., Shuster, D. L., and van der Beek, P.: Significant increase in relief of the European Alps during mid-Pleistocene glaciations, *Nature Geosciences*, **4**, 688–692, 2011.

Van Dijk, A.I.J.M., Bruijnzeel, L.A., Rosewell, C.J.: Rainfall intensity-kinetic energy relationship: A critical literature appraisal, *Journal of Hydrology*, **261**, 1–23, 2002.

VanSickle, J. and Beschta, R. L.: Supply–based models of suspended sediment transport in streams, *Water Resources Research*, **19**, 768–778, 1983.

Vetsch, D., Rousselot, P., Fäh, R. (2011) Flussgebietsmodellierung mit der Simulationssoftware BASEMENT, *Wasser Energie Luft*, **103(4)**

Vörösmarty, C. J., Meybeck, M., Fekete, B., Sharma, K., Green, P., Syvitski, J. P. M.: Anthropogenic sediment retention: major global impact from registered river impoundments, *Global and Planetary Change*, **39**, 169–190, 2003.

VAW-ETH, Glaciological reports (1881–2016). *"The Swiss Glaciers"*, Yearbooks of the Cryospheric Commission of the Swiss Academy of Sciences (SCNAT) published since 1964 by the Laboratory of Hydraulics, Hydrology and Glaciology (VAW) of ETH Zürich. **No. 1–134**, (http://glaciology.ethz.ch/swiss–glaciers/), 2015.

Vernon, A.J., Van der Beek, P.A., Sinclair, H.D., Rahn, M.K.: Increase in Late Neogene denudation of the European Alps confirmed by analysis of a fission–track thermochronology database, *Earth Planetary Sciences Letters*, **270(3-4)**, 316–329, 2008.

Walling, D. E.: Suspended sediment production and building activity in a small British basin, *IAHS–AISH, Spec. Publ.*, **113**, 137–144, 1974.

Walling, D. E.: Assessing the accuracy of suspended sediment rating curves for a small basin, *Water Resources Research*, **13**, 531–538, 1977.

Walling, D. E.: Tracing suspended sediment sources in catchments and river systems, *Science of the Total Environment*, **344**, 159–184, 2005.

Wang, H., Yang, Z., Wang, Y., Saito, Y., Liu, J. P.: Reconstruction of sediment flux from the Changjiang (Yangtze River) to the sea since the 1860s, *Journal of Hydrology*, **349**, 318–332, 2008.

Warrick, J. A., Trend analyses with river sediment rating curves, *Hydrological Processes*, **29**, 936–949, 2015.

Weber, C., Peter, A., and Zanini, F.: Spatio-temporal analysis of fish and their habitat: a case study on a highly degraded Swiss river system prior to extensive rehabilitation, *Aquatic Sciences*, **69**, 162–172, 2007.

Wen, L. J., Nagabhatla, N., Lü, S. H., Wang, S.Y.: Impact of rain snow threshold temperature on snow depth simulation in land surface and regional atmospheric model, *Adv. Atmos. Sci.*, **30**, 1449–1460, 2013.

Wick, L., Van Leeuwen, J. F. N., Van der Knaap, W. O., Lotter, A. F.: Holocene vegetation development in the catchment of Sägistalsee (1935 m asl), a small lake in the Swiss Alps. *Journal of Paleolimnology*, **30**, 261–272, 2003.

Wilcock, P. R., Kenworthy, S. T., and Crowe, J. C.: Experimental study of the transport of mixed sand and gravel, *Water Resources Research*, **37(12)**, 3349–3358, doi:10.1029/2001WR000683, 2001.

Wilcock, P. R. and Crowe J. C.: Surface-based transport model for mixed-size sediment. *Journal of Hydraulic Engineering*, **129**, 120–128, doi:10.1061/(ASCE)0733-9429(2003)129:2(120), 2003.

Wilks, D. S.: *Statistical Methods in the Atmospheric Sciences*, Academic Press, **467**, 1995.

Willgoose, G., Bras, R.L., and Rodriguez-Iturbe, I.: Results from a new model of river basin evolution, *Earth Surface Processes Landforms*, **16**, 237–254, 1991.

Williams, G.P., Wolman, M.G.: *Downstream effects of dams on alluvial rivers.* U.S. Geological Survey Professional Paper **1286**, U.S. Geological Survey, Reston, VA, 1984.

Wischmeier, W. H.: Rainfall erosion index for universal soil loss equation, *Soil Sci. Soc. Am. Proc.*, **23**, 246–249, 1959.

Wischmeier, W. H. and Smith, D. D.: *Predicting Rainfall Erosion Losses – A Guide to Conservation Planning*, Agric. Handbook, **No. 537**, Washington D.C., 58, 1978.

Wolman, M. G.: A method of sampling coarse river-bed material. *Eos, Transactions American Geophysical Union*, **35(6)**, 951–956, 1954. ISSN 2324-9250, doi:0.1029/TR035i006p00951, 1954.

Wood, J. L., Harrison, S., Turkington, T. A. R. and Reinhardt, L.: Landslides and synoptic weather trends in the European Alps, *Climatic Change*, **136**, 297–308, 2016.

Yager, E. M., Kirchner, J. W., and Dietrich, W. E.: Calculating bed load transport in steep boulder bed channels, *Water Resources Research*, **43**, W07418, doi:10.1029/2006WR005432, 2007.

Yang D., Kanae S., Oki T., Koike T., Musiake, K.: Global potential soil erosion with reference to land use and climate changes, *Hydrological Processes*, **17**, 2913–2928, doi: 10.1002/hyp.1441, 2003.

Yang, G., Chen, Z., Yu, F., Wang, Z., Zhao, Y., Wang, Z.: Sediment rating parameters and their implications: Yangtze River, China, *Geomorphology*, **85**, 166–175, 2007.

Zemp, M., Paul, F., Hoelzle, M., Haeberli, W.: *Glacier fluctuations in the European Alps, 1850–2000: an overview and spatio–temporal analysis of available data*, In: Orlove, B [et al.], Darkening Peaks: Glacier Retreat, Science, and Society, Berkeley, US, 152–167, 2008.

Zerathe, S., Lebourg, T., Braucher, R. and Bourles, D.: Mid–Holocene cluster of large-scale landslides revealed in the Southwestern Alps by ^{36}Cl dating. Insight on an Alpine-scale landslide activity, *Quaternary Science Reviews*, **90**, 106–27, 2014.